CHAIRS OF PHYSICAL CHEMISTRY

TECHNICAL UNIVERSITY OF MUNICH

Laboratory Course in Physical Chemistry for Fundamental Studies

Experiments Manual

The reproduction of this manual is funded by the tuition grant of the Chemistry Faculty

15th Edition (8 June 2026).

Editing, typing, and printing: Michele Piana, Karin Stecher, Alexander Ogrodnik, Sonja Uhl, Matthias Stecher, and Peter Kämmerer.

Chair of Technical Electrochemistry and Second Chair of Physical Chemistry

Table of Contents

1 Vapor-Pressure Curve and Boiling-Point Elevation

1.1 Context and aim of the experiment

In this experiment, the boiling point of a pure solvent as a function of pressure, i.e., its vapor-pressure curve, is measured. This is used to determine the vaporization enthalpy, the vaporization entropy, and the ebullioscopic constant of the solvent. Furthermore, an unknown substance is added to the solvent, and its molecular weight is determined from the measured boiling-point elevation [1.1 - 1.5].

1.1.1 Important concepts to know

Colligative properties, chemical potential, phase diagram, boiling point, triple point, critical point, ebullioscopic constant, vapor pressure, vapor pressure curve, Clausius-Clapeyron equation, enthalpy of vaporization, entropy of vaporization, ideal and non-ideal solution, non-associating solvent, Raoult's law, Henry's law, Gibbs' phase rule, molarity, molality, superheating of a solution.

1.1.2 Most common questions to be answered

- How can you graphically explain the effect of boiling-point elevation using the temperature dependence of the chemical potential of a solvent and its solution?
- Is the boiling-point elevation an enthalpy effect or an entropy effect? Explain your answer.
- How can you explain simply the effect of boiling-point elevation concerning the entropy of the system?
- Which characteristic distinguishes the phase diagram of water from those of most other solvents?
- In the expression for the ebullioscopic constant, the concentration is given as molality (mol/kg) instead of molarity (mol/L)? What is the advantage of this?

1.1.3 Further preparations before the experiment

Before experimenting, prepare a worksheet as follows:

Table 1.1-1: Example of the table to prepare for data collection and evaluation.

Pressure p (bar)	*Boiling temperature T_b (K)*
…	…
…	…
…	…
…	…

1.2 Theory

1.2.1 Phase diagrams

The *phase diagram* of a substance shows the regions of pressure p and temperature T at which its various phases (solid, liquid, or gas) have the minimum Gibbs free energy and are, thus, thermodynamically stable at equilibrium (Figure 1.1). The lines separating the regions are called *phase boundaries* and show the values of p and T at which two phases coexist in equilibrium.

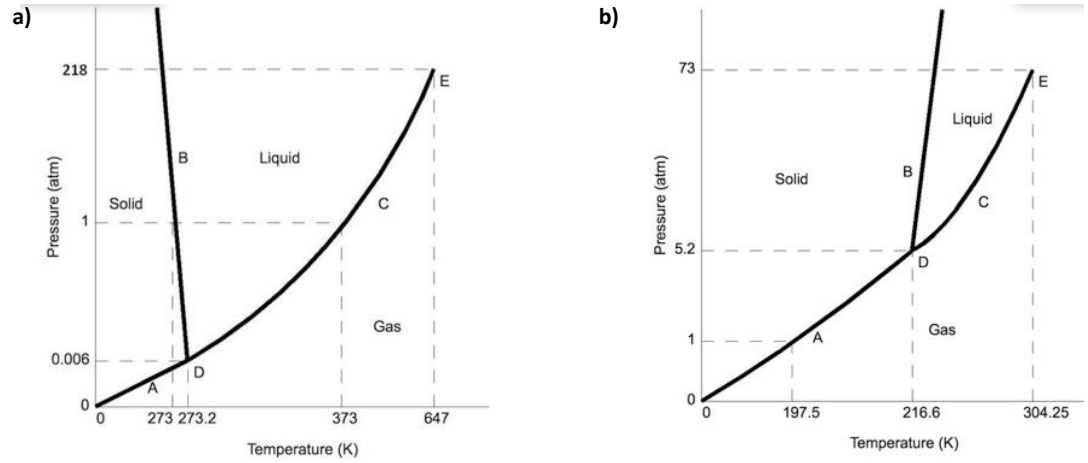

Figure 1.1: Phase diagram of **a)** water and **b)** CO_2. Phase boundaries are labeled with A, B, and C. D and E represent the triple point and the critical point, respectively.

The phase diagram illustrates several key properties of a substance, including its boiling point, standard boiling point, freezing point (also known as melting point), standard freezing point (also referred to as standard melting point), triple point, and *critical point*. The student must be familiar with these terms.

Figure 1.1 shows that, at the thermodynamic equilibrium, an arbitrary number of phases cannot exist simultaneously. This is stated in *Gibbs' phase rule*, which further allows the determination of the maximum possible degrees of freedom f at a particular position of the phase diagram. For liquids, this is

$$f = N - P + 2 \tag{1.1}$$

where P is the number of existing phases and N is the number of chemically independent components in the system. The Gibbs' phase rule is derived from the *Gibbs-Duhem equation*, which states that, in a thermodynamic system, not all intensive variables (such as temperature, pressure, molar quantities, etc.) can be varied independently.

1.2.2 Vapor pressure

Consider a liquid sample of a pure substance in a closed vessel. When the liquid and its vapor are in equilibrium, the same number of molecules leaves the liquid by vaporization and returns to the liquid by condensation. Under these conditions, the pressure of the vapor at a given temperature is called the *vapor pressure* of the liquid. The vapor pressure is independent of the presence of other components in the gas phase, e.g., air. In this case, the *partial pressure* of the liquid equals its vapor pressure at a specific temperature. Further heating of the liquid increases its vapor pressure. The temperature at which the vapor pressure of the liquid equals the external pressure is called the *boiling point*. At this temperature, vaporization can occur throughout the bulk of the liquid, and the vapor can expand freely into the surroundings. The condition of free vaporization throughout the liquid is called boiling.

During boiling, nucleation centers initiate bubble formation in the liquid. In the absence of nucleation centers, liquids could be overheated above their boiling temperature (***superheating***). To prevent boiling delay and ensure smooth boiling at the actual boiling point, nucleation centers, such as small pieces of sharp-edged glass, should be introduced as sources of bubbles.

Is the superheating a thermodynamic or a kinetic process?

Vaporization at a temperature T is accompanied by a change in molar enthalpy $\Delta_{vap}H$. This leads to the Clausius-Clapeyron equation for vaporization

$$\frac{dp}{dT} = \frac{\Delta_{vap}H}{T\Delta_{vap}V} \tag{1.2}$$

where $\Delta_{vap}V = V_m(g) - V_m(l)$ is the change in molar volume that occurs upon vaporization. Since the volume $V_m(l)$ of the liquid is negligible compared to the volume $V_m(g)$ of the vapor, we can write $\Delta_{vap}V \approx V_m(g)$. Additionally, the vapor can be treated as an ideal gas ($p \cdot V_m = R \cdot T$) and we can write

$$\frac{dp}{dT} = \frac{\Delta_{vap}H}{T\left(\frac{R \cdot T}{p}\right)} \tag{1.3}$$

Using $dp/p = d(\ln p)$ we can rearrange the equation (1.3) into the Clausius-Clapeyron equation, which describes how the vapor pressure varies with temperature

$$\frac{d(\ln p)}{dT} = \frac{\Delta_{vap}H}{R \cdot T^2} \tag{1.4}$$

The practical consequence of the equation (1.4) is that it allows us to predict how vapor pressure varies with temperature and how the boiling point varies with pressure (vapor-pressure curve). Using $dT/T^2 = -d(1/T)$ we obtain

$$\frac{d(\ln p)}{d(1/T)} = -\frac{\Delta_{vap}H}{R} \tag{1.5}$$

The phase boundary between the liquid phase and the gas phase is also called the ***vapor-pressure curve,*** and it is mathematically described by the equation (1.5). Plotting $\ln p$ as a function of $1/T$, a straight line with a slope $m = -\Delta_{vap}H/R$ will result. Assuming that $\Delta_{vap}H$ is independent of temperature, we can integrate the equation (1.4) to get

$$\ln p_1 - \ln p_2 = -\frac{\Delta_{vap}H}{R}\left(\frac{1}{T_1} - \frac{1}{T_2}\right) \tag{1.6}$$

Equation (1.6) allows calculation of $\Delta_{vap}H$.

For most of the non-associating solvents, i.e., solvents which do not show intermolecular interactions, the molar entropy of vaporization at boiling point and at standard pressure is given by the rule found by ***Pictet*** and ***Trouton***

$$\Delta S_{T_b} = \frac{\Delta_{vap}H}{T_b} \approx 88\frac{J}{K \cdot mol} \tag{1.7}$$

This means that, from the obtained $\Delta_{vap}H$ it is possible to estimate the boiling point T_b and vice versa, keeping in mind the assumption of non-associating solvents.

Give examples of non-associating and associating solvents.

1.2.3 Colligative properties and boiling-point elevation

In the case of a solute added to a pure solvent, a so-called osmotic pressure can be built, since the solute tends to occupy the whole volume of the solution. This is analogous to a gas prone to occupy the available volume. Using Fermi's words, "*the osmotic pressure of a dilute solution is equal to the pressure exerted by an ideal gas at the same temperature and occupying the same volume as the solution and containing a number of moles equal to the number of moles of the solutes dissolved in the solution*" [1.6]. In dilute solutions, the osmotic pressure depends on the number of solute particles present, not on their

identity. For this reason, it is called a colligative property (dependent on the number of particles). Because of this parallelism between solutions and gases, in case of dilute solutions, it is possible to use the ideal-gas law, according to Van't Hoff. [1.7]

$$p_B \cdot V = n_B \cdot R \cdot T \tag{1.8}$$

where n_B is the number of moles of the solute, V the volume of the solution, R the gas constant and T the absolute temperature. Since $n_B/V = c_B$

$$p_B = c_B \cdot R \cdot T \tag{1.9}$$

Solutions show a decreased vapor pressure Δp compared to the pure solvent (Figure 1.1). This can be related to the presence of the osmotic pressure and can be determined by ***Raoult's Law*** (assuming that the solute does not have an appreciable vapor pressure).

$$x_B = \frac{n_B}{n_B + n_A} = \frac{p_0 - p}{p_0} = \frac{\Delta p}{p_0} \tag{1.10}$$

where x_B is the molar fraction of the solute, p_0 is the vapor pressure of the pure solvent, p is the vapor pressure of the solution, n_B is the number of moles of the solute, n_A is the number of moles of the pure solvent. In the case of diluted solutions $n_A \gg n_B$, then

$$\frac{p_0 - p}{p_0} = \frac{n_B}{n_A} \tag{1.11}$$

At very low concentration, Raoult's Law turned out to be a good approximation for many solvents. Molecularly, this can be interpreted as the solvent molecules being in an environment very similar to that of pure liquid. For the solute, the situation is entirely different. Solvent molecules mainly surround it, so it experiences an entirely different environment than in its pure state. William Henry experimentally found a relationship that applies to the solute in a dilute solution (for the definition of *Henry's Law* (see paragraph 5.2.3).

Both boiling-point elevation and freezing-point depression (see Chapter 2) are directly correlated to the decreased vapor pressure of a solution compared to the pure solvent (Figure 1.2) and they are experimentally much easier to measure. In Figure 1.2 the black curve is the vapor-pressure curve of the pure solvent, while the green dotted curve is for the solution. Using the ebullioscopic method, the boiling points of the pure solvent ($T_{b,0}$) and the solution (T_b) at constant pressure p can be measured (generally at atmospheric pressure). For small temperature intervals, ($T_b - T_{b,0}$) the boiling points of the solution and pure solvent can be assumed linear for both curves. With these assumptions, the following equation applies

$$\frac{dp}{dT} \approx \frac{\Delta p}{\Delta T} = \frac{p_1 - p_0}{T_b - T_{b,0}} \longrightarrow p_1 - p_0 = (T_b - T_{b,0})\frac{dp}{dT} \tag{1.12}$$

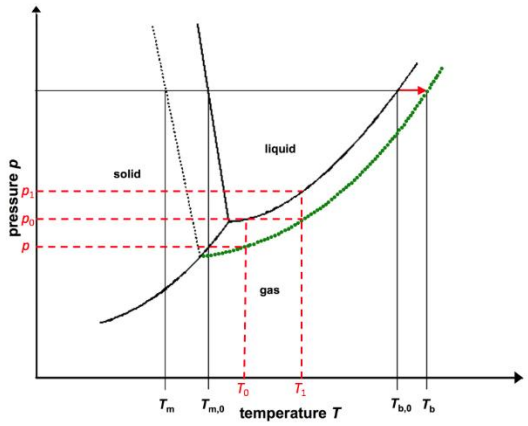

Figure 1.2: Phase diagram for a pure solvent (solid line) and its solution (dotted line). The vapor-pressure curve of the solution is highlighted in green. T_m, $T_{m.0}$, T_b, and $T_{b,0}$ are the freezing point and the boiling point for the solution and for the pure solvent, respectively.

Substituting (1.12) in the Clausius-Clapeyron equation (1.3) we obtain

$$\frac{p_1 - p_0}{p_0} = (T_b - T_{b,0})\frac{\Delta_{vap}H}{R \cdot T_{b,0}^2} \tag{1.13}$$

Assuming the parallelism of the two curves and using Raoult's law (1.11)

$$\frac{p_1 - p_0}{p_0} = \frac{p_1 - p}{p_0} == \frac{n_B}{n_A} = \frac{m_B \cdot M_A}{M_B \cdot m_A} \tag{1.14}$$

where m_B and M_B are the initial mass and molecular weight of the solute, while m_A and M_A are the initial mass and molecular weight of the solvent. Substituting equation (1.14) in (1.13) we obtain

$$T_b - T_{b,0} = \Delta T_b = \frac{M_A \cdot R \cdot T_{b,0}^2}{\Delta_{vap} H} \cdot \frac{m_B}{m_A \cdot M_B} \tag{1.15}$$

The first term on the right-hand side of the equation has a given constant value for each solvent. Thus, we can write the boiling point elevation as

$$\Delta T_m = C_{ebul} \cdot \frac{m_B}{M_B \cdot m_A} \qquad \text{where} \qquad C_{ebul} = \frac{M_A \cdot R \cdot T_{b,0}^2}{\Delta_{vap} H} \tag{1.16}$$

The constant C_{ebul}, the so-called ebullioscopic constant, specifies the boiling point increase occurring when one mole of a solute ($m_B/M_B = 1$ mol) is dissolved in 1 kg of solvent (m_A = 1 kg). Being M_B our unknown, it is possible to obtain it from the equation (1.16) by measuring the boiling-point elevation.

Equation (1.15) can also be derived from the difference in chemical potential μ between the pure solvent and the solution, as reported in the Appendix 1.5.1.

1.3 Experimental details and evaluation

1.3.1 Experimental execution

Vapor-pressure curve

The setup used to measure the vapor pressure curve is shown in Figure 1.3. The liquid solvent in the boiling flask **(1)** is heated with a heating mantel (**10**). A temperature sensor (**2**) is plugged into the boiling flask and measures the temperature inside the liquid (it should be slightly immersed). Additionally, a boiling capillary (3) is immersed in the solvent to prevent superheating. The vapor rises toward the condenser (4), which also serves as the connection to the vacuum pump (**5**). The vacuum pump evacuates the apparatus via a ballast piston (8).

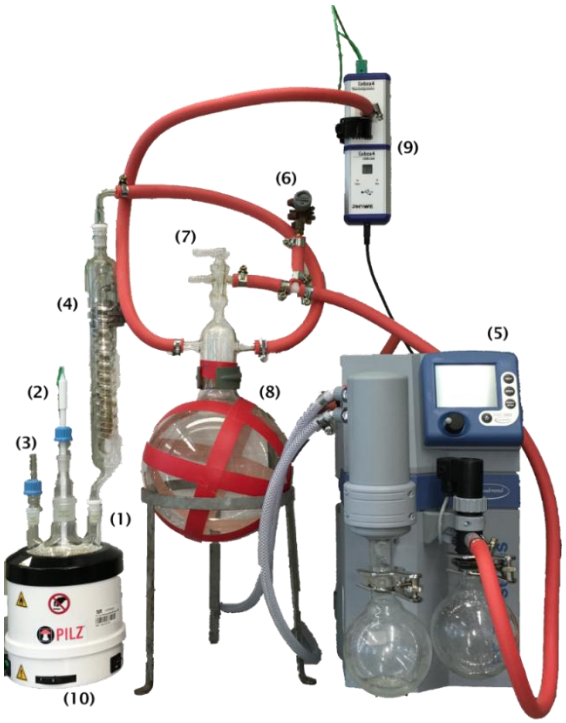

Figure 1.3: Setup for measuring the vapor pressure curve: (**1**) boiling flask, (**2**) temperature sensor, (**3**) boiling capillary, (**4**) condenser, (**5**) vacuum pump, (**6**) partial load valve, (**7**) valve, (**8**) ballast piston, (**9**) Cobra4 sensor unit, and **(10)** Heating mantel.

Turn on the cooling water and the pump (**5**), then evacuate the apparatus by carefully turning the partial-load valve (6). If the final vacuum (p = 200 mbar) is reached, a small heating stage (stage 5 or 6) is switched on to bring the liquid to a boil. Turn the partial load valve so that only the air flowing in through the boiling capillary is pumped out, thereby maintaining a constant pressure. Now the pressure and the corresponding boiling temperature can be read on the computer using the software provided (for instructions on how to use the software, see Chapter 12). In the next step, open the partial-load valve carefully and let the air slowly enter the apparatus (in increments of about 100 mbar). Again, turn the partial-load valve so that only the air flowing in through the boiling capillary is pumped out. At each measuring point, the adjusted pressure must equilibrate over time before the corresponding boiling temperature can be determined. This allows for a stable equilibrium value unaffected by any systematic error. Increase the pressure until you reach ambient pressure, then repeat the experiment, starting from high pressure and decreasing it to low pressure. The piston is pumped in increments of about 100 mbar, waiting until the pressure is constant, and then recording the pressure and the corresponding boiling temperature. **As pressure decreases, students need to allow the liquid to cool from one measuring point to the next, since the boiling point decreases with decreasing pressure.** When you have reached the final vacuum (p = 200 mbar), ventilate the equipment carefully, then turn off the pump (**5**) and the cooling water.

Boiling-point elevation

In the second part of the experiment, the molar mass M_X of an unknown substance must be determined by comparison between the boiling points of pure solvent and solutions of the unknown substance at different concentrations. For analysis, the vaporization enthalpy determined in the first part of the experiment is used. Finally, the calculated molecular mass should be used to identify the unknown substance.

To determine the boiling-point elevation, the apparatus in Figure 1.4, known as the Swietoslawski ebulliometer, is employed. The boiling vessel (**1**) is filled with 50 mL of solvent, and one or two boiling stones are added. The vessel is heated until the temperature remains constant (the boiling point is reached). Then, the students must briefly remove the temperature sensor (**2**) and fill the upper opening with 5 mL of the unknown liquid substance. This leads to a gradual increase in temperature until the new boiling point is reached. Then, again, 5 mL of the liquid are added, and the corresponding boiling point is determined similarly. To calculate the mass corresponding to 5 mL of the unknown substance at the experiment temperature and pressure, please refer to Table 1.5-1.

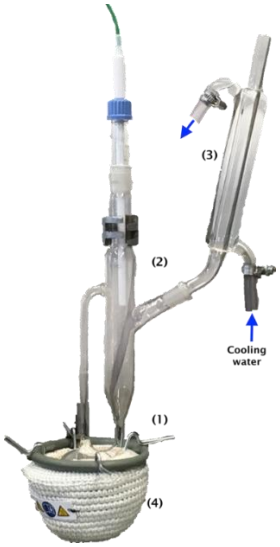

Figure 1.4: Setup for measuring the boiling point elevation: (**1**) boiling vessel, (**2**) temperature sensor, **(3)** Liebig refrigerator, and **(4)** heating mantel.

1.3.2 Data evaluation

- ☐ Plot the vapor pressure curve of the solvent drawing $\ln p$ against $1/T$ to obtain a straight line predicted by the equation (1.5).
- ☐ Determine $\Delta_{vap}H$ graphically from the slope of the line, and also calculate it according to equation (1.5).
- ☐ The boiling points determined in the experiment at the same pressure, going both upwards and downwards, are different. Provide a possible reason for this deviation between the two series of measurements.
- ☐ Use the determined $\Delta_{vap}H$ to calculate the ebullioscopic constant of the solvent using the equation (1.15). Further calculate $\Delta_{vap}S$ according to the rule found by Pictet and Trouton (equation (1.7)).
- ☐ Use the determined ebullioscopic constant and the measured increase in boiling point after addition of the unknown compound to calculate the molecular weight of the unknown substance according to the equation (1.16). The measured elevations in boiling point due to the addition of the unknown substance are defined as follows:

  $T_1 - T_0$ T_1 = Temperature after addition of the 1st portion of the pellets

  $T_2 - T_0$ T_2 = Temperature after addition of the 2nd portion of the pellets

  $T_2 - T_1$

  The 1st difference refers to m_1 (≡ mass of 1st portion), the 2nd difference to $m_1 + m_2$, and the 3rd to m_2.
- ☐ Using the average molecular weight of the unknown substance and knowing that it is a hydrocarbon (composed of carbon and hydrogen), determine its molecular formula.
- ☐ Perform an error analysis for all calculations.

1.4 Applications of the experiment and its theory

- ☑ Phases play an essential role in everyday life, for example, in the context of water (ice, liquid water, and water vapor).
- ☑ Pressure cooking pot.
- ☑ Cooking times are affected by alpine conditions, which are characterized by lower atmospheric pressure compared to ideal conditions.
- ☑ In organic and inorganic chemistry, the effect of boiling-point elevation can be applied to determine the molecular weight of newly synthesized molecules. It also allows the measurement of high-molecular-weight substances, which is essential in polymer science. [1.8, 1.9].
- ☑ Boiling-point elevation plays a vital role in food chemistry [1.10].
- ☑ The osmotic pressure is pharmaceutically essential, e.g., for the goal of achieving isotonic dosage forms [1.11].

1.5 Appendixes

1.5.1 Derivation of the boiling-point elevation from the chemical potential

The boiling-point elevation can also be derived from state functions that depend on both the measured temperature and pressure. One state function is called *Gibbs' free energy* G and it is related to the *enthalpy* H, to the *internal energy* U and to the *entropy* S as follows

$$G = H - T \cdot S = U + p \cdot V - T \cdot S \tag{1.17}$$

The partial derivative $\left(\frac{\partial G}{\partial n}\right)_{p,T}$ of the Gibbs' free energy with respect to the number of molecules n at constant pressure and temperature is defined as the chemical potential μ. Addition of a solute B to the pure solvent A changes the chemical potential of the latter to

$$\mu_{A,liquid} = \mu_{A,liquid,0} + R \cdot T \ln x_A \tag{1.18}$$

Where $\mu_{A,liquid,0}$ is the chemical potential of the pure liquid solvent A and $x_A = n_A/(n_A + n_B)$ is the molar fraction of the solvent. At a given pressure p, the variation of the chemical potential with temperature is proportional to the corresponding entropy S_A

$$\frac{\partial \mu_A}{\partial T} = -\frac{S_A}{n_A} \tag{1.19}$$

Figure 1.5 shows the temperature dependence of the chemical potential for a pure solvent and for a solution of the same solvent. This plot clearly demonstrates that adding a solute to a pure solvent results in a boiling-point elevation and a freezing-point depression.

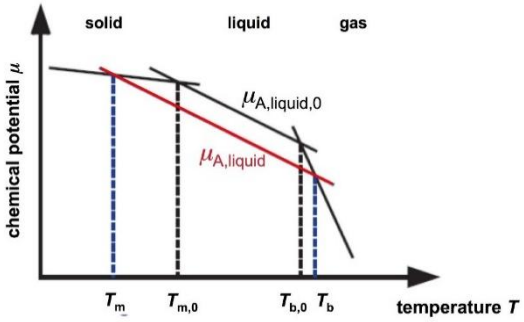

Figure 1.5: Chemical potential of a pure solvent *A* (black) and a solution made with it (red) as a function of temperature.

At the boiling point T_b, the liquid solvent and the solvent vapor are in equilibrium. This means that their chemical potentials are equal. Assuming that the solute B is not soluble in the solvent vapor, this yields

$$\mu_{A,gas} = \mu_{A,liquid} = \mu_{A,liquid,0} + R \cdot T_b \ln x_A \tag{1.20}$$

where $\mu_{A,gas}$ is the chemical potential of the pure gas A. Since the difference $\mu_{A,gas} - \mu_{A,liquid}$ is the molar Gibbs free energy of vaporization $\Delta_{vap}G$. Since $x_A = 1 - x_B$, then

$$\ln(1 - x_B) = \frac{\mu_{A,gas} - \mu_{A,liquid,0}}{R \cdot T} = \frac{\Delta_{vap}G}{R \cdot T} \tag{1.21}$$

Comparing equation (1.21) to the relationship of $\Delta_{vap}G$ with the molar enthalpy $\Delta_{vap}H$ and the molar entropy $\Delta_{vap}S$ of evaporation

$$\Delta_{vap}G = \Delta_{vap}H - T_b \cdot \Delta_{vap}S \tag{1.22}$$

we obtain

$$\ln(1 - x_B) = \frac{\Delta_{vap}H}{R \cdot T_b} - \frac{\Delta_{vap}S}{R} \tag{1.23}$$

Equation (1.23) neglects the small temperature dependence of $\Delta_{vap}H$ and $\Delta_{vap}S$. Considering the pure solvent ($x_B = 0$), equation (1.23) provides the relation between the melting point of the pure solvent $T_{b,0}$ and $\Delta_{vap}H$ and $\Delta_{vap}S$

$$\ln(1) = \left(\frac{\Delta_{vap}H}{R \cdot T_b} - \frac{\Delta_{vap}S}{R}\right) = 0 \tag{1.24}$$

By subtracting the equation (1.24) from equation (1.23) we obtain:

$$\ln(1 - x_B) = \frac{\Delta_{vap}H}{R}\left(\frac{1}{T_b} - \frac{1}{T_{b,0}}\right) \tag{1.25}$$

If B is present in a very low concentration ($x_B \ll 1$), the approximation $\ln(1 - x_B) \approx -x_B$) is valid, and we obtain

$$x_B \approx \frac{\Delta_{vap}H}{R}\left(\frac{1}{T_{b,0}} - \frac{1}{T_b}\right) \tag{1.26}$$

Since the boiling-point elevation is minimal ($T_b \approx T_{b,0}$), the term within the bracket can be written as

$$\left(\frac{1}{T_{b,0}} - \frac{1}{T_b}\right) = \frac{T_b - T_{b,0}}{T_{b,0} \cdot T_b} \approx \frac{\Delta T_b}{T_{b,0}^2} \tag{1.27}$$

where $\Delta T_b = T_{b,0} - T_b$ is the measured boiling-point elevation. Substituting equation (1.27) in equation (1.26), we can derive the boiling-point elevation

$$\Delta T_b \approx \left(\frac{R \cdot T_{b,0}^2}{\Delta_{vap}H}\right) \cdot x_B \tag{1.28}$$

Note that $\Delta T_m = T_{m,0} - T_m$ is defined oppositely compared to $\Delta T_b = T_b - T_{b,0}$ (see Chapter 2). This is done to obtain $\Delta T > 0$ in both cases. Using $x_B = n_B/n$ with $n \approx n_B$, $n_B = m_B/M_B$ and $n_A = m_A/M_A$ (where m is the mass in grams, while M is the molar mass in g/mol) we obtain

$$\Delta T_m = \left(\frac{R \cdot T_{b,0}^2}{\Delta_{vap}H}\right) \cdot \left(\frac{m_B \cdot M_A}{M_B \cdot m_A}\right) \tag{1.29}$$

that is precisely the equation (1.15), previously derived.

1.5.2 Density of the unknown substance at various temperatures and pressures

Table 1.5-1: Density of the unknown substance in g/cm^3 at various temperatures and pressures.

	Temperature T/K								
Pressure p/MPa	**283.15**	**293.15**	**303.15**	**313.15**	**323.15**	**333.15**	**343.15**	**353.15**	**363.15**
0.1	0.877	0.869	0.861	0.853	0.845	0.838	0.830	0.822	0.814
1	0.877	0.870	0.862	0.854	0.846	0.838	0.831	0.823	0.815
3	0.879	0.871	0.863	0.855	0.848	0.840	0.832	0.825	0.817
5	0.880	0.872	0.865	0.857	0.849	0.842	0.834	0.826	0.819
10	0.883	0.875	0.868	0.860	0.853	0.845	0.838	0.831	0.823
15	0.886	0.878	0.871	0.864	0.856	0.849	0.842	0.835	0.827
20	0.889	0.881	0.874	0.867	0.860	0.853	0.846	0.838	0.831
25	0.892	0.884	0.877	0.870	0.863	0.856	0.849	0.842	0.835
30	0.894	0.887	0.880	0.873	0.866	0.859	0.852	0.846	0.839
35	0.897	0.890	0.883	0.876	0.869	0.862	0.856	0.849	0.842
40	0.899	0.892	0.885	0.878	0.872	0.866	0.859	0.853	0.846
50	0.904	0.898	0.891	0.884	0.878	0.871	0.865	0.858	0.852
60	0.910	0.902	0.895	0.889	0.883	0.877	0.870	0.864	0.858

1.6 Literature

1.1 - H.D.B. Jenkins, Chemical Thermodynamics at a Glance, Chapter 52. Colligative Properties: Boiling Point, Wiley/Blackwell (2007).

1.2 - P.W. Atkins, Physical Chemistry, 6th ed., Oxford University Press, Oxford (1998), pp. 163-182.

1.3 - P.W. Atkins and J. de Paula, Atkins' Physical Chemistry, 8th ed., Oxford University Press, Oxford, (2006) pp. 136-156.

1.4 - S. G. Wedler, *Lehrbuch der Physikalischen Chemie*, 6th ed., Wiley/VCH (2012).

1.5 - R. Brdicka, *Grundlagen der Physikalischen Chemie,* 15th ed., Wiley/VCH (1981).

1.6 - E. Fermi, *Thermodynamics* by Prentice-Hall, 1937 - Dover Publications, Inc., New York, NY (1956), Chapter VII, The thermodynamics of dilute solutions, pp. 113-130. http://gutenberg.net.au/ebooks13/1305021p.pdf (accessed on 25 October 2024).

1.7 - J.H. van't Hoff, "The Role of Osmotic Pressure in the Analogy between Solutions and Gases", in: "Memoirs on The Modern Theory of Solution", by Pfeffer, van't Hoff, Arrhenius, and Raoult; translated and edited by Harry C. Jones, Harper & Brothers Publishers, New York and London, (1899), pp. 11-43. https://archive.org/details/moderntheoryofso00jonerich (accessed on 25 October 2024).

1.8 - R.S. Lehrle and T.G. Majury, A thermistor ebulliometer for high molecular weight measurements*, Journal of Polymer Science*, **29**, (1958) pp. 219-234.

1.9 - H. Morawetz, Measurement of Molecular Weight of Polyethylene by Menzies-Wright Boiling Point Elevation Method*, Journal of Polymer Science*, **6**, (1951) pp. 117-121.

1.10 - G.H. Crapiste and J.E. Lozano, Effect of Concentration and Pressure on the Boiling Point Rise of Apple Juice and Related Sugar Solutions*, Journal of Food Science*, **53**, (1988) pp. 865-868.

1.11 - K.A. Connors and S. Mecozzi, *Thermodynamics of Pharmaceutical Systems: An Introduction for Students of Pharmacy,* Chapter 9. Colligative properties, John Wiley & Sons Inc., Hoboken, NJ, USA, (2010).

2 Freezing-Point Depression

2.1 Context and aim of the experiment

As discussed in Chapter 1, dissolving particles in a pure solvent decreases the vapor pressure, thereby increasing the boiling point. Similarly, a decrease in the vapor pressure of a solution lowers its freezing temperature. The effect of freezing-point depression is discussed and applied in the experiment described in this chapter. Note that both effects have a similar theoretical background. [2.1 - 2.6]

In this experiment, the freezing points of water and various aqueous solutions are measured. The results are used to determine the cryoscopic constant of water. Furthermore, an unknown substance is added to the solvent, and the observed freezing-point depression is used to calculate its molecular weight. The measured data are further used to determine the degree of dissociation of sodium sulfate in water.

2.1.1 Important concepts to know

Colligative properties, chemical potential, phase diagram, freezing point, triple point, critical point, cryoscopic constant, vapor pressure, vapor-pressure curve, Clausius-Clapeyron equation, enthalpy of fusion, entropy of fusion, ideal and non-ideal solution, Raoult's law, Henry's law, molality, molarity, Gibbs' phase rule, supercooling of a solution.

2.1.2 Most common questions to be answered

- How can you graphically explain the effect of freezing point depression using the temperature dependence of the chemical potential of a solvent and its solution?
- Is the freezing point depression an enthalpy effect or an entropy effect? Explain your answer.
- How can you explain simply the impact of freezing point depression regarding the entropy of the system?
- Which characteristic distinguishes the phase diagram of water from those of most other solvents?
- In the expression for the cryoscopic constant, the concentration is given as molality (mole/kg) rather than molarity (mole/l)? What is the advantage of this?

2.1.3 Further preparations before the experiment

Before experimenting, prepare a worksheet as follows:

Table 2.1-1: Example of the table to prepare for data collection and evaluation.

Solution, conditions	*Freezing point T_m (K)*
…	…
…	…
…	…

2.2 Theory

2.2.1 Phase diagrams

To understand the effect of freezing-point depression, it is essential to know the concepts of phase diagrams and the associated terms of solid phase, liquid phase, gaseous phase, thermodynamic equilibrium, Gibb's free energy, phase boundary, boiling point, freezing point (also called melting point), standard boiling point, standard freezing point, triple point and critical point and with the statement of the Gibb's phase rule. The students must be familiar with all these terms (see paragraph 1.2).

2.2.2 Colligative properties

Solutions show a decreased vapor pressure Δp compared to the pure solvent (see Figure 2.1 and paragraph 1.2.3). Both the boiling-point elevation (see Chapter 1) and the freezing-point depression are directly related to this observation. In dilute solutions, both effects only depend on the number of solute particles present, not on their identity. For this reason, they are referred to as colligative properties. Another example of a colligative property is the osmotic pressure.

Similar to the vapor pressure curve, but in the opposite direction, the phase boundary between the solid phase and the liquid phase is shifted for a solution, in comparison to the pure solvent.

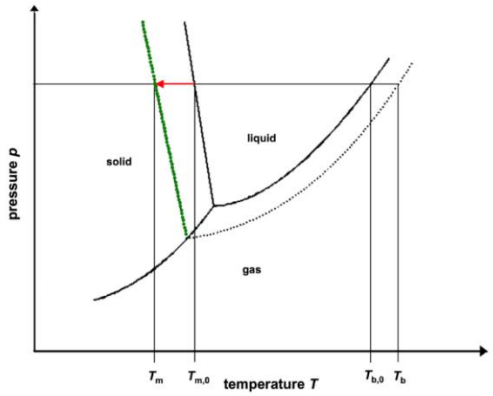

Figure 2.1: Phase diagram for a pure solvent (solid line) and its solution (dotted line). The vapor-pressure curve is highlighted in green. T_m, $T_{m.0}$, T_b, and $T_{b,0}$ are the freezing points and the boiling points for the solution and for the pure solvent, respectively.

2.2.3 Derivation of freezing-point depression from chemical potential

Any property of substances (pure or mixtures) can be derived from state functions, which are related to both the measured temperature and pressure. The *Gibbs free energy* G is a state function and it is related to others, like the *enthalpy* H, *internal energy* U and *entropy* S as follows

$$G = H - T \cdot S = U + p \cdot V - T \cdot S \tag{2.1}$$

The partial derivative $\left(\frac{\partial G}{\partial n}\right)_{p,T}$ of the Gibbs free energy with respect to the number of molecules n at constant pressure and temperature is defined as the chemical potential m. Addition of a solute B to the pure solvent A changes the chemical potential of the latter to

$$\mu_{A,liquid} = \mu_{A,liquid,0} + R \cdot T \ln x_A \tag{2.2}$$

Where $\mu_{A,liquid,0}$ is the chemical potential of the pure liquid solvent A and $x_A = n_A/(n_A + n_B)$ is the molar fraction of the solvent. At a given pressure p, the variation of the chemical potential with temperature is proportional to the corresponding entropy S_A

$$\frac{\partial \mu_A}{\partial T} = -\frac{S_A}{n_A} \tag{2.3}$$

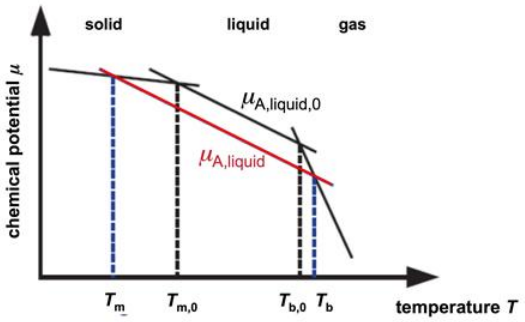

Figure 2.2: Chemical potential of a pure solvent *A* (black) and a solution made with it (red) as a function of temperature.

At the freezing point T_m, the solid solvent and the liquid solvent are in equilibrium. This means that their chemical potentials are equal. Assuming that the solute B is not soluble in the gas solvent, this yields

$$\mu_{A,solid} = \mu_{A,liquid} = \mu_{A,liquid,0} + R \cdot T_m \ln x_A \tag{2.4}$$

where $\mu_{A,solid}$ is the chemical potential of the pure solid A. Since the difference $\mu_{A,liquid} - \mu_{A,solid}$ is the molar Gibbs free energy of fusion $\Delta_{fus}G$. Since $x_A = 1 - x_B$, then

$$\ln(1 - x_B) = \frac{\mu_{A,solid} - \mu_{A,liquid,0}}{R \cdot T} = -\frac{\Delta_{fus}G}{R \cdot T} \tag{2.5}$$

Comparing equation (2.5) to the relationship of $\Delta_{fus}G$ with the molar enthalpy $\Delta_{fus}H$ and the molar entropy $\Delta_{fus}S$ of fusion

$$\Delta_{fus}G = \Delta_{fus}H - T_m \cdot \Delta_{fus}S \tag{2.6}$$

we obtain

$$-\ln(1 - x_B) = \frac{\Delta_{fus}H}{R \cdot T_m} - \frac{\Delta_{fus}S}{R} \tag{2.7}$$

Equation (2.7) neglects the small temperature dependence of $\Delta_{fus}H$ and $\Delta_{fus}S$. Considering the pure solvent ($x_B = 0$), equation (2.7) provides the relation between the melting point of the pure solvent $T_{m,0}$ and $\Delta_{fus}H$ and $\Delta_{fus}S$

$$\ln(1) = -\left(\frac{\Delta_{fus}H}{R \cdot T_m} - \frac{\Delta_{fus}S}{R}\right) = 0 \tag{2.8}$$

By subtracting the equation (2.8) from equation (2.7) we obtain:

$$\ln(1 - x_B) = \frac{\Delta_{fus}H}{R}\left(\frac{1}{T_{m,0}} - \frac{1}{T_m}\right) \tag{2.9}$$

If B is present in a very low concentration ($x_B \ll 1$) the approximation $\ln(1 - x_B) \approx -x_B$) is valid, and we obtain

$$x_B \approx \frac{\Delta_{fus}H}{R}\left(\frac{1}{T_m} - \frac{1}{T_{m,0}}\right) \tag{2.10}$$

Since the freezing-point depression is minimal ($T_m \approx T_{m,0}$), the term within the bracket can be written as

$$\left(\frac{1}{T_m} - \frac{1}{T_{m,0}}\right) = \frac{T_{m,0} - T_m}{T_{m,0} \cdot T_m} \approx \frac{\Delta T_m}{T_{m,0}^2} \tag{2.11}$$

where $\Delta T_m = T_{m,0} - T_m$ is the measured melting-point depression. Substituting equation (2.11) in equation (2.10), we can derive the freezing-point depression

$$\Delta T_m \approx \left(\frac{R \cdot T_{m,0}^2}{\Delta_{fus}H}\right) \cdot x_B \tag{2.12}$$

Note that $\Delta T_m = T_{m,0} - T_m$ is defined oppositely compared to $\Delta T_b = T_b - T_{b,0}$ (see Chapter 1). This is done to obtain $\Delta T > 0$ in both cases. Using $x_B = n_B/n$ with $n \approx n_A$, $n_B = m_B/M_B$ and $n_A = m_A/M_A$ (where m is the mass in grams, while M is the molar mass in g/mol) we obtain

$$\Delta T_m = \left(\frac{R \cdot T_{m,0}^2}{\Delta_{fus} H}\right) \cdot \left(\frac{m_B \cdot M_A}{M_B \cdot m_A}\right) \tag{2.13}$$

The first term to the right has a given constant value for each solvent. Thus, we can write the freezing-point depression as

$$\Delta T_m = C_{cryo} \cdot \frac{m_B}{M_B \cdot m_A} \qquad \text{where} \qquad C_{cryo} = \frac{R \cdot T_{m,0}^2 \cdot M_A}{\Delta_{fus} H} \tag{2.14}$$

The constant C_{cryo}, called cryoscopic constant, specifies the freezing-point decrease occurring when one mole of a solute (m_B/M_B =1 mol) is dissolved in 1 Kg of solvent (m_A = 1 Kg). Since M_B is our unknown, it is possible to derive it from the equation (2.14) by measuring the freezing-point depression.

$$M_B = C_{Cryo} \frac{m_B}{m_A \Delta T_m} \tag{2.15}$$

The freezing-point depression can be derived from Raoult's Law analogously to the boiling-point elevation (chapter 1). Take care that you are also familiar with this and with *Henry's law* (chapter 5).

2.2.4 *Supercooling of a liquid*

At the freezing temperature, nucleation centers form, from which the freezing of the liquid begins. If these nucleation centers are missing, liquids may be cooled below their freezing temperatures. This is a process called *supercooling*. A small external perturbation, such as carefully knocking the test tube, usually triggers the freezing process suddenly. As a result, the temperature increases until it reaches the freezing point.

Is the supercooling a thermodynamic or a kinetic process?

2.3 Experimental details and evaluation

2.3.1 *Experimental execution*

The setup used to determine the freezing point is shown in Figure 2.3a and Figure 2.3b in all its parts. It is made of a special glass tube (**1**) that is cooled by a cold mixture (**7**) (Figure 2.3b) consisting of water, ice, and sodium chloride.

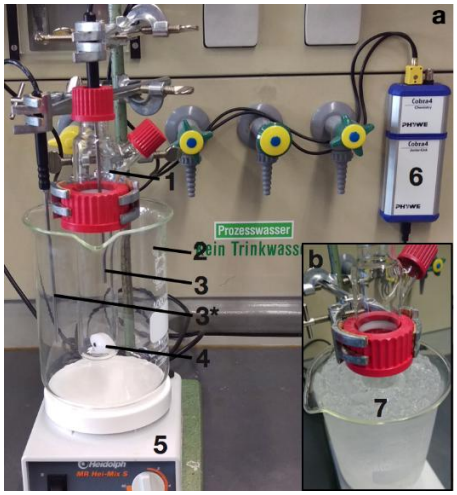

Figure 2.3: a - Workplace for freezing-point experiments and its parts. Glass tube (**1**), 1000 ml beaker (**2**), temperature sensors? (**3, 3***), stirring bar (**4**), magnetic stirrer (**5**), Cobra4 unit (**6**). **b -** Cold mixture used to cool the glass tube (**7**)

Turn on the Cobra4 unit (**6**), the computer, and open the "Excel" software and the software "measure" (see Chapter 12 for basic instructions on using the software).

Prepare the cold mixture by mixing water, ice, and sodium chloride in the 1000 mL beaker (**2**). The amounts of the components of the cold mix must be chosen to obtain a temperature of T < -10 °C. Fill the 1000 mL beaker with ice. Add

deionized water up to the 800 mL calibration mark. Since part of the ice is melting, add more ice until it stops melting. To prevent the water from overflowing, part of it needs to be periodically poured into the basin. Once the ice has stopped melting, pour sodium chloride onto the surface of the ice-water mixture and immediately begin stirring with a glass rod to dissolve the salt. Check the temperature using the temperature sensor (**3***). If T > -10 °C, add more salt and repeat the dissolving-stirring procedure as described above. The temperature of the cold mixture increases over time; therefore, it must be checked after each measurement and adjusted by adding ice and salt as needed.

Clean the glass tube with deionized water. Carefully add the stirring bar (4). **To avoid breaking the glass tube, ensure the stirring bar does not fall from the top to the bottom.**

In the first measurement, the freezing point of pure water is determined. Fill the glass tube with 25 mL of deionized water using a pipette, and mount it in the beaker with the cold mixture as deeply as possible. Place the first temperature sensor (**3**) in the middle of the glass tube. **Ensure that it does not touch either the stirring bar or the glass tube**. Turn on the magnetic stirrer (**5**). Place the second temperature sensor (**3***) into the cold mixture in the beaker. This is used to monitor the temperature of the cold mixture, ensuring it stays below -10 °C.

Start the measurement. The measurement can be stopped if the temperature stays constant for one minute. Remove the glass tube from the cold mixture and liquefy the frozen sample by warming it with tap water from outside (or by hand). The same sample can be used for the following measurements. The freezing point of pure water has to be determined three times. Calculate the average of the results for further data analysis. **The following measurements on the solutions have to be performed only twice. For further data analysis, always take the average of the two individual results**.

For the determination of the cryoscopic constant of water, prepare two solutions of urea in deionized water (**solutions A and B**) for the following measurements:

Solution A: 2.5 g of urea in 25 mL of solution in deionized water
Solution B: 1.5 g of urea in 25 mL of solution in deionized water

The following measurements are performed to identify an unknown substance by determining its freezing point. The unknown substance is available on the bench. Prepare the two following solutions (**solutions C and D**):

Solution C: 1 g of unknown substance in 25 mL of solution in deionized water
Solution D: 2 g of unknown substance in 25 mL of solution in deionized water

In the last measurements, the degree of dissociation of sodium sulfate is determined. For this, prepare the following solution (**solution E**):

Solution E: 0.75 g of sodium sulfate in 25 mL of solution in deionized water

2.3.2 Data evaluation

- ☐ Determine the freezing point of pure water.
- ☐ Plot temperature vs. time for the two solutions of different urea concentrations and use this to determine the cryoscopic constant of water.
- ☐ Determine the molecular weight of the unknown substance according to the equation (2.15).
- ☐ Determine the degree of dissociation of sodium sulfate using the experimentally determined cryoscopic constant of water.
- ☐ Perform an error analysis for all calculations.

2.4 Applications of the experiment and its theory

- ☑ In organic and inorganic chemistry, freezing-point depression can be used to determine the molecular weight of newly synthesized molecules. This method is called cryoscopy. Cryoscopy is also used in food science [2.7 - 2.9].
- ☑ Application of road salt to prevent ice formation on pavements and streets in winter.
- ☑ Anti-freezing agents in the car radiator to prevent freezing of the liquid cooling system.
- ☑ Anti-freezing agents (e.g., glucose, glycerol, urea) are produced naturally in the bodies of some insects and frogs [2.10].
- ☑ Analysis of freezing point depression is essential in polymer science. [2.11]

2.5 Literature

2.1 - P.W. Atkins, Physical Chemistry, 6th ed., Oxford University Press, Oxford (1998), pp. 163-182.

2.2 - P.W. Atkins and J. de Paula, Atkins' Physical Chemistry, 8th ed., Oxford University Press, Oxford (2006), pp. 136-156.

2.3 - R.E. Dickerson, H.B. Gray, M.Y. Darensbourg and D.J. Darensbourg, *Prinzipien der Chemie,* 2nd ed. (1988).

2.4 - G. Wedler, *Lehrbuch der Physikalischen Chemie*, 6th ed., Wiley/VCH (2012).

2.5 - W.J. Moore, *Grundlagen der Physikalischen Chemie,* 1st ed., de Gruyter (1990).

2.6 - R. Brdicka, *Grundlagen der Physikalischen Chemie,* 15th ed., Wiley/VCH (1981).

2.7 - C.S. Chen, Effective Molecular Weight of Aqueous Solutions and Liquid Foods from the Freezing Point Depression*, Journal of Food Science*, **51** (1986) 1537-1539.

2.8 - C.S. Chen, Thermodynamic Analysis of the Freezing and Thawing of Foods: Enthalpy and Apparent Specific Heat*, Journal of Food Science*, **50** (1985) 1158-1162.

2.9 - J.B. Lahne and S.J. Schmidt, Gelatin-Filtered Consommé: A Practical Demonstration of the Freezing and Thawing Processes*, Journal of Food Science*, **9** (2010) 53-58.

2.10 - K.B. Storey and J.M. Storey, Natural Freezing Survival in Animals*, Ann. Rev. of Ecology and Systematics*, **27** (1996) 365-386.

2.11 - B.B. Boonstra, F.A. Heckman and G.L. Taylor, Anomalous freezing point depression of swollen gels, *Journal of Applied Polymer Science*, **12** (1986) 223-247.

3 Joule-Thomson Effect

3.1 Context and aim of the experiment

This experiment aims to measure and interpret the Joule-Thomson coefficient of various gases. The students are supposed to understand how the Joule-Thomson coefficient relates to the intermolecular forces in general and to the van der Waals parameters, a, b and the second viral coefficient B, in particular. A quantitative comparison of these parameters with the experimental results will be performed. Finally, the influence of temperature on the Joule-Thompson effect will be illustrated graphically and discussed within the concept of inversion temperature [3.1 - 3.6].

3.1.1 Important concepts to know

Ideal and real gas: Lennard-Jones potential, van der Waals forces, dispersive London forces, van der Waals' equation of state, Clausius' virial expansion

Joule-Thomson-Coefficient: first law of thermodynamics, enthalpy, isenthalpic processes, inversion curve of the Joule-Thomson-Coefficient

3.1.2 Most common questions to be answered

- What is the difference between a *reversible adiabatic*, a *reversible isothermal*, and an *isenthalpic* (Joule-Thomson) *expansion*? Show these differences in a $p-V$-diagram and explain what is happening along the Lennard-Jones-potential. How does the *internal energy* U, the *enthalpy* H, the *entropy* S and the *temperature* T change during the processes?
- Why does a real gas usually cool down during an isenthalpic expansion? What happens to an ideal gas? In which situation does a real gas warm up instead of cooling down?
- Which qualitative relation exists between the Joule-Thomson effect (depending on the variable p) and the Lennard-Jones potential (depending on the variable r)?
- Which criteria need to be considered when looking for a gas with maximum Joule-Thomson effect? Which of the gases investigated in this experiment would you start with and why?

3.1.3 Further preparations before the experiment

Before performing the experiment, prepare a worksheet as follows:

Table 3.1-1: Example of the table to prepare for data collection and evaluation.

Overpressure p (bar)	T_1 *(K)*	p_1 *(bar)*	$\frac{1}{n}\sum_{i=1}^{n}\Delta T_i$ *(K)*	$\frac{\Delta T_\downarrow+\Delta T_\uparrow}{2}$ *(K)*
0.8 (p ↓)				
0.8 (p ↑)				
0.6 (p ↓)				
0.6 (p ↑)				
0.4 (p ↓)				
0.4 (p ↑)				
0.2 (p ↓)				
0.2 (p ↑)				
0 (p ↓)				
0 (p ↑)				

T_1 and p_1 stand for the ambient temperature and the ambient pressure, respectively. $p\downarrow$ and $p\uparrow$ indicate the series of measurements going from high to low pressure and from low to high pressure, respectively. $\frac{\Delta T_\downarrow + \Delta T_\uparrow}{2}$ denotes the average of the temperature differences obtained from the two measurement series.

3.2 Theory

An *adiabatic, irreversible expansion* (= *isenthalpic, see below) of a real gas across a throttle (nozzle) generally results in a reduction in* temperature. Such an effect is not expected in ideal gases, as it arises from *intermolecular interactions*.

3.2.1 Internal energy and intermolecular interactions

The internal energy U consists of the *kinetic energy* (energy of the translational, rotational, and vibrational degrees of freedom) of the molecules and of their *potential energy*, which, in our case, results from *intermolecular interactions*. The contributions to U can be specified by the following differential equation

$$dU = \left(\frac{\partial U}{\partial T}\right)_V dT + \left(\frac{\partial U}{\partial V}\right)_T dV \tag{3.1}$$

The first term in the equation (3.1) corresponds to the kinetic energy, while the second term arises from intermolecular interactions. Furthermore

$$\left(\frac{\partial U}{\partial T}\right)_V = C_V \tag{3.2}$$

where C_V denotes the heat capacity at constant volume and depends on the number of thermodynamically active *degrees of freedom*. Each degree of freedom retains the energy $R \cdot T/2$ and thus contributes to $R/2$ to the heat capacity. Furthermore

$$\left(\frac{\partial U}{\partial V}\right)_T = p_{cohesion} \tag{3.3}$$

where $p_{cohesion}$ is the cohesion pressure. Since the differential is performed at constant temperature, i.e., at constant kinetic energy, this term is a measure of the intermolecular interactions: any change of volume results in a shift in the *average distance* $\langle r \rangle$ and, accordingly, of the interaction between the molecules.

Let us now consider the special case of an *adiabatic* expansion (meaning that there is no heat exchange) into a vacuum (meaning that there is no work transferred to the surroundings). According to the *first law of thermodynamics*, the internal energy U must remain constant, i.e., $dU = 0$. At ordinary values of pressure and temperature, the attractive interactions dominate and, consequently, an increase in the average distance $\langle r \rangle$ of the molecules increases the interaction energy (compare Lennard-Jones potential, Figure 3.1).

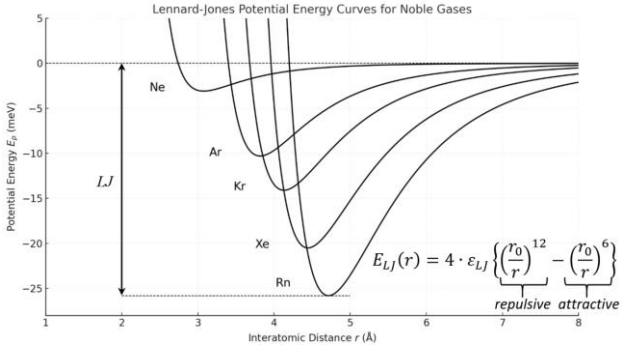

Figure 3.1: The Lennard-Jones-potential is the intermolecular interaction (potential energy) between two uncharged particles plotted as a function of the distance r for noble gases. It has a minimum at $r_{min} = 2^{1/6} \cdot r_0$ where r_0 is the radius at which $E_{LJ} = 0$. The depth of the well is the intermolecular binding energy ε_{LJ}. The r_0 increases with increasing atomic mass, while simultaneously the binding energy becomes stronger and stronger. Note that for theoretical calculations of Joule-Thomson-coefficients, the $1/r^{12}$ term is usually replaced by an exponential term (exp-6 potential) [3.1].

At intermolecular distances $r < r_{LJ}$ repulsion occurs between molecules (Pauli principle), if $r > r_{LJ}$ attraction prevails (due to London dispersion force: instantaneous dipole–induced dipole forces). Since for an expansion into a vacuum the intermolecular distance r increases to infinity ($r \to \infty$), the interaction energy, i.e., the interaction term $\left(\frac{\partial U}{\partial V}\right)_T dV$, increases. If the constraints of the experiment have been chosen to prohibit the flow of energy from the surroundings ($dU = 0$), the kinetic term $\left(\frac{\partial U}{\partial T}\right)_V dT$ must decrease. Consequently, the amount of interaction energy required for expansion can only be extracted from the internal kinetic degrees of freedom, which explains the decrease in temperature. The fewer degrees of freedom available, i.e., the smaller the heat capacity, the more substantial the temperature decrease will be.

3.2.2 The Joule-Thomson-Experiment

Joule's first attempt to verify intermolecular interactions failed, since the experiments were not conducted under adiabatic conditions. To detect the temperature change, he used a surrounding heat bath. However, due to its high heat capacity, the heat bath provided all the energy necessary for expansion to the vacuum, and thus the proposed decrease in temperature was not detectable. In 1842, Joule and Thomson carried out the experiment under improved constraints (Figure 3.2). *i)* The temperature change was not detected in a surrounding heat bath, but directly in the adiabatically expanding gas (by thermal insulation of the gas from its surroundings); *ii)* the experiment was conducted in a quasi-stationary mode, by leading a continuous stream of gas through a throttle (or nozzle), generating a pressure drop from the initial pressure $p_{initial}$ in front of the throttle to the final pressure p_{final}. (*Note that in our experiment p_{final} corresponds to the external pressure p_1*). The continuously flowing gas from the throttle provides freshly cooled gas for a longer period, making temperature changes easier to detect.

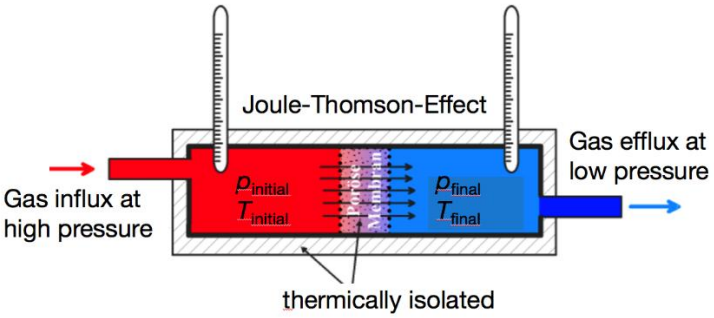

Figure 3.2: Adiabatic Joule-Thomson experiment. A continuously flowing gas stream generates a pressure drop across a throttle, causing the gas to expand against intermolecular forces. The stronger the attraction, the larger the detectable temperature decrease will be.

In the new experiment, the temperature changes were significant enough to detect even minor pressure differences. The Joule-Thomson coefficient is the temperature change per pressure unit:

$$\mu_{JT} = \left(\frac{\partial T}{\partial p}\right)_H \tag{3.4}$$

If multiplied by the heat capacity of the gas, μ_{JT} is related to the change of the Lennard-Jones potential induced by the change of the average distance $\langle r \rangle$ of the molecules with pressure.

3.2.3 Thermodynamic analysis of the Joule-Thomson effect

Since the Joule-Thomson experiment (Figure 3.4) is performed under adiabatic conditions (meaning that there is no heat flow from the system to the surroundings), we conclude from the first law of thermodynamics that $\Delta U = w$ (for the first law of thermodynamics, see also paragraph 5.2.1). Then we calculate the work, w, performed by the gas per unit time (Figure 3.3). For this, consider that before passing the throttle the gas will have the volume $V_{initial}$, the pressure $p_{initial}$, and the

temperature $T_{initial}$. We can imagine a piston on the left side pressing the entire volume of gas through the bottleneck. By this, the system will have to perform the work:

$$w_{initial} = -p_{initial} \cdot (0 - V_{initial}) \tag{3.5}$$

Behind the throttle, the same amount of gas will flow out, but now it will have the volume V_{final}, since it experiences the pressure p_{final} (since the final pressure is smaller, volume V_{final} will be larger). While proceeding, the gas will push away whatever is in its way and thus will do the work:

$$w_{final} = -p_{final} \cdot (V_{final} - 0) \tag{3.6}$$

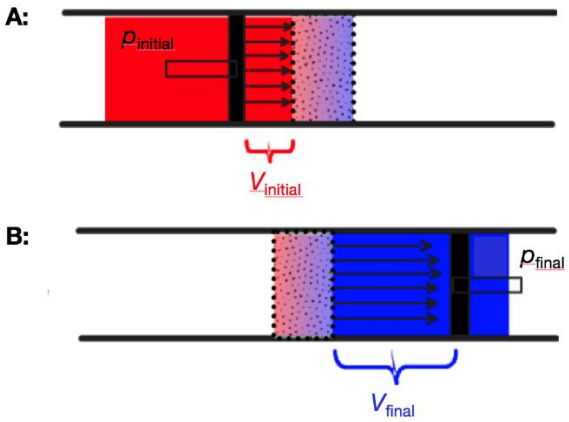

Figure 3.3: Closer look at the change in volume going from **A:** $V_{initial}$ to **B:** V_{final} during the Joule-Thomson experiment.

The total work w_{tot} is then given by

$$w_{tot} = w_{initial} + w_{final} = p_{initial} \cdot V_{initial} - p_{final} \cdot V_{final} \tag{3.7}$$

and should equal the change in internal energy

$$w_{tot} = \Delta U \tag{3.8}$$

Now we can calculate the change in enthalpy:

$$\begin{gathered} \Delta H = \Delta U + p_{final}V_{final} - p_{initial}V_{initial} = \\ = p_{initial} \cdot V_{initial} - p_{final} \cdot V_{final} + p_{final} \cdot V_{final} - p_{initial} \cdot V_{initial} = 0 \end{gathered} \tag{3.9}$$

Equation (3.9) shows that $\Delta H = 0$, i.e., enthalpy does not change during the process. Such a process is called an ***isenthalpic process***. Therefore, we can specify the Joule-Thomson coefficient more rigorously and end up with the equation (3.4). With the restriction of $\Delta H = 0$, the Joule-Thomson coefficient can now be derived theoretically. We insert $\left(\frac{\partial T}{\partial p}\right)_H$ as the first term in Euler's chain rule (or triple product rule)

$$\left(\frac{\partial x}{\partial y}\right)_z \cdot \left(\frac{\partial y}{\partial z}\right)_x \cdot \left(\frac{\partial z}{\partial x}\right)_y = -1 \tag{3.10}$$

Proceeding with the cyclic exchange of variables, we obtain

$$\left(\frac{\partial T}{\partial p}\right)_H \cdot \left(\frac{\partial p}{\partial H}\right)_T \cdot \left(\frac{\partial H}{\partial T}\right)_p = -1 \tag{3.11}$$

In equation (3.11) we can identify the molar heat capacity C_p at constant pressure

$$C_p = \left(\frac{\partial H}{\partial T}\right)_p \tag{3.12}$$

Using the previous equation, the expression for the Joule-Thomson coefficient becomes

$$\mu_{JT} = \left(\frac{\partial T}{\partial p}\right)_H = -\frac{1}{\left(\frac{\partial H}{\partial T}\right)_p \cdot \left(\frac{\partial p}{\partial H}\right)_T} = -\frac{\left(\frac{\partial H}{\partial p}\right)_T}{\left(\frac{\partial H}{\partial T}\right)_p} \Rightarrow \mu_{JT} = -\frac{1}{C_p} \cdot \left(\frac{\partial H}{\partial p}\right)_T \tag{3.13}$$

For ideal gases, we know that internal energy depends only on temperature, not on pressure or volume. In this case, enthalpy is also a function of the temperature only, thus, the term $\left(\frac{\partial H}{\partial p}\right)_T = 0$ results in $\mu_{JT} = 0$. This is different for real gases. In the following, it is shown that in this case, $\left(\frac{\partial H}{\partial p}\right)_T \neq 0$ and that this term reflects intermolecular interactions. For the derivation of $\left(\frac{\partial H}{\partial p}\right)_T$ equations (3.14) and (3.15) need to be introduced. The *Gibbs' fundamental equation of thermodynamics* expresses the total differential of the enthalpy as

$$dH = T \cdot dS + V \cdot dp \tag{3.14}$$

and mathematically represents a summary of the first and the second law of thermodynamics.

The *Maxwell equation*

$$\left(\frac{\partial S}{\partial p}\right)_T = -\left(\frac{\partial V}{\partial T}\right)_p \tag{3.15}$$

mathematically reflects the fact that the Gibbs' energy $G = H - TS$ is a conserved quantity. Formally dividing the equation (3.14) by dp gives

$$\left(\frac{\partial H}{\partial p}\right)_T = T \cdot \left(\frac{\partial S}{\partial p}\right)_T + V \tag{3.16}$$

and further insertion of the equation (3.15) provides

$$\left(\frac{\partial H}{\partial p}\right)_T = -T \cdot \left(\frac{\partial V}{\partial T}\right)_p + V \tag{3.17}$$

Finally, a combination of equations (3.17) and (3.13) provides

$$\mu_{JT} = \frac{1}{C_p} \cdot \left\{ T \cdot \left(\frac{\partial V}{\partial T}\right)_p - V \right\} \tag{3.18}$$

For an ideal gas, the thermal expansion coefficient α (in general $\equiv \frac{1}{V} \cdot \left(\frac{\partial V}{\partial T}\right)_p$) can be calculated easily by

$$\alpha_{ideal} = \frac{1}{V} \cdot \left(\frac{\partial V}{\partial T}\right)_p = \frac{p}{nRT} \cdot \left(\frac{\partial \left(\frac{nRT}{p}\right)}{\partial T} \right)_p = \frac{1}{T} \tag{3.19}$$

Using this relation, the equation (3.18) becomes

$$\mu_{JT} = \frac{V}{C_p} \cdot \{\alpha T - 1\} = \frac{V}{C_p} \cdot \left\{ \frac{\alpha}{\alpha_{ideal}} - 1 \right\} \tag{3.20}$$

The deviation of the thermal expansion in a real gas from the thermal expansion in an ideal gas results from intermolecular interactions. Attractive forces lead to smaller expansion, while repulsive forces enhance thermal expansion. Consequently, we find three different situations for the Joule-Thomson effect:

a) $\alpha = \alpha_{ideal} \Longrightarrow \mu_{JT}^{ideal\ gas} = 0$

b) $\alpha > \alpha_{ideal} \Longrightarrow \mu_{JT} > 0 \Longrightarrow dT < 0$, the gas cools down

c) $\alpha < \alpha_{ideal} = \frac{1}{T} \Longrightarrow \mu_{JT} < 0 \Longrightarrow dT > 0$, the gas warms up

Both α and α_{ideal} change with temperature, but differently. Thus, the Joule-Thomson coefficient is a function of temperature and may even change sign at the so-called *inversion temperature* T_{invers}, where $\mu_{JT}^{T_{invers}} = 0$. This is shown in Figure 3.4. Here, the temperature T is plotted as a function of pressure p at constant enthalpy H. The corresponding theoretical derivation is given in the paragraph 3.2.4 and appendix 3.5.4.

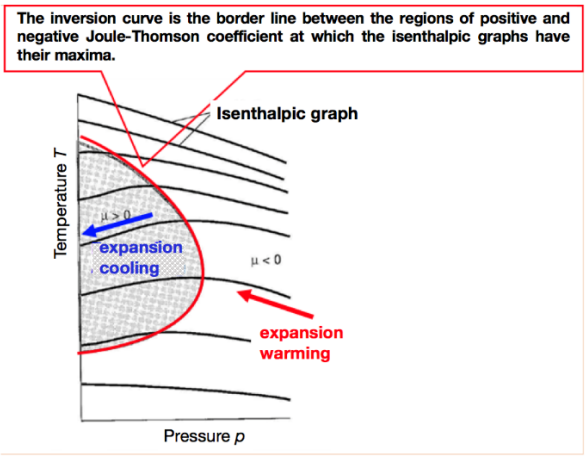

Figure 3.4: Isenthaplic processes in a $p-T$ diagram at constant enthalpy. μ_{JT} is the slope of the isenthalpic graph.

3.2.4 Derivation of the expansion coefficient and the Joule-Thomson coefficient

As already shown before, we need the expansion coefficient α of the real gas to calculate the Joule-Thomson coefficient μ_{JT}. We start by calculating $\frac{\partial V_m}{\partial T}$. Since solving the van der Waals equation of state for the volume is very cumbersome (cubic equation!), instead, we solve the equation for the pressure and write the derivative with time

$$p = \frac{RT}{V-b} - \frac{a}{V_m^2} \Big| \cdot \frac{\partial}{\partial T} \tag{3.21}$$

From this, we obtain a simpler equation with terms containing $\frac{\partial V_m}{\partial T}$, which is easier to solve

$$\begin{aligned} \frac{\partial p}{\partial T} = 0 = \frac{\partial}{\partial T}\left(\frac{RT}{V_m - b}\right) - \frac{\partial}{\partial T}\left(\frac{a}{V_m^2}\right) = \\ = \frac{R(V_m-b) - RT}{(V_m-b)^2} \cdot \frac{\partial V_m}{\partial T} - \frac{-2a}{V_m^3} \cdot \frac{\partial V_m}{\partial T} \end{aligned} \tag{3.22}$$

we order the terms

$$\frac{R}{(V_m-b)} = \left\{\frac{RT}{(V_m-b)^2} - \frac{2a}{V_m^3}\right\} \cdot \frac{\partial V_m}{\partial T} \tag{3.23}$$

and after introducing a common denominator for the term in $\left\{\frac{RT}{(V_m-b)^2} - \frac{2a}{V_m^3}\right\}$

$$\frac{RTV_m^3 - 2a(V_m-b)^2}{(V_m-b)^2 \cdot V_m^3} \tag{3.24}$$

we can solve for $\frac{\partial V_m}{\partial T}$

$$\frac{\partial V_m}{\partial T} = \frac{\frac{R}{(V_m-b)}}{\frac{RTV_m^3 - 2a(V_m-b)^2}{(V_m-b)^2 \cdot V_m^3}} = \frac{R(V_m-b)\cdot V_m^3}{RTV_m^3 - 2a(V_m-b)^2} \tag{3.25}$$

Cancelling $R \cdot V_m^3$ leads to

$$\frac{\partial V_m}{\partial T} = \frac{(V_m-b)}{T - \frac{2a}{RV_m} \cdot \left(\frac{V_m-b}{V_m}\right)^2} \tag{3.26}$$

Finally, we obtain the expansion coefficient

$$\alpha = \frac{1}{V_m} \cdot \frac{\partial V_m}{\partial T} = \frac{(V_m-b)}{V_m \cdot T - \frac{2a}{R} \cdot \left(\frac{V_m-b}{V_m}\right)^2} \tag{3.27}$$

or, by introduction into the equation (3.20), the Joule-Thomson coefficient

$$\mu_{JT} = \frac{V_m}{C_p}\left(\frac{(V_m - b)}{V_m - \frac{2a}{RT}\cdot\left(\frac{V_m - b}{V_m}\right)^2} - 1\right) \tag{3.28}$$

For further insights, see the appendix 3.5.4.

3.2.5 Calculation of the inversion curve using the van-der-Waals equation of state

The inversion curve can be directly calculated from the van der Waals equation without any further approximations. We get the sign change at $\mu_{JT} = 0$ at the inversion temperature. According to the equation (3.20), $\alpha = 1/T$ under these conditions, and we get

$$\alpha = \frac{(V_m - b)}{V_m \cdot T - \frac{2a}{R}\cdot\left(\frac{V_m - b}{V_m}\right)^2} = \frac{1}{T} \tag{3.29}$$

Now, the terms of T and V have to be ordered, and the expression is inserted in the van-der-Waals equation (see appendix 3.5.5). This reveals the following expression for the inversion curve

$$p_{inv} = \sqrt{\frac{8aRT_{invers}}{b^3}} - \frac{3}{2}\cdot\frac{RT_{invers}}{b} - \frac{a}{b^2} \tag{3.30}$$

***Important**:* here, we have the inversion curve given as pressure as a function of temperature (Figure 3.5). One could, in principle, solve for T, which would make things much more complicated. It is much easier to calculate $p(T)$ and plot it as a $p-T$-diagram. After that, one may change the axes by mirroring with respect to the diagonal. For a sketch, one may simply combine a rising $\sqrt{T}$-graph (horizontal parabola) and a linearly falling T-graph (straight line with negative slope). Of course, the inversion curve is only valid for positive values of p.

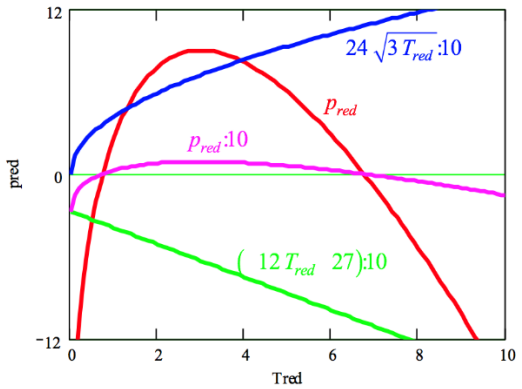

Figure 3.5: Inversion curve in reduced coordinates in a *p*-*T*-diagram.

3.3 Experimental details and evaluation

Your supervisor will provide the connection to two unknown gases, which should be identified by experimental determination of their Joule-Thomson coefficients μ. This can be determined experimentally by measuring the temperature T_{comp} of the gas in its compressed state at $p = p_{comp}$ and the temperature T_{exp} in its expanded state at $p = p_1$, where p_1 is the ambient pressure. Plotting $\Delta p = p_0 - p_1$ vs. $\Delta T = T_{comp} - T_{exp}$ should provide a straight line with a slope $m = \mu$. (Note that T_{comp} equals the ambient temperature, and it is named T_1 in the software used in this experiment)

For each gas, two series of measurements are performed. The first series of measurements starts at an overpressure of 0.8 bar and decreases to ambient pressure, with pressure steps of Δp = -0.2 bar. The second series is performed in the opposite direction, starting from ambient pressure and increasing to an overpressure of 0.8 bar, with pressure steps of

increment p = 0.2 bar. Thus, altogether there are four series of measurements to perform, each consisting of five individual measurements. The data are used to determine the Joule-Thomson coefficient graphically using equation (3.4).

Further, the Joule-Thomson coefficient should be determined theoretically using the equation (3.28) from the theory. The required van-der-Waals parameters are given in the appendix 3.5.3.

3.3.1 Experimental execution

The setup used to measure the Joule-Thomson coefficient is shown in Figure 3.6 and Figure 3.7 in all its parts. The glass tube **(1)** is equipped with a restrictor **(2)** and wrapped in transparent plastic for safety. At one end of the glass tube, there is an opening (3) where the gas under investigation flows in, and at the other end, there is an opening **(4)** where the gas flows out. The high-pressure part **(5)** of the glass tube is developed to withstand overpressures up to 1,0 bar. A copper capillary **(6)** is used to equilibrate the flowing gas at ambient temperature. Two temperature sensors **(7)** measure the temperature of the gas flowing through the glass tube. The temperature sensors are positioned near the restrictor, one in front and the other behind it. This allows measuring the temperature of the gas before ($T = T_{comp}$) and after ($T = T_{exp}$) it flows through the restrictor. After passing the second sensor, the temperature of the flowing gas will equilibrate to the surrounding temperature. The pressure sensor **(8)** is positioned next to the opening through which the gas flows. A needle valve **(9)** is used to regulate the pressure **(9)**.

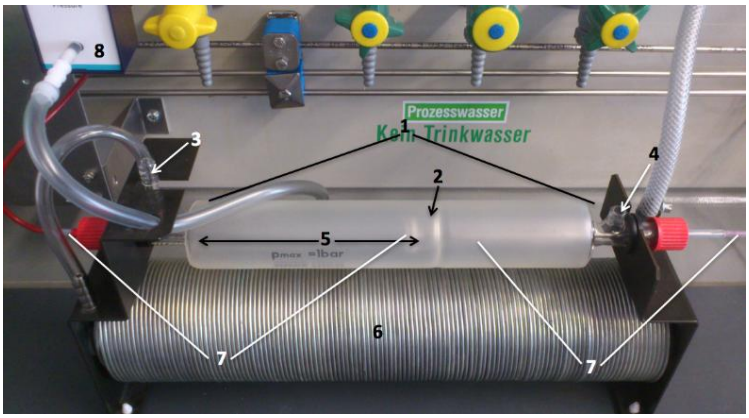

Figure 3.6: - Setup in all its parts used to determine the Joule-Thomson coefficient. (**1**) glass tube, **(2)** restrictor, **(3)** opening for gas influx, **(4)** opening for gas efflux, **(5)** high-pressure part, (6) copper capillary, (7) temperature sensors, and (**8**) pressure sensor.

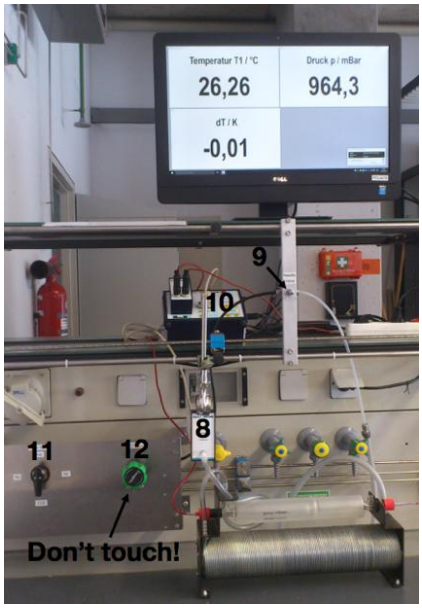

Figure 3.7: - Setup in all its parts used to determine the Joule-Thomson coefficient. (**8**) pressure sensor, **(9)** needle valve, **(10)** Cobra3 unit, **(11)** main valve, and **(12)** regulator.

During the measurement, the gas flows into the high-pressure part of the glass tube. Because of the restrictor, the pressure increases ($p = p_{comp}$). After flowing through the restrictor, the gas expands to the ambient pressure $p = p_1$ and as a result, it cools down from T_{comp} to T_{exp}. Remind that T_1 corresponds to the ambient temperature.

Turn on the Cobra3 Unit **(10)**, the computer, and open the "measure" software (see appendix 3.5.1 for basic instructions on using the software). Before you start the first experiment, the temperature of the setup and the gas must be equilibrated to the ambient temperature T_1. Monitor T_1 for about 10 minutes before the first experiment starts, to ensure it is constant. Furthermore, keep in mind to write down the value of the ambient pressure p_1. To allow the first gas under investigation to flow through the experimental setup, switch the main valve (11) to the appropriate position. Use the needle valve **(9)** to regulate the desired pressure (for the first experiment p equals an overpressure of 0.80 ± 0.01 bar). Wait four minutes before starting the data collection.

Important: The regulator **(12)** for the main gas line pressure must not be touched. It is adjusted to ensure the pressure in the glass cell does not exceed 1 bar, thereby preventing the glass cell from bursting.

During a running measurement, the software continuously collects the temperature difference $\Delta T = T_{comp} - T_{exp}$, the temperature T_1 and the pressure p in the high-pressure part of the glass tube (Figure 3.8).

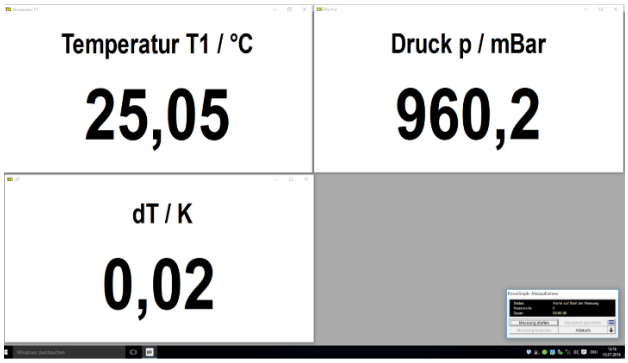

Figure 3.8: - Parameters collected and monitored by the software.

Important: the needle valve is a regulating valve, not a closing valve. Therefore, you need to close the main valve to stop gas flow completely. **Don't try to close the needle valve too tightly.**

Important: before starting the measurements for the second gas, flush the system with the new gas for 4 minutes, applying an overpressure of about 0.4 bar to completely purge the first gas.

More instructions to treat the collected data are reported in the appendix 3.5.2.

3.3.2 Data evaluation

- ☐ Determine the averages of the ambient temperature T_1, the pressure p and the temperature difference ΔT measured in the glass tube for each experiment. ***Important:*** During evaluation, compare the series of measurements from high to low pressure to the series from low to high pressure. If there are any deviations between the two corresponding values, calculate the average of the two.
- ☐ Determine the Joule-Thomson coefficients graphically according to the equation (3.4).
- ☐ Determine the Joule-Thomson coefficients theoretically according to the equation (3.28) and compare the results to the experimental results. Use the data to identify the gases.
- ☐ Calculate (equation (3.30)) and draw the complete inversion curve of CO_2 using the corresponding van-der-Waals coefficients and the heat capacity C_p provided in Table 3.5-1.
- ☐ Perform an error analysis for all calculations.

3.4 Applications of the experiment and its theory

- ☑ Hampson-Linde cycle (liquefaction of air).
- ☑ Due to the decrease in pressure by transferring gas from soil to pipelines, the gas cools down, and the surrounding area of the pipelines runs the risk of freezing [3.5].
- ☑ Leakage of high-pressure gas from a pipeline [3.6].
- ☑ Risk of freezing of diving regulators.
- ☑ Separation of gaseous mixtures by gas permeation, e.g., enrichment of oxygen from air and separation of methane from biogas [3.7].
- ☑ Generation of molecular beams for spectroscopy (Knudsen beam, supersonic beam).
- ☑ Mode of operation of refrigerators and heat pumps.

3.5 Appendixes

3.5.1 Basic instructions to use the software

- ☐ Turn on the Cobra3 Unit.
- ☐ Turn on the computer.
- ☐ Log in to your account using your LRZ-username.
- ☐ Open the Phywe "***measure***" software that you can find at the path C:\Program Files (x86)\PHYWE\measure\measure.exe.
- ☐ Start the measurement by clicking on the red button in the upper left corner (Figure 3.9).

Figure 3.9: Starting the interface in the Phywe "measure" software.

- ☐ Click on "Weiter" in the appearing window (Figure 3.10).

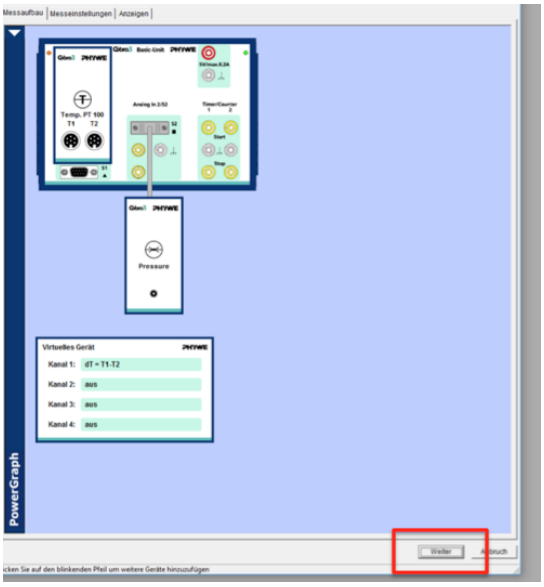

Figure 3.10: Starting the interface in the Phywe "measure" software.

- ☐ Write down the value of the ambient pressure.
- ☐ Switch the main valve to the position of the first gas under investigation.
- ☐ Use the needle valve to set the gas pressure to an overpressure of 0.80 ± 0.01 bar.
- ☐ Wait four minutes before you start the experiment.
- ☐ Start the experiment by clicking on "*Messung starten*" (Figure 3.11)

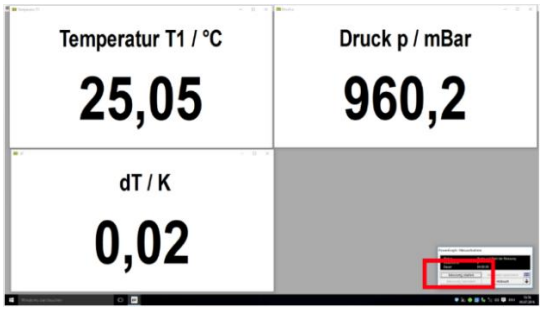

Figure 3.11: Starting an experiment.

- ☐ The measurement takes 20 seconds and stops automatically.

3.5.2 *Instruction for data treatment*

- ☐ After completing one series of measurements, the data are processed before the next series begins.
- ☐ Use the computer software to calculate the averages of the ambient temperature, the pressure, and the temperature difference ΔT measured in the glass tube. This is done individually for each measurement in the series. To choose a single experiment, click on the corresponding measuring window. Choose the desired parameter (T_1, p, ΔT) in the upper taskbar (Figure 3.12) by double clicking. The parameter needs to appear as the y-axis label.

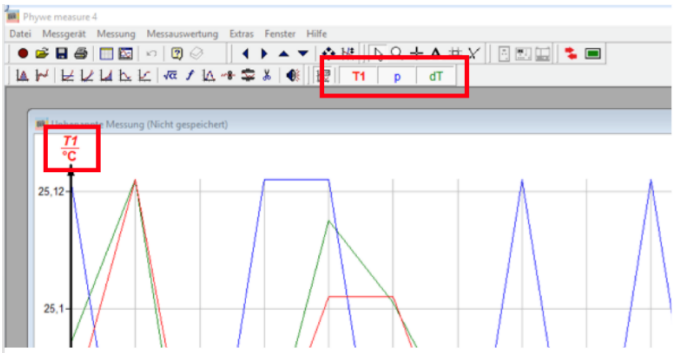

Figure 3.12: Data evaluation.

- ☐ To calculate the average values, click on "Messauswertung" → "Mittelwert bilden" (Figure 3.13).

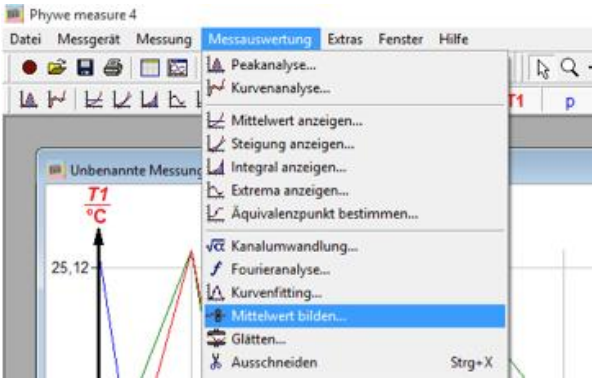

Figure 3.13: Data evaluation.

☐ Click on “Berechne” (Figure 3.14) to obtain the average value of the chosen parameter.

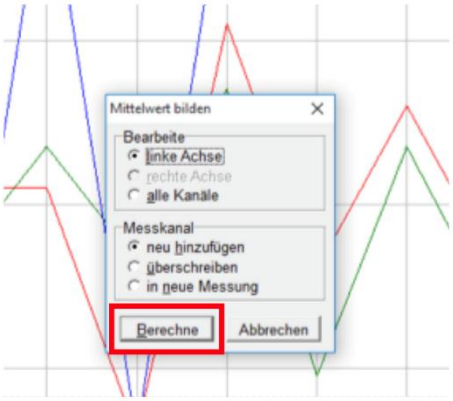

Figure 3.14: Data evaluation

☐ Export of the processed data to Excel: For this, click on “Messung” in the “measure” software → “Messwerte exportieren” (Figure 3.15).

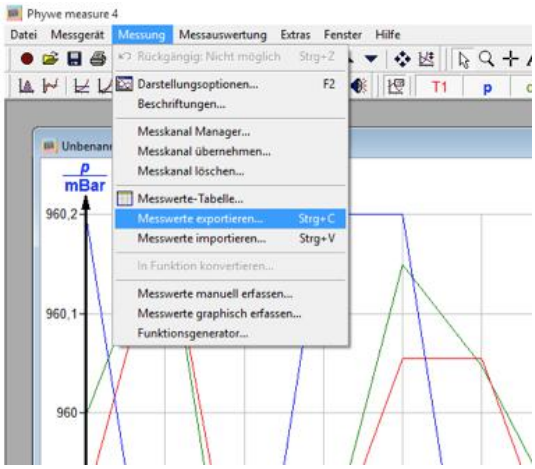

Figure 3.15: Data export.

☐ “In Zwischenablage kopieren” (Figure 3.16). Then open Excel and paste the values.

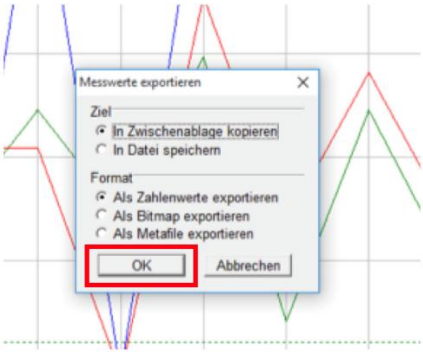

Figure 3.16: Data export.

☐ Go back to the “measure” software and close the measuring window corresponding to the data you have just analyzed.

☐ Repeat the procedure for all measurements within the measuring series.

3.5.3 Van-der-Waals parameters

Table 3.5-1: Van-der-Waals coefficients *a* and *b* and heat capacity C_p for different gases.

	a ($l^2 \cdot bar/mol^2$)	*b* (*l*/*mol*)	C_p ($J/(K \cdot mol)$)
CO_2	3.592	0.04267	37.14
He	0.03457	0.0237	20.79
N_2	1.39	0.03913	29.14

3.5.4 Further implementations in the derivation of the Joule-Thomson coefficient for real gases

$$\frac{\alpha}{\alpha_{ideal}} = \frac{(V_m - b)}{V_m - \frac{2a}{RT} \cdot \left(\frac{V_m - b}{V_m}\right)^2} = \frac{(V_m - b)}{(V_m - b) + b - \frac{2a}{RT} \cdot \left(\frac{V_m - b}{V_m}\right)^2} \Rightarrow \frac{\alpha}{\alpha_{ideal}} < 1 \quad \text{if } b > \frac{2a}{RT} \cdot \left(\frac{V_m - b}{V_m}\right)^2 \tag{3.31}$$

Insertion into van-der-Waals equation:

$$b \cdot \left(\frac{V_m}{V_m - b}\right)^2 = b \cdot \left(1 + \frac{b}{V_m - b}\right)^2 = b \cdot \left(1 + b \cdot \frac{p + \frac{an^2}{V^2}}{nRT}\right)^2 > \frac{2a}{RT} \tag{3.32}$$

This can be summarized as follows

$$\left.\begin{array}{l} \mu_{JT} < 0 \Rightarrow heating \\ \mu_{JT} > 0 \Rightarrow cooling \end{array}\right\} \Leftrightarrow \frac{\alpha}{\alpha_{ideal}} \text{ is } \begin{cases} < 1 \; for \; b \cdot \left(\frac{V_m}{V_m - b}\right)^2 > \frac{2a}{RT} \; repulsion \; is \; dominant \\ > 1 \; for \; b \cdot \left(\frac{V_m}{V_m - b}\right)^2 < \frac{2a}{RT} \; attraction \; is \; dominant \end{cases}$$

Again, we have difficulties with inserting V_m from the van-der-Waals equation. To avoid higher powers of V_m we can exploit a virial expansion instead and drop higher powers of V_m. Thus, we could reconstruct the isenthalpic curves in a $T - p$ diagram.

In equation (3.31), the term $b - \frac{2a}{RT} \cdot \left(\frac{V_m - b}{V_m}\right)^2$ is the only one that may change its sign. Furthermore, we can see from equation (3.32):

a) $\left(\frac{V_m}{V_m - b}\right)$ is always larger than 1. The larger b (repulsion), the larger the term $b \cdot \left(\frac{V_m}{V_m - b}\right)^2$ will be, the more negative μ_{JT} is $\Rightarrow$ repulsion dominates, leading to heating!

b) The larger a is compared to RT, the larger the term $\frac{2a}{RT}$ will be, the more positive μ_{JT} is $\Rightarrow$ attraction dominates, leading to cooling!

The exact position of the sign change of μ_{JT} can be delineated with the inversion line.

3.5.5 Further implementations in the derivation of the inversion temperature for real gases

Ordering the terms of the equation (3.29) and insertion into the van-der-Waals equation

$$V_m - b = V_m - \frac{2a}{RT}\cdot\underbrace{\left(\frac{V_m - b}{V_m}\right)^2}_{\left(1-\frac{b}{V_m}\right)^2} \Rightarrow \left(1-\frac{b}{V_m}\right)^2 = \frac{bRT}{2a} \Rightarrow \frac{1}{V_m} = \frac{1}{b} \pm \sqrt{\frac{RT}{2ab}} \tag{3.33}$$

$$p = \frac{1}{V_m}\cdot\frac{RT}{1-b\frac{1}{V_m}} - a\cdot\frac{1}{V_m^2} = \left(\frac{1}{b} - \sqrt{\frac{RT}{2ab}}\right)\cdot\frac{RT}{\underbrace{1-b\left(\frac{1}{b}-\sqrt{\frac{RT}{2ab}}\right)}_{+\sqrt{\frac{2aRT}{b}}}} - a\cdot\left(\frac{1}{b}-\sqrt{\frac{RT}{2ab}}\right)^2 \tag{3.34}$$

$$= \left(\frac{1}{b}-\sqrt{\frac{RT}{2ab}}\right)\cdot\sqrt{\frac{2aRT}{b}} \qquad -a\cdot\left(\frac{1}{b^2}-\frac{2}{b}\cdot\sqrt{\frac{RT}{2ab}}+\frac{RT}{2ab}\right)^2$$

$$p = \sqrt{\frac{2aRT}{b^3}} - \frac{RT}{b} - \frac{a}{b^2} + \sqrt{\frac{2aRT}{b^3}} - \frac{RT}{2b} \tag{3.35}$$

3.5.6 *Virial coefficient*

The Joule-Thomson coefficient is closely related to the *second viral coefficient* (B in the equation (3.36) and B_V in the equation (3.37):

$$Z = 1 + B\cdot p + C\cdot p^2 + \cdots \tag{3.36}$$

$$Z = 1 + \frac{B_V}{V} + \frac{C_V}{V^2} + \cdots \tag{3.37}$$

Digression: The second virial coefficient is a handy quantity, since it is directly related to the Lennard-Jones pair interaction potential $E_{JT}(r)$. Since in a gas the distances between particles are statistically distributed, one has to integrate any pair interaction potential $U(r)$ over all possible distances between the particles. This relation is quantified by cluster integrals derived in statistical mechanics. It turns out that (because of the integration) it is difficult to derive the exact form of $U(r) = E_{JT}(r)$.

3.6 Literature

3.1 - P.W. Atkins, Physical Chemistry, 6th ed., Oxford University Press, Oxford (1998), pp. 45-90.

3.2 - P.W. Atkins and J. de Paula, Atkins' Physical Chemistry, 8th ed., Oxford University Press, Oxford (2006), pp. 28-67.

3.3 - G. Wedler, *Lehrbuch der Physikalischen Chemie*, 6th ed., Wiley/VCH (2012).

3.4 - R. Brdicka, *Grundlagen der Physikalischen Chemie,* 15th ed., Wiley/VCH (1981).

3.5 - K.C. Cheng and J.-W. Ou, Joule-Thomson Effects on Turbulent Graetz Problems for Gas Flow in Pipes with uniform wall temperature, *The Canadian Journal of Chemical Engineering*, **56** (1978) 31-36.

3.6 - R. Tu, Q. Xie, J. Yi, K. Li, X. Zhou, and X. Jiang, An Experimental Study on the Leakage Process of High-Pressure CO_2 from a Pipeline Transport System*, Greenhouse Gases: Science and Technology*, **4** (2014) 777-784.

3.7 - R. Rautenbach and W. Dahm, Oxygen and Methane enrichment – a Comparison of Module Arrangements in Gas Permeation*, Chemical Engineering & Technology*, **10** (1987) 256-261.

4 Combustion Enthalpy via Bomb Calorimetry

4.1 Context and aim of the experiment

In this experiment, the internal energy released by the combustion of an organic compound is measured using bomb calorimetry. From the measured internal energy of the reaction at constant volume, the reaction enthalpy of the combustion of the compound can be determined [4.1 - 4.3].

4.1.1 Important concepts to know

First law of thermodynamics, work, heat, internal energy, state function, intensive and extensive properties, reaction enthalpy, exothermic and endothermic reaction, exergonic and endergonic reaction, calorimetry, combustion enthalpy, adiabatic system, heat capacity at constant volume, heat capacity at constant pressure.

4.1.2 Most common questions to be answered

- Why is the heat capacity at constant pressure C_p always larger than that at constant volume C_V?
- Consider a certain amount of heat being released during the combustion of a sample in a calorimeter. Would the induced ΔT be higher if the measurement were performed at constant volume or at constant pressure? Why?
- What is the statement of the first law of thermodynamics?
- What is the definition of enthalpy?
- What are the definitions of exergonic, endergonic, exothermic, and endothermic reactions?
- What are the prerequisites for a combustion reaction to occur?

4.1.3 Further preparations before the experiment

Before performing the experiment, prepare a worksheet for all five measurements as follows:

Table 4.1-1: Example of the table to prepare for data collection and evaluation.

sample	ΔT *[K]*	$\Delta T_{average}$ *[K]*	$-\frac{m_{cal} \cdot \Delta_r H_{cal}}{M_{cal} \cdot \Delta T_{cal,average}}$ *[J/K]*	$C_{cal} \cdot \Delta T_{average}$ *[J]*
benzoic acid m_{cal}=				
sucrose $m_{sucrose}$=				

4.2 Theory

The energy of a chemical reaction can be partly absorbed or released as heat and partly utilized or expended as work. Calorimetry is the most established method for studying heat transfer during chemical and physical reactions.

4.2.1 Heat transactions, internal energy, and reaction enthalpy

In thermodynamics, the total energy of a system is called its *internal energy* U. The internal energy is the sum of the kinetic and the potential energy of all molecules in the system. It is a *state function* because it is path-independent. This means its value depends only on the current state of the system, not on how it was reached. Variables like pressure p, temperature T, volume V and the amount of substance n characterize the thermodynamic state itself. Changing one of these state variables changes the internal energy. The internal energy is also an extensive property, meaning it is additive across subsystems. Take care to be familiar with the terms *"intensive" and "extensive" property*. According to the first law of thermodynamics, the change in internal energy dU of a system is generally given by the amount of energy δq absorbed or released by the system in the form of heat and the work δw done on or by the system

$$dU = \delta q + \delta w \tag{4.1}$$

Work and heat are not state functions and therefore their prefix in the equation (4.1) is "δ" instead of "d" to express infinitesimal changes. A measurable change in internal energy during the reaction of a system (*internal reaction energy*) is thus given by

$$\Delta_r U = q + w \tag{4.2}$$

In equation (4.1), the work can be further separated into expansion work δw_{exp} and work exceeding the expansion work δw_e. The latter could be the electrical work of driving a current through a circuit.

$$dU = \delta q + \delta w_{exp} + \delta w_e \tag{4.3}$$

If the system is kept at constant volume, it cannot do expansion work, thus $\delta w_{exp} = 0$. If the system is further incapable of doing any other kind of work, then $\delta w_e = 0$ too, and equation (4.3) becomes

$$dU_V = \delta q_V \tag{4.4}$$

The subscript in dU_V and δq_V implies a change at constant volume. If the system passes from state A to state B and during this exchanges heat with the surroundings, the measurable change in internal reaction energy is given by

$$\Delta_r U_V = q_V \tag{4.5}$$

Equation (4.5) indicates that, when a change of state happens in a system at constant volume, by measuring the energy supplied to it ($q_V > 0$, endothermic reaction) or obtained from it as heat ($q_V < 0$, exothermic reaction), we are actually measuring the change in its internal energy. Comparison of equation (4.5) to the definition of enthalpy

$$\mathrm{d}H = dU + p \cdot dV + V \cdot dp \tag{4.6}$$

and assuming that both volume and pressure of the system are constant (e.g., the involved components are either liquid or solid), then $\Delta_r V$ and $\Delta_r p$ thus $p \cdot \Delta_r V$ and $V \cdot \Delta_r p$ can be neglected, and the reaction enthalpy equals the internal reaction energy

$$\Delta_r H_{V,p} = \Delta_r U_{V,p} \tag{4.7}$$

Thus, we can conclude that, measuring q_V released or absorbed as heat during a reaction at constant volume directly reveals the corresponding reaction enthalpy $\Delta_r H_{V,p}$.

4.2.2 Combustion reactions

Generally, the prerequisites for a combustion reaction to occur are *i)* the presence of an adequate amount of an inflammable compound that must be *ii)* in contact with an oxidant (generally oxygen) and *iii)* a high enough ignition temperature in the surroundings of the inflammable compound. The latter point is necessary to overcome the activation energy of the combustion reaction and thus initiate the reaction (ignition). As soon as part of the compound burns, the heat released thereby provides the activation energy for further combustion. For the definition and meaning of the activation energy, see the chapter 8.

Combustion reactions are usually exothermic, i.e., they release energy as heat. For those kinds of reactions, the standard reaction enthalpy $\Delta_r H^0 < 0$. Take care that you are familiar with the difference between exothermic/endothermic and exergonic/endergonic reactions and with the meaning of the superscript "0". The enthalpy of combustion of a specific compound corresponds to its heating value (HV), also called calorific value (CV). During combustion, water is produced either as liquid or vapor. If water is produced as a liquid, the amount of heat released is maximum, since no heat is lost to vaporize the water, providing the so-called higher heating value (HHV or higher calorific value, HCV). If water is produced as vapor, the amount of heat released is lower, since some heat is lost as the enthalpy of vaporization of water, providing the so-called lower heating value (LHV or lower calorific value, LCV).

4.2.3 *Bomb calorimetry*

Bomb calorimetry is the most established method to determine the combustion enthalpy at constant volume of hydrocarbons. A schematic representation of a bomb calorimeter is shown in Figure 4.1.

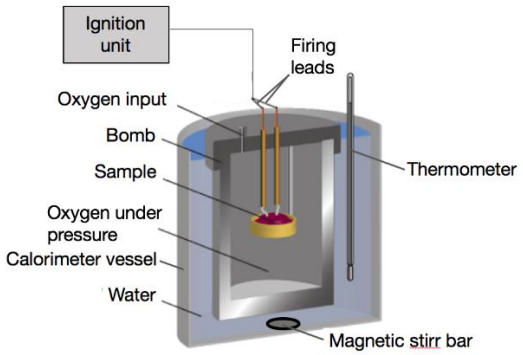

Figure 4.1: Schematic representation of the design of a bomb calorimeter (adapted from [4.4]).

The calorimeter consists of a calorimetric bomb in which the combustion reaction occurs. The calorimetric bomb is designed to withstand heat and pressure and acts as a closed system. It is immersed in a stirred Dewar (also called a calorimeter vessel) filled with a known volume of water. The water in the Dewar prevents heat flow from the calorimeter to its surroundings. Thus, the combustion reaction occurs under *adiabatic conditions*. Further, an ignition unit is used to initiate combustion of the sample by applying a short electric spark. This is necessary to overcome the activation energy of the combustion reaction (see chapter 8). The calorimetric bomb is usually made of stainless steel, and therefore, the combustion reaction occurs at *constant volume*. Often, a small amount of water is present in the calorimeter bomb to ensure the water vapor is saturated. The advantage is that the heat of vaporization of water does not need to be accounted for in subsequent data analysis.

During the measurement, a known amount of sample is ignited and burned to completion in an oxygen-rich environment, ensuring rapid, complete combustion. Since the combustion reaction takes place at constant volume and the pressure increase due to gaseous products is assumed to be negligible, equations (4.5) and (4.7) are valid. It would be possible to estimate, at first approximation, the change in pressure upon combustion by calculating the moles of gas produced and using the ideal gas equation. The heat of combustion released is absorbed by the water in the calorimetric vessel and results in a measurable temperature increase $\Delta T = T_{final} - T_{initial}$. To convert ΔT to a reaction heat, the heat capacity of the calorimeter has to be known (for the definition and meaning of the heat capacity and for the discrimination of the heat capacity at either constant volume or constant pressure, see references [4.1, 4.2]). This can be determined by burning a fixed mass of a calibration sample (often benzoic acid, see equation (4.8)) for which the combustion heat is precisely known.

$$2\ C_6H_5COOH(s) + 15O_2(g) \rightarrow 14CO_2(g) + 6H_2O(l) \tag{4.8}$$

Alternatively, the calibration can be done by measuring ΔT upon applying a known amount of heat by passing a current from a source of known potential through a heater for a known period of time. Using the strategy of burning a calibration sample, the heat capacity of the calorimeter C_{cal} can be determined via the equations

$$Q = -\frac{m_{cal} \cdot \Delta_r H_{V,p,cal}}{M_{cal}} \tag{4.9}$$

$$C_{cal} = \frac{Q}{\Delta T_{cal}} \tag{4.10}$$

where $\Delta_r H_{V,p,cal}$ denotes the molar combustion enthalpy of the calibration sample (-3228 ± 4 kJ/mol for benzoic acid [4.5]). m_{cal} is the amount of the used calibration substance and is given by the mass of the burned pellet minus the mass of the igniter wire. M_{cal} is the molecular mass of the calibration substance. ΔT_{cal} is the measured temperature change during the combustion of the calibration substance.

Since the enthalpy is a state function, according to Hess's law [4.1], any standard enthalpy of reaction $\Delta_r H^0$ can be calculated from the standard enthalpy of formation $\Delta_f H^0$ of each reactant and product, multiplied by their stoichiometric coefficient in the reaction, according to the equation

$$\Delta_r H^0 = \sum_{Products,\ j} \nu_j \cdot \Delta_f H_j^0 - \sum_{Reactants,\ i} \nu_i \cdot \Delta_f H_i^0 \tag{4.11}$$

4.3 Experimental details and evaluation

In this experiment, the combustion of sucrose is investigated using bomb calorimetry. The corresponding stoichiometric reaction is

$$C_{12}H_{22}O_{11}(s) + 12O_2(g) \rightarrow 12CO_2(g) + 11H_2O(l) \tag{4.12}$$

The recorded data are used to calculate the heat capacity of the calorimeter C_{cal}, the internal reaction energy $\Delta_r U_{V,p}$ and from this, the reaction enthalpy $\Delta_r H_{V,p}$ for reaction (4.12).

4.3.1 *Experimental execution*

The setup used to determine the heat transfer during combustion is shown from Figure 4.2 to Figure 4.5.

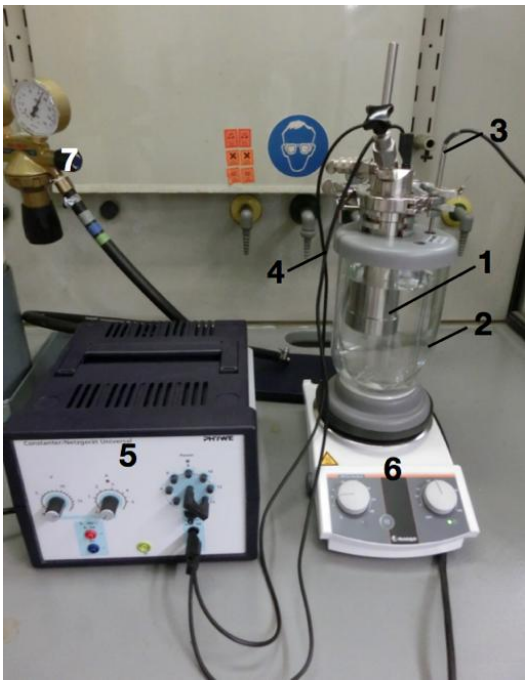

Figure 4.2: Calorimetric setup used for the determination of heat transfer during a chemical reaction; **(1)** calorimetric bomb, **(2)** calorimeter vessel, **(3)** temperature sensor, **(4)** black connector cords/firing leads, **(5)** power supply of the ignition unit, **(6)** magnetic stirrer, and **(7)** outlet valve.

The calorimetric bomb (**1**) is immersed in the calorimeter vessel (**2**), also called a dewar. Further, a temperature sensor (**3**) is immersed in the calorimeter vessel. The temperature sensor is connected to the digital temperature meter and measures the water temperature in the calorimeter vessel. The black connector cords (**4**) connect the power supply (**5**) of the ignition unit to the calorimetric bomb (for details, see Figure 4.3).

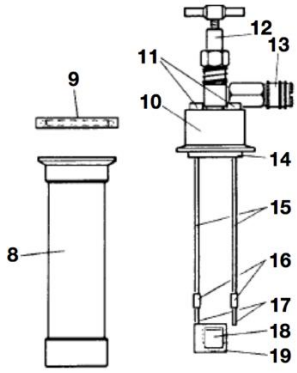

Figure 4.3: Individual parts of the calorimeter bomb: (**8**) pressure vessel, (**9**) O-ring-seal, (**10**) lid, (**11**) 4 mm connection socket, (**12**) control valve of the bomb, (**13**) quick-lock-coupling, (**14**) ceramic-disc, (**15**) nickel-electrode, (**16**) ferrule, (**17**) contacts for the nickel electrode, (**18**) quartz sample vessel and (**19**) sample vessel bracket.

The water in the calorimeter must be stirred before, during, and after the measurement using a magnetic stirrer (6) to ensure homogeneous temperature. A detailed view of the calorimetric bomb and its coupling parts is shown in Figure 4.3 and Figure 4.4, respectively. Figure 4.5 shows the details of the pressure reducer of the oxygen pressure cylinder.

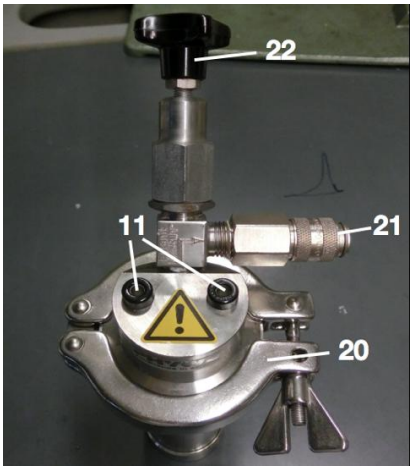

Figure 4.4: Coupling parts of the calorimeter bomb. **(11)** 4mm connection socket, **(20)** clamping ring, **(21)** quick connector, and **(22)** control valve of the calorimetric bomb.

Figure 4.5: Pressure reducer on the oxygen cylinder. **(7)** outlet valve, **(23)** work manometer, **(24)** main valve of the oxygen bottle, and the venting connection **(25)**.

Fill the calorimeter vessel (**2**) with 850 ± 1 g of deionized water using the technical balance available in the lab. Carefully place the magnetic stirring bar in the calorimeter vessel and switch on the magnetic stirrer (**6**).

The investigated substances, sucrose and benzoic acid, are available as powders. To ensure rapid combustion during the reaction, the surface area of the substances must be large. To achieve this, only benzoic acid must be ground in a mortar. Weigh about 450 mg of substance in a weighing dish. After this, cut a piece about 10 cm long from the iron wire and weigh it. An iron wire will be necessary to ignite the substance. Form the iron wire in such a manner that a small coil is formed in the middle to provide a good grip on the pellet later.

Use the pellet-pressing die, place it in a vertical position, and insert the small steel rod in the cylinder to close the bottom end of the borehole. Carefully insert the coil of the iron wire into the borehole, such that the ends of the wire are positioned in the guiding grooves of the pellet press. Insert the large rod from above and press briefly on the coil of the iron wire. Fill the hole with the weighted substance using a funnel. Again, insert the large rod from above and compress the substance a little. Now fit the assembled pellet-pressing die into the vice and carefully apply pressure so that a solid pellet forms from the substance. Take care not to shear off the ends of the ignition wire during preparation of the pellet. To get the pellet out of the press, hold the pellet press over a plastic pan and turn it upside down. Grasp the long steel rod in the closed hole and use a rubber mallet to help you remove the pellet. Weigh the pellet with an accuracy of 1 mg using the analytical balance. **It is essential to apply the right pressure during pellet preparation. If the pellet is too compact, then combustion is hindered. On the other hand, the pellet will fall apart if the applied pressure is too small.**

Now, the pellet can be introduced into the calorimetric bomb. To do this, carefully place the pellet in the quartz sample vessel (**18**) using a spatula. Take care that the coil of the iron wire is positioned near the vessel head, because the pellet should be located above the center of the sample vessel, so that it can burn there after the ignition wire has burned out. This is important for the proper combustion of the substance. The sample vessel can now be fixed in the sample vessel bracket (**19**). Subsequently, fix the lid and the corresponding components (**11**-**13**) to a stand using a clamp, and fix the sample vessel bracket (**19**) by introducing the ends of the iron wire in the contacts for the nickel electrode (**17**) using tweezers. The iron wire ends need to be wrapped around the nickel electrodes (**15**); then push the ferrules (**16**) downwards to secure the iron wire. Finally, the nickel electrode and the sample vessel bracket, including the sample, are introduced into the pressure vessel. Ensure that the O-ring seal (**9**) is dust-free and that the lid (**10**) is correctly placed. The calorimetric bomb is closed using the clamping ring (**20**). Subsequently, the prepared calorimetric bomb is immersed as deeply as possible in the water-filled calorimetric vessel and clamped to the stand. Ensure that the quick connector (**21**) of the calorimeter bomb and the clamping ring (**20**) are pointing in the same direction, so that there is sufficient space for the temperature sensor (**3**) to be introduced. Fix the temperature sensor so its tip is at about the same height as the sample in the bomb.

Before filling the calorimetric bomb with oxygen, ensure the outlet valve (**7**) is fully closed. Introduce the pressure hose in the quick connector (**21**) of the calorimetric bomb. Ensure that the venting connection (**25**) is closed, then open the main valve (**24**) of the oxygen bottle and check that the pressure at the workmanometer (**23**) is adjusted to 9 bar. Open the outlet valve (**7**) while keeping the control valve (**22**) of the calorimetric bomb closed. Once the pressure remains constant, open the control valve (**22**) of the calorimetric bomb carefully to allow oxygen to flow into the bomb. Once the calorimetric bomb is filled with oxygen, close its control valve (**22**), the main valve (**24**), and the outlet valve (**7**) of the oxygen bottle, and slowly and carefully open the venting connection (**25**). **Be sure that the power supply is turned off**, introduce the black connector cords (**4**) of the power supply (**5**) in the connection socket (**11**) of the lid and adjust the voltage of the power supply to 15 V. The power supply needs to be employed manually to initiate the combustion; this is done just turning on the main switch on the backside of the power supply.

The measurements are carried out using the Cobra 4 software (called “Measure”). For basic instructions on how to use the software and how to handle the power supply to initiate the combustion, see Chapter 12.

Important: After every experiment, **release excess oxygen** and the gases evolved during the reaction **before opening the calorimetric bomb**. To do this, open the venting connection (**25**), then slowly and carefully open the control valve (**22**) of the calorimetric bomb. **The supervisor must be present when the students execute this procedure for the first time.** The calorimetric bomb may only be opened and disassembled after all gases have been purged. To purge the pressure hose before the next measurement, open the outlet valve (7) slightly for a few seconds after closing the venting connection (**25**).

The nickel electrode needs to be cleaned after each experiment using a paper towel to remove residues from the iron wire and carbon black.

The first measurements deal with the determination of the heat capacity C_{cal} of the calorimeter by analyzing the combustion of benzoic acid. The experiment on the combustion of benzoic acid must be performed three times, and the average of the determined single ΔT values is used for the calculation of C_{cal}. In subsequent measurements, the heat released during the combustion of sucrose is determined. This experiment must be performed three times as well, and the average of the determined ΔT values is, together with C_{cal}, used to determine the enthalpy of the combustion of sucrose.

4.3.2 *Data evaluation*

☐ Select the regression mode of the software by clicking on the corresponding button in the toolbar above the opened temperature-time diagram (Figure 4.6).

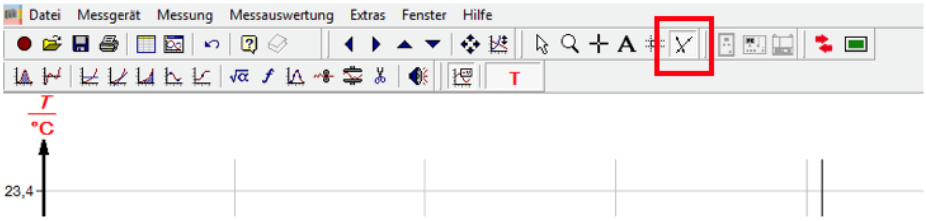

Figure 4.6: Selecting the regression mode in the software.

☐ Determine ΔT from the temperature-time diagram. For this, define two regression lines matching the data points before and after the transition, respectively (Figure 4.7). Draw an auxiliary line parallel to the ordinates in a way that F1 = F2. The endpoints of the line AB need to be prolonged parallel to the x-axis to reveal ΔT (Figure 4.7).

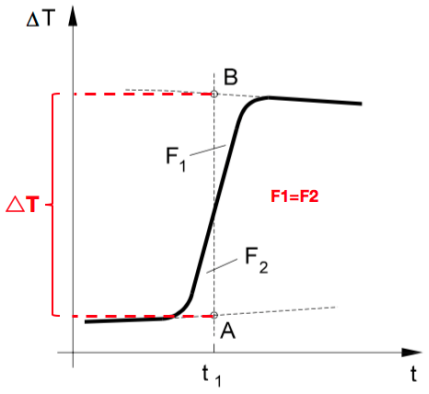

Figure 4.7: Graphical determination of ΔT. F1 and F2 are the areas defined by the data points in the transition, the auxiliary line AB, and the two regression lines. Original picture adapted from reference [4.9].

☐ To see the defined ΔT click on “Messauswertung” → “Kalorimetrie” → “Ergebnisse einzeichnen” (Figure 4.8).

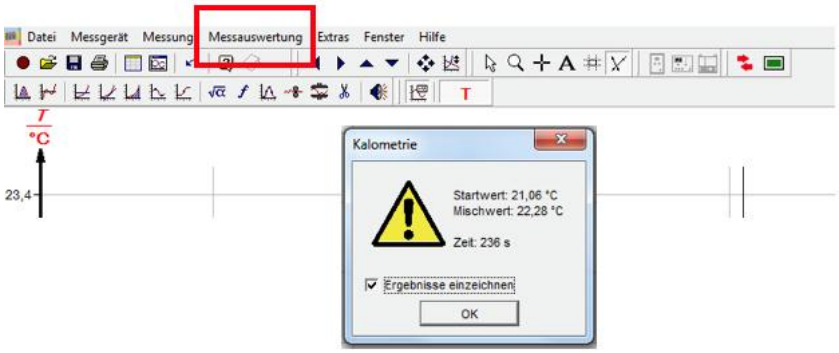

Figure 4.8: Getting the graphically defined ΔT.

- ☐ Determine the heat capacity C_{cal} of the calorimeter, applying equations (4.7) and (4.10) to the data collected on the combustion reaction of benzoic acid. Check if the mass of the iron wire can be neglected in these calculations.
- ☐ Determine the molar combustion enthalpy of sucrose using the experimentally determined C_{cal} and compare it with the literature value.
- ☐ Calculate for all the combustion reactions considered their standard combustion enthalpy from the standard enthalpies of formation of reactants and products available from [4.10].
- ☐ Perform an error analysis for all calculations.

4.4 Applications of the experiment and its theory

- ☑ Combustion enthalpies determined by calorimetric measurements are used to indirectly determine the enthalpy of formation of inorganic and organic chemical compounds (Hess's law). This is important for the thermodynamic investigation of flammable substances. Furthermore, combustion enthalpies are used to calculate standard reaction energies and enthalpies of any chemical reaction [4.6].
- ☑ Combustion reactions are very important reactions that provide energy, e.g., the combustion of alkanes in power stations, heating installations, and combustion engines. Their higher heating value is the maximum energy that they could provide.
- ☑ Determination of calorific values of fuel oils, motor fuels, flammable waste (waste combustion and recycling industry), explosive agents, building materials (chalk and cement industry), etc. [4.7].
- ☑ Determination of calorific values of foods is the method by which food calories are measured. [4.8].

4.5 Literature

4.1 - P.W. Atkins, Physical Chemistry, 6th ed., Oxford University Press, Oxford (1998), pp. 45-84.

4.2 - P.W. Atkins and J. de Paula, Atkins' Physical Chemistry, 8th ed., Oxford University Press, Oxford (2006), pp. 28-60.

4.3 - G. Wedler, *Lehrbuch der Physikalischen Chemie*, 6th ed., Wiley/VCH (2012).

4.4 - P.W. Atkins & J.de Paula, Atkins' Physical Chemistry, 10th ed., Oxford University Press, Oxford (2014), p. 72.

4.5 - http://webbook.nist.gov/cgi/cbook.cgi?ID=C65850&Mask=2 (accessed on 16 September 2016).

4.6 - Y.V. Maksimuk, G.J. Kabo, V.V. Simirsky, A.A. Kozyro & V.M. Sveruk, Standard Enthalpies of Formation of Some Methyl Esters of Benzene Carboxylic Acids, *J. Chem. Eng. Data,* **43** (1998) 293-298.

4.7 - S.M. Akers, J.L. Conkle, S.N. Thomas & K. B. Rider, Determination of the Heat of Combustion of Biodiesel Using Bomb Calorimetry, *Journal of Chemical Education,* **83** (2006) 260-262.

4.8 - R.P. Stout, F.E. Nettleton & L.M. Price, Bomb Calorimetry: The Energy Content of Pizza, *Journal of Chemical Education,* **62** (1985) 438-439.

4.9 - http://www.imn.htwk-leipzig.de/~pfestorf/praktikum/Kalorimetrie.pdf (accessed on 16 September 2016).

4.10 - http://webbook.nist.gov/chemistry/ (accessed on 28 March 2017).

5 Mixing Enthalpy of Binary Mixtures

5.1 Context and aim of the experiment

In this experiment, the binary mixture of two liquids is investigated. Calorimetric measurements are performed to determine the enthalpy change upon mixing as a function of composition. The individual contributions to the total mixing enthalpy are determined by calculating the partial molar mixing enthalpies for both components. [5.1, 5.2].

5.1.1 Important concepts to know

Chemical potential, ideal solution, ideal dilute solution, real solution, mixing entropy, mixing enthalpy, Gibbs energy of mixing, endothermic process, exothermic process, intermolecular forces, power, electrical work, calorimetry, partial molar volume, partial molar Gibbs energy, partial molar mixing enthalpy, Raoult's law, Henry's law.

5.1.2 Most common questions to be answered

- How can you explain a negative partial molar volume for a liquid mixture?
- What is the driving force for the mixing of two pure liquids to form an ideal solution?
- How can you explain the different boiling points of pure water and pure acetone by means of intermolecular interactions?
- What is an excess function, and how is it used to describe real solutions?

5.1.3 Further preparations before the experiment

Before performing the experiment, prepare a worksheet as follows:

Table 5.1-1: Example of the table to prepare for data collection and evaluation.

Mixture	ΔT_{exp} *(°C)*	ΔT_{cal} *(°C)*	W_{el} *(J)*	q_{exp} *(J)*
…	…	…	…	…
…	…	…	…	…
…	…	…	…	…
…	…	…	…	…
…	…	…	…	…
…	…	…	…	…

5.2 Theory

Here, we consider a binary mixture consisting of the components A and B that do not react with each other. To describe the mixture by its equilibrium properties, the term partial molar quantity has to be introduced. This enables us to describe the contribution of each component to a certain total quantity of the sample.

5.2.1 Partial molar volume

The partial molar volume V_i of a substance in a mixture is the change in volume per mole of A added to a large volume of the mixture. For substances A and B in a binary mixture, it is given by

$$V_A = \left(\frac{\partial V}{\partial n_A}\right)_{p,T,n_B} \tag{5.1}$$

and

$$V_B = \left(\frac{\partial V}{\partial n_B}\right)_{p,T,n_A} \tag{5.2}$$

In equations (5.1) and (5.2) the subscripts indicate that the pressure, temperature, and amount of the other component are constant. The partial molar volumes of the components depend on the actual composition of the mixture. Molecularly, the dependence on the actual composition can be explained by the fact that changing the composition changes the molecular environment and thus the intermolecular forces acting between the molecules. Be aware that partial molar volumes need not be positive.

When the partial volumes of both components of a binary mixture at the composition of interest are known, the total volume of the mixture can be calculated by

$$V = n_A \cdot V_A + n_B \cdot V_B \tag{5.3}$$

5.2.2 Partial molar Gibbs' energy

As described in chapters 1 and 2, the *chemical potential* μ of a substance i is the derivative of the Gibbs' free energy G with respect to the number of moles n_i

$$\mu_i = \left(\frac{\partial G}{\partial n_i}\right)_{p,T,n'} \tag{5.4}$$

Thus, the chemical potential corresponds to the molar Gibbs energy G_m. For the components A and B in a binary mixture, the chemical potentials μ_A and μ_B at a certain composition are given by the partial molar Gibbs energies

$$\mu_A = \left(\frac{\partial G}{\partial n_A}\right)_{p,T,n_B} \tag{5.5}$$

and

$$\mu_B = \left(\frac{\partial G}{\partial n_B}\right)_{p,T,n_A} \tag{5.6}$$

The dependence of the total Gibbs energy of a binary mixture on its composition is then given by

$$G = n_A \cdot \mu_A + n_B \cdot \mu_B \tag{5.7}$$

Comparison to

$$G = H - T \cdot S = U + p \cdot V - T \cdot S \tag{5.8}$$

reveals that the chemical potential further shows how the internal energy U, the enthalpy H and the Helmholtz energy $A = U - TS$ depend on the composition of the mixture.

$$\mu_A = \left(\frac{\partial G}{\partial n_A}\right)_{p,T,n_B} = \left(\frac{\partial U}{\partial n_A}\right)_{S,V,n_B} = \left(\frac{\partial H}{\partial n_A}\right)_{S,p,n_B} = \left(\frac{\partial A}{\partial n_A}\right)_{V,T,n_B} \tag{5.9}$$

Thus, the chemical potential describes how all extensive equilibrium properties depend on the solution composition. This is why it is so important to understand the thermodynamic properties of mixtures.

5.2.3 Chemical potential of liquids

The chemical potential and its dependence on liquid composition provide the basis for understanding liquid mixtures. In the following, this is discussed for ideal solutions and ideal-dilute solutions. At equilibrium, the chemical potential of a pure

substance A in its vapor phase equals its chemical potential in the liquid phase. The chemical potential of the pure liquid A is then given by

$$\mu_{A,liquid,pure} = \mu_A^0 + R \cdot T \cdot \ln p_{A,pure} \tag{5.10}$$

where, μ_A^0 is the standard chemical potential of A, that is identical to the molar Gibbs energy G_m of the pure gas at $p = p^0 = 1$ bar, and $p_{A,pure}$ is the vapor pressure of pure liquid A. If a solute is present in the liquid, then the chemical potential of A in the liquid is $\mu_{A,liquid}$ and its vapor pressure is p_A. Then

$$\mu_{A,liquid} = \mu_A^0 + R \cdot T \cdot \ln p_A \tag{5.11}$$

Combining equation (5.10) and (5.11) eliminates the standard chemical potential of the gas, and we obtain

$$\mu_{A,liquid} = \mu_{A,liquid,pure} + R \cdot T \cdot \ln \frac{p_A}{p_{A,pure}} \tag{5.12}$$

François Raoult experimentally found a relationship between the vapor pressure and the composition of the liquid. His experiments on liquid mixtures showed that the ratio of the partial vapor pressure of each component to its vapor pressure, if present as a pure liquid, is approximately equal to the mole fraction of the component in the mixture, with $x_A = n_A/n_{tot}$. This observation is called ***Raoult's law***

$$p_A = x_A \cdot p_{A,pure} \tag{5.13}$$

This relation is used to define ideal solutions, which obey Raoult's law throughout the whole composition range. For the chemical potential of an ideal solution, it thus follows that

$$\mu_{A,liquid} = \mu_{A,liquid,pure} + R \cdot T \cdot \ln x_A \tag{5.14}$$

For ideal solutions, both the solvent and the solute obey Raoult's law. At very low solute concentrations, it proved to be a good approximation for many solvents. In this case, x_A in equation (5.14) approaches 1, i.e., the liquid is almost pure and $p_A \to p_{A,pure}$. Molecularly, this can be interpreted by assuming that, in such a dilute solution, the solvent molecules are in an environment very much like that in the pure liquid and hence behave nearly as if they were pure. Let us now consider the case that $x_A \to 0$, i. e., A becomes the solute. The average molecule A in the solution is then mainly surrounded by molecules B and experiences an entirely different environment than in the pure solution. William Henry experimentally found a relationship that applies to solutes in dilute solutions. In ***Henry's law***, the proportionality constant is no longer the vapor pressure $p_{A,pure}$ of the pure substance, but an empirical constant K_A and equation (5.13) becomes

$$p_A = x_A \cdot K_A \tag{5.15}$$

Combination of equation (5.13) and (5.15) can be used to define an ideal dilute solution in which the solvent obeys Raoult's law and the solute obeys Henry's law.

5.2.4 *Liquid mixtures of ideal solutions*

First, we consider liquids that form an ideal solution upon mixing. This provides the background for understanding the deviations from ideal behavior exhibited by real solutions that take intermolecular interactions into account. For the case of mixing the liquids A and B to form an ideal solution, the change in Gibbs' energy upon mixing can be calculated by

$$\Delta_{mix}G = n \cdot R \cdot T \cdot (x_A \cdot \ln x_A + x_B \cdot \ln x_B) \tag{5.16}$$

with $n = n_A + n_B$, $x_A = n_A/n$ and $x_B = n_B/n$. The mixing entropy $\Delta_{mix}S$ describes the change in disorder upon mixing and is given by

$$\Delta_{mix}S = -\left(\frac{\partial \Delta_{mix}G}{\partial T}\right)_{p,n_A,n_B} = -n \cdot R \cdot (x_A \cdot \ln x_A + x_B \cdot \ln x_B) \tag{5.17}$$

In the case of an ideal solution, the mixing enthalpy $\Delta_{mix}H = 0$ since the intermolecular interactions between A and A, between B and B and between A and B are all equal. At this point, it is important to note that the definition of an ideal solution differs from that of an ideal gas. An ideal gas particle is treated as a hard point mass; that is, it has virtually no volume. Collisions between ideal gas particles are elastic, so no intermolecular forces are involved. In an ideal solution,

intermolecular interactions are present, but the average interactions in the mixture are the same as those in the pure liquids. As mentioned above, ideal liquid mixtures can be described by the implementation of Raoult's law throughout the complete composition range. Indeed, some mixtures obey Raoult's law very well, especially when the components are structurally similar.

The fact that $\Delta_{mix}H = 0$ for ideal solutions leads to $\Delta_{mix}G = -T\Delta_{mix}S$. The fact that $\Delta_{mix}S > 0$ upon mixing of ideal solutions reveals that $\Delta_{mix}G < 0$ and thus mixing is always spontaneous.

5.2.5 *Liquid mixtures of real solutions*

Now we consider that the intermolecular interactions (see Table 5.2-1) in the pure liquids A and B and in the binary mixture of A and B are different. Compared to ideal solutions where $\Delta_{mix}H = 0$, this leads to a change in enthalpy upon mixing.

For mixtures of real solutions, the thermodynamic properties are usually expressed in terms of an *excess function*, which is the difference of the observed thermodynamic property in the real mixture compared to its value for an ideal solution. Since its value equals zero in ideal mixtures, the excess enthalpy $\Delta_{mix}H$ in real mixtures equals the observed change in enthalpy upon mixing and can thus be determined directly from experiments. A widely used method for determining excess enthalpy is *differential calorimetry*. This method allows direct determination of the change in heat q_{exp} upon mixing from the measured change in temperature ΔT_{exp} via

$$q_{exp} = q_{cal} \cdot \frac{\Delta T_{exp}}{\Delta T_{cal}} \tag{5.18}$$

where Q_{cal} is the heat used to obtain a change in temperature ΔT_{cal} and must be determined as part of the calorimetric experiment calibration. q_{cal} equals the electrical work W_{el} that must be applied to achieve a change in temperature of ΔT_{cal} in the solution. W_{el} can be determined from the integration of the applied power P over time

$$q_{cal} = W_{el} = \int_{t_0}^{t} P \cdot dt \tag{5.19}$$

At constant pressure, q_{exp} equals the change in enthalpy $\Delta_{mix}h_i$ upon addition of a certain amount of one of the components A and B to the other or to a mixture of both. The enthalpy is here written as a small letter, since its value is not yet correlated to the amount of substance n_A and n_B. If one of the components is added successively to the second component, the total mixing enthalpy is obtained simply by integration of the individual enthalpy values $\Delta_{mix}h_i$

$$\Delta_{mix}h = \sum_i \Delta_{mix}h_i \tag{5.20}$$

From this, the molar mixing enthalpy could be calculated by taking into account the amount of substances via

$$\Delta_{mix}H = \frac{\Delta_{mix}h}{n_A + n_B} \tag{5.21}$$

$\Delta_{mix}H > 0$ indicates an *endothermic mixing* process that absorbs energy as heat while $\Delta_{mix}H < 0$ indicates an *exothermic mixing* process that releases energy as heat.

Application of

$$\Delta_{mix}H = \Delta_{mix}H_A \cdot x_A + \Delta_{mix}H_B \cdot x_B \tag{5.22}$$

and conversion reveals that the partial molar mixing enthalpies $\Delta_{mix}H_A$ and $\Delta_{mix}H_B$ of the components A and B of a binary mixture are given by

$$\Delta_{mix}H_A = \left(\frac{\delta\Delta_{mix}H}{\delta x_A}\right) x_B + \Delta_{mix}H \tag{5.23}$$

$$\Delta_{mix}H_B = \left(\frac{\delta\Delta_{mix}H}{\delta x_B}\right) x_A + \Delta_{mix}H \tag{5.24}$$

Table 5.2-1 gives an overview of intermolecular interactions that may contribute to $\Delta_{mix}H$. Make sure you are familiar with it.

Table 5.2-1: Overview of intermolecular forces

Type of interaction	*Interacting species*	*Strength*
Ionic interaction	Ion-ion	~ 1/r
Ion-dipole	Ion-dipole	~ $1/r^2$
Dipole-dipole	Dipole-dipole	~ $1/r^3$
Ion-induced dipole	Ion-induced dipole	~ $1/r^4$
Debye forces	Dipole-induced dipole	~ $1/r^6$
Van-der-Waals (VdW) forces or London dispersion forces	Induced dipole-induced dipole	~ $1/r^6$
hydrogen bonding	A-H ... B, where A and B are highly electronegative, and B possesses a lone pair of electrons	Stronger than VdW forces, weaker than ionic interactions

In real solutions, the excess entropy $\Delta_{mix}S$ equals its value in ideal solutions, thus the excess Gibbs energy $\Delta_{mix}G = \Delta_{mix}H$.

5.2.6 Properties of acetone and water and their interactions

In this experiment, we use calorimetry to determine the mixing enthalpy of different water-acetone mixtures. The two polar solvents are miscible in any ratio. Acetone-water mixtures serve as a model system for binary non-ionic mixtures and are the subject of intensive research. Spectroscopic studies and molecular dynamics simulations have provided quite a detailed insight into the complex dynamics and structural properties of these systems. [5.3, 5.4] As a basis to understand what is going on in these binary mixtures, it is important to be familiar with the structure of both solvents (Figure 5.1). Acetone is a planar molecule with a polar double bond between the carbon and oxygen atoms. It belongs to the group of aprotic solvents, meaning that it cannot release protons. Water has a bent structure and belongs to the group of protic solvents, meaning that protons can be released from its structure. The polarity of water is significantly higher compared to that of acetone.

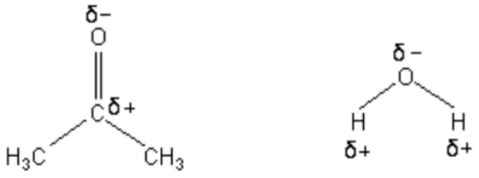

Figure 5.1: Structure of acetone (left) and water (right). δ- and δ+ indicate the polarity of both molecules and stand for the partial negative charge on the oxygen atom and the partial positive charge on the carbon atom or the hydrogen atoms, respectively.

A crucial property of water is that it can simultaneously donate and accept hydrogen bonds. This is the basis for the formation of an intermolecular hydrogen-bond network in water, and the corresponding attraction between neighboring water molecules is responsible for the unique properties of liquid water. Compared to this, acetone can only accept hydrogen bonds, but not donate them. This indicates that hydrogen bonds cannot form in pure acetone. However, in mixtures with water, hydrogen bonds can form between the oxygen atom of acetone and a water hydrogen atom. The properties of acetone-water mixtures proved to be very complex and are still not fully understood. Recent studies have shown that the

tetrahedral structure of water is lost as the acetone concentration increases; however, below very high acetone concentrations ($x_{acetone} \leq 0.7$), most water molecules remain hydrogen-bonded to other water molecules. [5.3] Only above this concentration, water molecules start to undergo hydrogen bonding with acetone molecules, and the formed water-acetone hydrogen bonds turned out to be quite strong.

5.3 Experimental details and evaluation

5.3.1 Experimental execution

In this experiment, seven water-acetone mixtures of different compositions are investigated (Table 5.3-1). The individual components need to be weighed with an accuracy of ± 0.1 g.

Important: The water bath temperature must be equilibrated to the actual temperature in the calorimeter after each measurement. This takes quite a long time, and to save time, it is reasonable to weigh the solvent in the Erlenmeyer flask for the subsequent measurement in the meantime.

Table 5.3-1: Composition of the seven investigated water-acetone mixtures.

Mixture	$x_{acetone}$	*Solvent in the calorimeter*	*Solvent in the Erlenmeyer flask*
1	0.1	432 g water	154 g acetone
2	0.2	mixture **1**	194 g acetone
3	0.9	464 g acetone	16 g water
4	0.8	mixture **3**	20 g water
5	0.6	mixture **4**	60 g water
6	0.5	mixture **5**	49 g water
7	0.4	mixture **6**	72 g water

The experimental setup for calorimetric determination of the mixing enthalpy is shown in Figure 5.2. Turn on the equipment for calorimetric measurement, the computer, and the Cobra 4 Mobile-Link (**1**). Open the Cobra 4 measure software (**2**) (for basic instructions on how to use the software, see Chapter 12).

For the first measurement, add 432 g of deionized water into the calorimeter vessel (**3**). Insert the magnetic stirring bar into the calorimeter vessel and turn on the magnetic stirrer (**4**). **Take care not to turn on the heating unit by mistake!** Insert the heating coil with the temperature sensor (**5**) into the solvent by introducing it through the lid hole of the calorimetric vessel. **To ensure proper immersion of the heating coil in the liquid, the heating coil socket needs to be positioned under the lid.** Turn on the thermostat (**6**) and ensure that the water level in the bath (**7**) is high enough for the cooling coil (**7***) to be properly immersed. Adjust the thermostat temperature to the actual temperature in the calorimetric vessel. The thermostat temperature can be adjusted by pressing the yellow button (**6***) twice. The display starts blinking, and the set temperature can be adjusted using the buttons (**6***) with the up and down arrows. Finally, the yellow button must be pressed once to confirm the temperature to set. **Do not forget to open the cooling water valve (8)!**

Figure 5.2: Experimental set-up with all its parts. (**1**) Cobra 4 USB-Link, (**2**) measure software, (**3**) calorimeter, (**4**) magnetic stirrer, (**5**) heating coil with sockets and temperature sensor, (**6**) thermostat with (**6***) buttons to set the temperature, (**7**) water bath of thermostat with (**7***) cooling coil, (**8**) cooling water valve, (**9**) digital high-resolution thermometer with (**9***) temperature sensor and (**10**) power supply for the calorimeter.

Weigh 154 g of acetone in a 250 mL Erlenmeyer flask. Insert the temperature sensor (**9***) of the digital high-resolution thermometer (**9**) into the hole in the rubber stopper, then close the Erlenmeyer flask. ***Be sure the sensor is immersed properly in the solution.*** Immerse the Erlenmeyer flask in the water bath and let it equilibrate. **To prevent the flask from tilting, be sure it is securely fastened. Furthermore, the liquid in the flask must be completely immersed to ensure proper temperature equilibration.**

Wait until the temperature of the acetone in the Erlenmeyer flask and the temperature of the water in the calorimeter differ by less than 0.2 °C. Then, the measurement can be started (for basic instructions on how to use the software, see Chapter 12). After collecting data points at the starting temperature for one minute, the equilibrated acetone is added through the third opening in the lid of the calorimeter. **Use a funnel for this procedure to avoid spillage!** Mixing leads to a change in temperature ΔT_{exp}. As soon as the mixing process is complete, the mixture temperature re-equilibrates. If this equilibrium is reached, the mixture temperature remains constant. When the temperature stops changing, wait 1 minute before performing the electrical calibration to determine the calorimeter total heat capacity. To do this, turn on the power supply (**10**) using a voltage of 10 V. This induces continuous heating of the liquid in the calorimeter vessel and the corresponding supplied energy (q_{cal}) is measured by the system. Stop the heating process as soon as the increase in temperature (ΔT_{cal}) corresponds approximately to the temperature difference (ΔT_{exp}) measured in the previous mixing experiment. Then, wait until the temperature has equilibrated again and let the measurement run for another minute before stopping the experiment. The measurements of the other mixtures are executed similarly.

For the mixtures 3 to 7 (see Table 5.3-1) water is added to either acetone or to an acetone-water mixture provided in the calorimeter vessel. Here, a 100 ml Erlenmeyer flask is used to weigh in and equilibrate the water temperature. Unlike acetone, water is not volatile, and therefore it is not necessary to close the flask with a rubber stopper. Instead, use a stand clamp to secure the temperature sensor.

Important: The temperature of the mixture in the calorimeter vessel decreases with time between two experiments. This must be taken into account when adjusting the thermostat set temperature. Before mixing the components, it is always very important to ensure that the temperature difference between the two mixing components is less than 0.1 °C. If

necessary, the thermostat temperature needs to be adjusted. If the water temperature in the thermostat needs to be cooled, add ice to accelerate the process.

5.3.2 *Data evaluation*

- ☐ Determine ΔT_{exp}, ΔT_{cal} and W_{el} by integrating the power curve P for each mixing experiment and use the results to calculate q_{exp} according to the equation (5.18) and (5.19)
- ☐ Determine ΔT_{exp} and ΔT_{cal} from the temperature-time diagram. For this, define two regression lines matching the data points before and after the transition, respectively (Figure 5.3). Draw an auxiliary line parallel to the ordinates in a way that F1 = F2. The endpoints of the line AB need to be prolonged parallel to the x-axis to reveal ΔT.

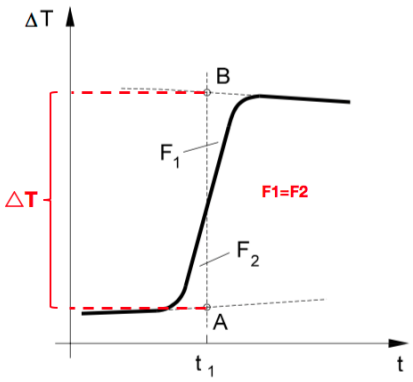

Figure 5.3: Graphical determination of ΔT. F1 and F2 are the areas defined by the data points in the transition, the auxiliary line AB, and the two regression lines. Original picture adapted from reference [4.9].

- ☐ Note the intercept time of ΔT_{exp} and ΔT_{cal}.
- ☐ Select the power-time-profile by clicking on the red capital P (Figure 5.4).

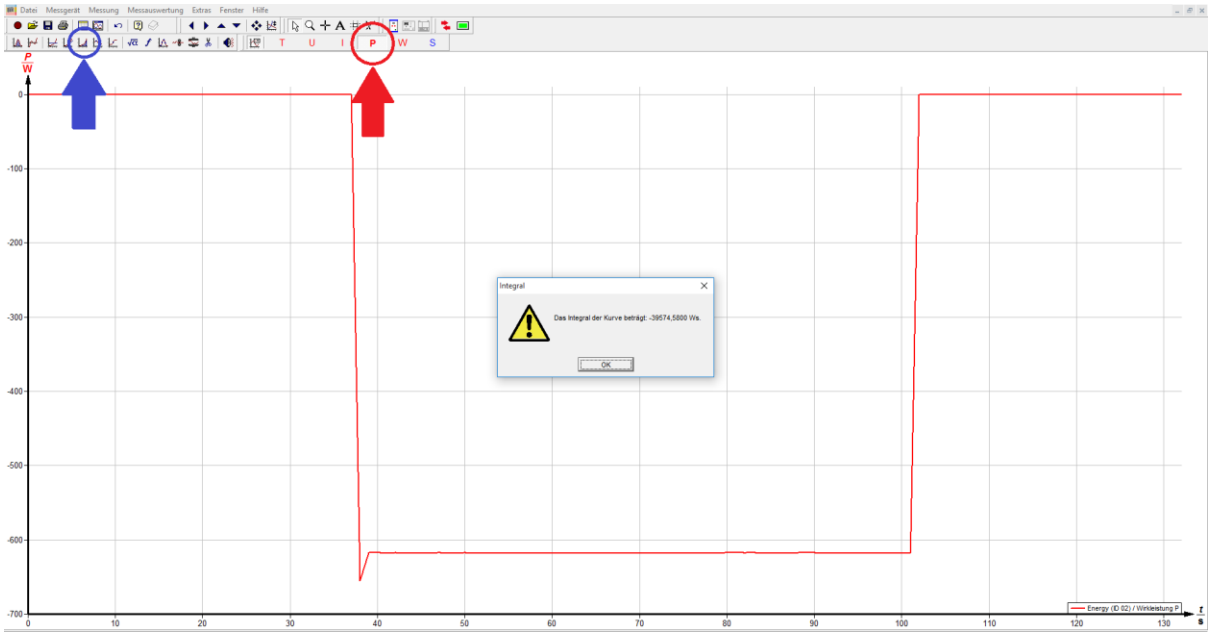

Figure 5.4: Selection of the power-time-profile (red box) and activation of the integration option (blue box) of the software.

- ☐ Integrate the entire curve using the integration option of the software  (Figure 5.4). As soon as the integration procedure is completed, the corresponding electrical work W_{el} is automatically given in units of W s.
- ☐ Calculate the mixing enthalpies $\Delta_{mix}H$ according to the equation (5.20) and (5.21). For experiments starting from a mixture provided in the calorimetric vessel, the mixing enthalpy of that mixture must also be accounted for. Its value must be added to the measured mixing enthalpy from the actual experiment.
- ☐ Plot $\Delta_{mix}H$ versus the mole fraction of acetone.
- ☐ Calculate the partial molar mixing enthalpies for acetone ($\Delta_{mix}H_{acetone}$) and water ($\Delta_{mix}H_{water}$) according to the equations from (5.22) to (5.24) and plot the results as a function of the mixture composition.
- ☐ Perform an error analysis for all calculations

5.4 Applications of the experiment and its theory

- ☑ Henry's law states that the quantity of a gas that will dissolve in a liquid is proportional to the partial pressure of the gas and its solubility coefficient. This is directly connected to decompression sickness in diving sports. The higher the pressure (the greater the diving depth), the more gas (air) is absorbed into the blood and tissues. Similarly, the impaired respiration due to the decreased solubility of oxygen in blood at high altitudes can be explained. Generally, Henry's law, Raoult's law, and mixing enthalpies are important to understand the absorption of gases into liquids [5.5].
- ☑ Mixing enthalpies play an important role in physics, chemistry, and technology, e.g., for the theoretical calculation of complex phase diagrams, for the description of mixed phases, and in the development of alloys [5.6 - 5.9].
- ☑ In addition to other requirements, a positive mixing enthalpy is necessary for liquid segregation.

5.5 Literature

5.1 - P.W. Atkins, Physical Chemistry, 6th ed., Oxford University Press, Oxford (1998), pp. 163-176.

5.2 - P.W. Atkins and J. de Paula, Atkins' Physical Chemistry, 8th ed., Oxford University Press, Oxford (2006), pp. 136-150.

5.3 - D.S. Venables and Ch.A. Schmuttenmaer, Spectroscopy and Dynamics of Mixtures of Water with Acetone, Acetonitrile, and Methanol*, Journal of Chemical Physics*, **113** (2000) 11222-11236.

5.4 - A. Perera and F. Sokolic, Modeling Nonionic Aqueous Solutions: The Acetone-Water Mixture*, The Journal of Chemical Physics*, **121** (2004) 11272.

5.5 - W. Shi and E.J. Maginn, Molecular Simulation of Ammonia Absorption in the Ionic Liquid 1-ethyl-3-methylimidazolium bis(trifluoromethylsulfonyl)imide([emin][Tf_2N])*, AIChE Journal*, **55** (2009) 2414-2421.

5.6 - W. López-Pérez, N. Simon-Olivera, R. González-Hernández and J.A. Rodríguez, First-Principles Study of the Structural, Electronic, and Thermodynamic Properties of $Sc_{1-x}Al_xAs$ Alloys*, Physica Status Solidi (B)*, **250** (2013) 2163-2173.

5.7 - E. Hayer, L. Komarek, P. Bros and M. Gaune-Escard, Enthalpy of Mixing of Liquid Gold-Tin Alloys*, ChemInform*, **12** (1981).

5.8 - R. Lueck, H. Wang and B. Predel, Calorimetric Determination of the Mixing Enthalpy of Liquid Cobalt-Zirconium Alloys*, ChemInform*, **24** (1993).

5.9 - F. Sommer, J.J. Lee and B. Predel, Calorimetric Investigations of Liquid Alkaline Earth Metal Alloys*, Berichte der Bunsengesellschaft für Physikalische Chemie*, **87** (1983) 792-797.

6 Equilibrium Thermodynamics

6.1 Context and aim of the experiment

At equilibrium, the chemical dye Rhodamine B exists as a mixture of its lactone and zwitterion forms. In this experiment, absorption spectroscopy is used to determine the Gibbs free energy, the reaction enthalpy, and the reaction entropy for the formation of the zwitterion form of Rhodamine B at different temperatures [6.1 - 6.3].

6.1.1 Important concepts to know

Thermodynamics, equilibrium constant, reaction kinetics, reaction rate, reaction rate constant, Gibbs energy, reaction enthalpy, reaction entropy, transition-state theory, Le Chatelier's principle, dye, chromophore, absorption spectroscopy, absorption, transmission, absorption spectra, Lambert-Beer's law, single and dual-beam spectrophotometer.

6.1.2 Most common questions to be answered

- What is the prerequisite to determine a concentration by means of UV-Vis spectrophotometry?
- What is the advantage of a dual-beam spectrophotometer, compared to a single beam spectrophotometer?
- What is an absorption spectrum, and what determines its shape?
- Rhodamine B is a chemical dye. What are its applications in biochemistry?
- What's the definition of an endothermic and an exothermic reaction? How do they differ in terms of the influence of temperature on the reaction rate constant?
- What is the driving force of a chemical reaction?
- How can a chemical equilibrium be shifted?
- What is the meaning of the transition state of a chemical reaction?

6.1.3 Further preparations before the experiment

Before performing the experiment, prepare a worksheet as follows:

Table 6.1-1: Example of the table to prepare for data collection and evaluation (# stands for the series of measurements).

#	A $T = 55°C$	A $T = 50°C$	A $T = 45°C$	A $T = 40°C$	A $T = 35°C$	A $T = 30°C$	A $T = 25°C$	A $T = 20°C$	A $T = 15°C$
1	…	…	…	…	…	…	…	…	…
2	…	…	…	…	…	…	…	…	…
3	…	…	…	…	…	…	…	…	…
(4)	…	…	…	…	…	…	…	…	…

6.2 Theory

6.2.1 Equilibrium thermodynamics

We consider a chemical equilibrium reaction of the type

$$A \underset{k_{-1}}{\overset{k_1}{\rightleftarrows}} B \tag{6.1}$$

Here, k_1 and k_{-1} are the rate constants for the formation of B and A, respectively. Figure 6.1 shows the free energy surface of such an equilibrium reaction between two compounds, as the free energy G^0 of the reaction at standard state (also called Gibbs' free energy) as a function of a certain reaction coordinate, which describes the progression of the reaction, followed by a certain experimental observable.

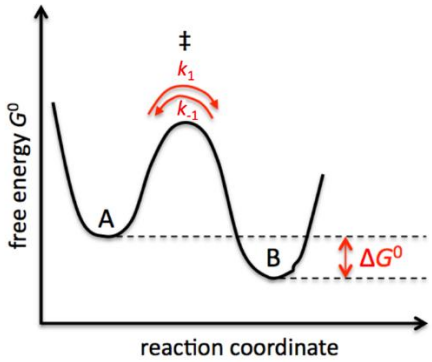

Figure 6.1: The free energy surface of an equilibrium reaction between the compounds A and B separated by the transition state (‡).

Taking the stability of *B* as a reference, the stability of *A* can be expressed by the difference in Gibbs' free energy ΔG^0 between A and B according to the Van't Hoff equation

$$\Delta G^0 = -R \cdot T \ln K \tag{6.2}$$

with

$$K = \frac{[B]_{eq}}{[A]_{eq}} = \frac{k_1}{k_{-1}} \tag{6.3}$$

K is the equilibrium constant and $[A]_{eq}$ and $[B]_{eq}$ are the concentrations of A and B at the equilibrium. At constant temperature and pressure, the reaction is spontaneous in the direction of decreasing Gibbs energy. The equilibrium between A and B can be shifted by a change in external conditions. The Gibbs fundamental equation (6.4) shows that the equilibrium can be perturbed by pressure p, temperature T or changes in chemical potential m, e. g., upon addition of chemical compounds that affect the equilibrium.

$$d\Delta G^0 = \Delta V^0 \cdot dp - \Delta S^0 \cdot dT + \sum_i \Delta \mu_i^0 \cdot dn_i \tag{6.4}$$

ΔV^0, ΔS^0 and $\Delta \mu_i^0$ are the changes in volume, entropy, and chemical potential upon formation of B. The definition of the Gibbs energy ($G = H - TS$) reveals an additional relationship for ΔG^0

$$\Delta G^0 = \Delta H^0 - T \cdot \Delta S^0 \tag{6.5}$$

Here, ΔH^0 is the change in enthalpy upon formation of *B*. Inserting equation (6.5) into equation (6.2) reveals the contributions of the reaction entropy and the reaction enthalpy to the equilibrium constant

$$\ln K = \frac{\Delta S^0}{R} - \frac{\Delta H^0}{R \cdot T} \tag{6.6}$$

The reaction enthalpy ΔH gives the enthalpy change per mole. The reaction is called endothermic if it absorbs energy as heat from its surroundings ($\Delta H > 0$) and exothermic if it releases energy as heat to the environment ($\Delta H < 0$). The superscript zero further indicates that all species involved in the reaction are in their standard states, namely in their pure

form at a pressure p = 1 bar at the specified temperature. The standard enthalpy may thus be reported for any temperature. The conventional temperature for reporting thermodynamic data is 298.15 K (25°C).

6.2.2 Effect of temperature on an equilibrium reaction

Changing the temperature perturbs the equilibrium, resulting in a new equilibrium with different concentrations of A and B. The *principle of Le Chatelier* predicts that the system at equilibrium readjusts itself to counteract the effect of the applied change. Regarding the effect of changing the temperature on a chemical equilibrium, this means that: *i)* the equilibrium will shift in the endothermic direction if the temperature is raised, because then energy is absorbed as heat and the temperature rise is opposed and *ii)* the equilibrium will shift in the exothermic direction if the temperature is lowered, because then energy is released and the reduction in temperature is opposed. This can be summarized in the following way:

- Exothermic reactions: increasing the temperature favors the reactants.
- Endothermic reactions: increasing the temperature favors the products.

Writing the expression $\Delta G = \Delta H - T \cdot \Delta S$ in the form $-\Delta G/T = -\Delta H/T + \Delta S$ reveals some insight into the thermodynamic basis of this behavior. For an exothermic reaction, $-\Delta H/T$ corresponds to a positive change of entropy of the surroundings and favors the formation of products. When the temperature is raised, $-\Delta H/T$ decreases, and the increasing entropy of the surroundings has a less important role. As a result, the equilibrium shifts to the left. For an endothermic reaction, the principal factor is the increasing entropy of the reaction system. The importance of the unfavorable change of entropy of the surroundings is reduced if the temperature is raised (because then $-\Delta H/T$ is smaller), and the reaction can shift towards the products. Quantitatively, this is described by the equation (6.6). According to this equation, a plot of $\ln K$ versus $1/T$ (*Van't Hoff plot*) yields a straight line with the slope $m = -\Delta H^0/R$ and the intercept $b = \Delta S^0/R$. Thus, it is quite easy to determine ΔH^0 and ΔS^0 graphically. However, it must be taken into account that the reaction enthalpy and the reaction entropy are dependent on temperature due to changes in heat capacity ΔC_p with temperature (for the meaning of the heat capacity, also see chapter 4). $\Delta C_p \neq 0$ leads to a curved line in the Van't Hoff plot. However, if the investigated temperature range and the temperature dependence of the heat capacity are small, then a straight line can be assumed. Usually, the Van't-Hoff-plot method is accurate enough to determine the reaction enthalpy and entropy.

6.2.3 Absorption spectroscopy

In this experiment, an equilibrium reaction is investigated using UV-Vis absorption spectroscopy. All optical spectroscopic methods are based on the principle that electromagnetic radiation is irradiated to the object under investigation, absorbed, scattered, and then reemitted. As its name suggests, UV-Vis absorption spectroscopy measures the absorption of light in the UV-Vis range (100 nm - 760 nm). A prerequisite for light absorption is the presence of a *chromophore,* which is the part of a molecule that is responsible for light absorption due to its electronic transitions. The possible electronic transitions (mainly $\pi \rightarrow \pi^*$, $n \rightarrow \pi^*$ and $n \rightarrow \sigma^*$) are excited by light absorption and together with their rotational and vibrational levels they determine the specific shape (position, width, and intensity of spectral lines) of the *absorption spectrum*.

The *Lambert-Beer law* (equation (6.7)) quantitatively describes the absorption of electromagnetic radiation by a substance in solution. This law assumes that the absorbing substance is homogenously distributed, that no light scattering occurs, and that no other photoreactions are taking place in the solution. The absorbance A of monochromatic light (meaning with a given wavelength λ, and thus with a given energy) by a dissolved substance is then given by

$$A = \log \frac{I_0}{I} = \varepsilon \cdot c \cdot d \tag{6.7}$$

Here, I_0 and I are the intensity of the irradiated light and of the light leaving the sample, respectively. c is the molar concentration of the light-absorbing substance, d is the thickness of the irradiated sample in cm, and ε is the substance-specific molar absorption coefficient in M^{-1} cm^{-1}. If the substance under investigation absorbs light in the wavelength range used, the equation (6.7) can thus be used to determine its concentration. Instead of the absorbance A, the transmittance T is often used to quantify the effect of light absorption. Both parameters are directly related

$$T = \frac{I}{I_0} \tag{6.8}$$

and thus

$$A = -\log T \tag{6.9}$$

According to Lambert-Beer law (equation (6.7)), an absorption spectrum is a plot of the extinction coefficient e as a function of the wavelength λ of the irradiated light. Note that the shape of the spectrum further depends strongly on the solvent due to interactions of the substance with the solvent dipoles, due to collisions with solvent molecules, and possibly also due to hydrogen bond formation.

Two major devices are used to perform spectrophotometric measurements. In single-beam spectrophotometers, as in this experiment, the sample and the reference must be measured separately. In contrast to this, double-beam spectrophotometers (Figure 6.2) compare the light intensity between two light paths, one path containing a reference sample and the other a test sample. The reference and the sample are alternately measured using a chopper mirror that switches the light between the optical paths.

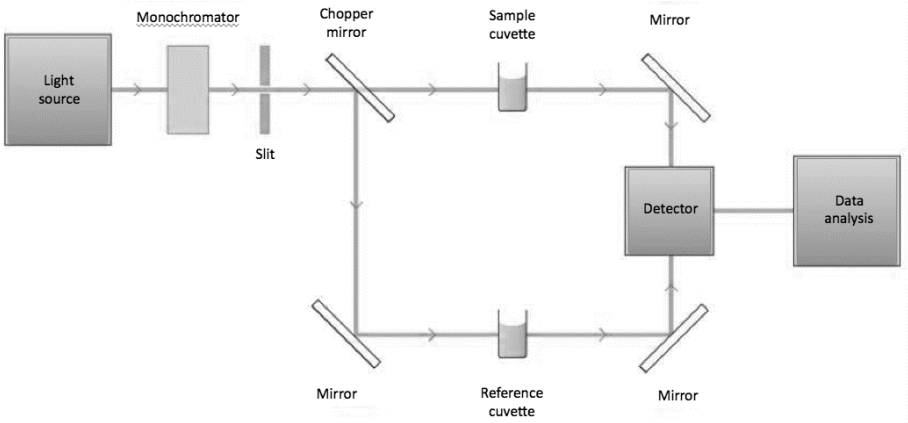

Figure 6.2: Setup of a dual-beam spectrophotometer.

6.2.4 The reaction of Rhodamine B

In this experiment, the parameters ΔG, ΔH and ΔS of an equilibrium reaction are determined using spectrophotometry. Here, the chemical dye Rhodamine B chloride is used. In solution, Rhodamine B chloride is present in an equilibrium of two different structures (Figure 6.3). On the one hand, there is the colorless lactone form (L) of Rhodamine B; on the other hand, the chromatic zwitterionic form (Z). Increasing the temperature favors the colorless lactone form.

Do you know why the lactone is colorless while the zwitterion is colored?

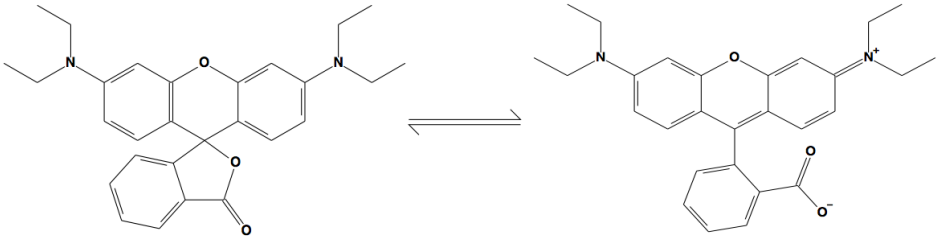

Figure 6.3: Equilibrium structures (left: lactone, right: zwitterion) of Rhodamin B in solution.

Since the lactone is colorless and the zwitterion is chromatic, the equilibrium concentrations can be determined using UV-Vis absorption spectroscopy. Knowing the equilibrium concentrations allows calculation of the equilibrium constant $K = [Z]/[L]$. To be able to determine K as a function of temperature, the absorbance of the pure Z-form must be known. This value can be determined from measurements of Rhodamine B chloride in strong acids. However, this is not part of this experiment, and the corresponding value of the molar absorption coefficient of the pure Z-form (ε = 13.0·10^4 M^{-1} cm^{-1}) is provided.

6.3 Experimental details and evaluation

6.3.1 Experimental execution

The experiment aims to determine ΔG, ΔH und ΔS for the formation of the zwitterion form of Rhodamine B, either in ethanol or in 1-propanol. The two Rhodamine B solutions A and B are provided at the bench:

Solution A: 8·10^{-6} M Rhodamine B in ethanol

Solution B: 8·10^{-6} M Rhodamine B in 1-propanol

The students may decide for themselves which solution they want to start with. Figure 6.4 shows the single beam spectrophotometer used to characterize the equilibrium reaction under investigation.

Figure 6.4: Spectrophotometer used to study the equilibrium reaction of Rhodamine B.

Before measurements of Rhodamine B solutions can be performed, the spectrophotometer must be calibrated using a base correction. This must be done for each measurement series individually, meaning once before the measurements in the first solvent and once before the measurements in the second alcohol. Check if the provided cuvettes (**1 cm inner width**) are clean and dry. To perform the base correction, fill one cuvette with the corresponding pure alcohol, place it in the cuvette

holder, equilibrate it at $T = 25\ °C$ and close the sample chamber. The temperature can be adjusted by setting the temperature controller.

Figure 6.5: Controller for the temperature adjustment of the cell holder.

To adjust the requested temperature, set the switch "TEMP. CONTROL" to "OFF". Turn the knob labeled "TEMP.ADJUSTMENT" to the left ("DOWN") to decrease, or to the right ("UP") to increase the temperature of the temperature-controlled cell holder. Then set the switch "TEMP. CONTROL" to "ON".

Figure 6.6: The temperature-controlled cell holder.

In "Mode menu" (Figure 6.7), select "Spectrum" to change to the "Spectrum menu" and start the base correction "BaseCorr" (Figure 6.8) by pressing F1.

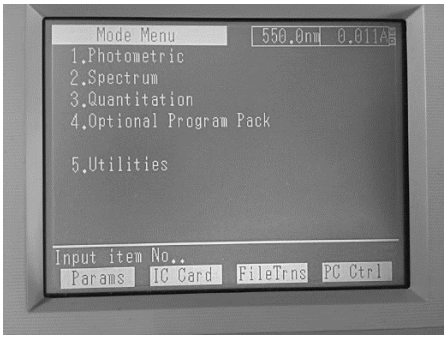

Figure 6.7: The “MODE menu”.

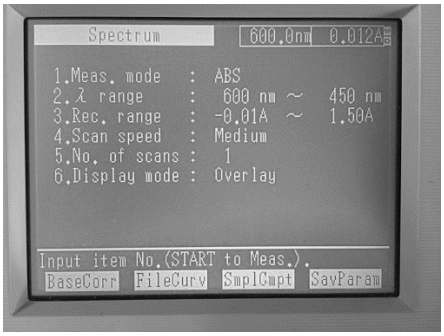

Figure 6.8: The “Spectrum menu”; press F1 (“BaseCorr”) to start the base correction.

When the measurement is finished, empty the cuvette into the waste can for “Halogenfreie Lösungsmittel”. Clean and dry the cuvette as described above and fill it with the corresponding Rhodamine B solution. Put the cuvette in the cuvette holder. Cover the cuvette with the insulator cap equipped with the thermocouple and close the sample chamber. **Take care of the Ni- Cr/Ni temperature sensor!**

Think about why it is important to close the cuvettes. What would happen if the cuvettes were open? What would be the consequences of that?

In a first step, the students determine the wavelength (λ_{max}) of maximum absorbance for the corresponding Rhodamine B solution. To perform this, the students must measure three absorbance spectra of the Rhodamine B solution over the range from 450 to 600 nm at three different temperatures (15, 25, and 40 °C). To start the measurement, press the START/STOP button, and a spectrum like in Figure 6.10 will appear. To obtain the wavelength of maximum absorbance, press F2 (PEAK button).

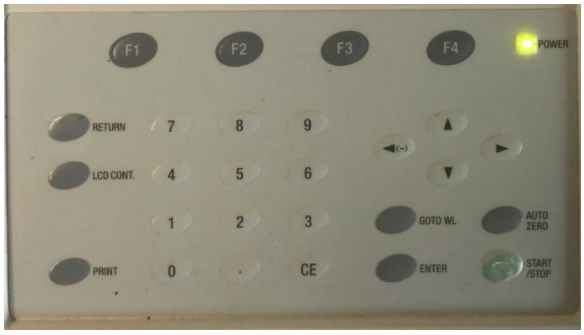

Figure 6.9: The keyboard of the single beam spectrometer.

In the following measurements, the absorbance at the wavelength of its maximum is determined as a function of temperature. To perform these measurements, go back to the “Mode menu” (Figure 6.7) of the spectrometer and choose "Photometric". Adjust the wavelength to the determined maximum of absorbance. Heat the cuvette to T = 60 °C and measure the absorbance spectrum by pressing the “START/STOP” button (Figure 6.9). If the set temperature of T = 60 °C is reached, and the corresponding absorbance is written down, the temperature should then be set to T = 10 °C. As a result, the solution in the cuvette begins to cool. Follow the actual temperature in the cuvette on the computer display and read the temperature in maximum steps of ΔT = 5 °C down to T = 15 °C. For each temperature, press the “START/STOP” button and record the actual absorbance value! Please collect three series of measurements from high to low temperature for each Rhodamine B solution to obtain enough values to estimate the error. The thereby collected absorbance values are stored in a table (Figure 6.11) in the spectrometer software.

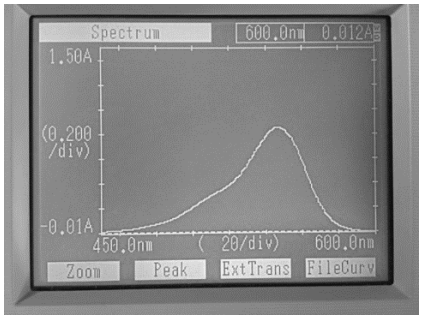

Figure 6.10: In the "Spectrum menu", press F2 ("Peak") to get the wavelength of maximum absorbance.

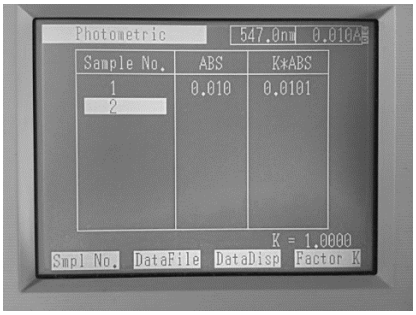

Figure 6.11: The table with the stored absorbance values.

Right after collecting the absorbance values, you should manually fill them into the prepared spreadsheet (similarly to Table 6.1-1)

After emptying and cleaning all cuvettes, repeat the measurements for the second Rhodamine-B solution.

6.3.2 *Data evaluation*

- ☐ Determine the concentration of the zwitterion form of Rhodamine B as a function of temperature, using the Lambert-Beer law. For this, it is necessary to calculate the absorbance $A(100\%)$ of the pure Z-form, meaning that all Rhodamine B is present in its zwitterion form, using the given molar extinction coefficient. The molar ratio χ_Z of the zwitterion form at a certain temperature is then given by

$$\chi_Z = \frac{A(T) \cdot \rho(15\,°C)}{A(100\%) \cdot \rho(T)} \tag{6.10}$$

  where $\rho(15\,°C)$ is the density of the solvent at 15 °C and $\rho(T)$ the density of the solvent at the measuring temperature T. $A(T)$ is the absorbance at the measuring temperature. Values for the density of the used solvents are provided in the lab. The temperature dependence of the density can be assumed to be linear.
- ☐ Use the relation $\chi_L = 1 - \chi_Z$ to determine the equilibrium constant according to the equation (6.3) for all the measurements and for both Rhodamine B solutions.
- ☐ Determine ΔG, ΔH und ΔS for the formation of the zwitterion form of Rhodamine B in both solvents. Discuss the size and the sign of the results. Why does the equilibrium move to the lactone form with increasing temperature?
- ☐ Perform an error analysis for all calculations.

6.4 Applications of the experiment and its theory

- ☑ In quantitative analyses of molecules that absorb light in the UV-Vis range of the electromagnetic spectrum, their concentration can be determined by absorption spectroscopy. Furthermore, this allows us to derive equilibrium constants, dissociation constants, and reaction kinetics.

- ☑ Since the absorption spectrum is specific to each compound, its measurement enables the identification and purity analysis of molecules in solution.
- ☑ UV-Vis absorption spectroscopy enables trace analysis, e.g., the determination of ethanol concentration in blood.
- ☑ Rhodamine dyes are widely used as fluorescent probes, owing to their high absorption and broad fluorescence in the visible region of the electromagnetic spectrum [6.4].
- ☑ Equilibrium reactions are ubiquitous in chemistry and in biology; some examples are: saturated solutions above a precipitate (e.g., $Ag^+ + Cl^- \leftrightarrows AgCl$), ester formation from acid and alcohol, phase equilibria, formation of crystals and flowstones, etc. The analysis of the corresponding equilibrium thermodynamics is important for the characterization and understanding of these systems [6.5, 6.6].

6.5 Literature

6.1 - D.A. Hinkley and P.G. Seybold, *J. Chem. Education,* **64**, (1987) 382-384.

6.2 - P.W. Atkins, Physical Chemistry, 6th ed., Oxford University Press, Oxford (1998), pp. 215-242.

6.3 - P.W. Atkins and J. de Paula, Atkins' Physical Chemistry, 8th ed., Oxford University Press, Oxford (2006), pp. 200-215.

6.4 - Beija, M., Afonso C.A.M., and Martinho J.M.G., Synthesis and applications of Rhodamine derivatives as fluorescent probes*, Chem. Soc. Rev.*, **38** (2009) 2410-2433.

6.5 - L. Stixrude and C. Lithgow-Bertelloni, Thermodynamics of mantle minerals*, Geophysical Journal International*, **184** (2011) 1180-1213.

6.6 - K. Sakurai, M. Oobatake and Y. Goto, Salt-dependent monomer-dimer equilibrium of bovine β-lactoglobulin at pH 3*, Protein Science*, **10** (2001) 2325-2335.

7 The Electromotive Force and Its Dependence on Activity and Temperature

7.1 Context and aim of the experiment

The following experiment concerns thermodynamics in electrochemistry. In more detail, the students will use the standard hydrogen electrode to measure the thermodynamic (also called reversible) potential of half-cell redox reactions, as reported in the so-called electrochemical series; those reactions are used in common reference electrodes. Furthermore, the students will calculate and measure the voltage of a galvanic cell, the Daniell cell, as a function of the concentration of the ionic species involved and of the temperature [7.1, 7.2], using Nernst and Gibbs-Helmholtz equations.

7.1.1 Important concepts to know

Electromotive force (emf), electrochemical series, activity, Debye-Hückel limiting law, Nernst equation, electrode potential, reference electrode, electrodes from first to fourth kind, standard hydrogen electrode (SHE), Daniell cell, Gibbs-Helmholtz equation.

7.1.2 Most common questions to be answered

- What is an electrochemical cell, and how could you build it? Which reaction occurs at the cathode and which at the anode?
- What is the difference between activity and concentration? Why is activity used?
- How can you measure the standard thermodynamic potential E^0 (formerly *emf*) of an electrochemical cell?
- Which equation correlates cell potential with the activities of the species involved?
- How can you thermodynamically relate cell potential variation with temperature at constant pressure $\left(\frac{\partial E}{\partial T}\right)_p$?

7.1.3 Further preparations before the experiment

Before performing the experiment, prepare a few worksheets as follows:

Table 7.1-1: Example of the table to prepare for data collection and evaluation of the various reference potentials.

Electrode	*Measured potential [mV]*		*Calculated potential [mV]*	
	vs. SHE	*vs. calomel*	*vs. SHE*	*vs. calomel*
calomel				
Ag/AgCl				

Table 7.1-2: Example of the table to prepare for data collection and evaluation of the voltage of the Daniell cell as a function of concentration of ionic species.

Daniell cell	*Measured potential [mV]*	*Calculated potential [mV]*	$\ln a_{Zn^{2+}}/a_{Cu^{2+}}$
	…	…	…

Table 7.1-3: Example of the table to prepare for data collection and evaluation of the voltage of the Daniell cell as a function of temperature.

Daniell cell	*Potential [mV]*	*Temperature [K]*
	…	…
	…	…
	…	…

7.2 Theory

7.2.1 Activity and concentration

In concentrated solutions, the strong interactions of the dissolved ionic species with each other, not only with the solvent, become relevant. To use real solutions and be able to physically model them, the concentration b_i in mol/kg (*molality*) of a dissolved species i must be replaced with a "*thermodynamically effective quantity*" a_i, denominated *activity*. This physical quantity is dimensionless, and it is obtained by dividing the molality b_i of the species i by the standard molality $b^0 = 1$ mol/kg. The relationship between concentration and activity is then

$$a_i = \gamma_i \cdot \frac{b_i}{b^0} \quad (\text{with } \lim_{b_i \to 0} \gamma_i = 1) \tag{7.1}$$

where b_i is the concentration in mol/kg of a dissolved species i and γ_i is its *activity coefficient*.

In the case of a solution of a salt, the physico-chemical methods constantly refer to the *mean ionic activity* $a_{i_\pm}$, since both ions must be dissolved to maintain electroneutrality in the solution. The mean ionic activity of an electrolyte is defined as the geometric mean of the ion activities

$$a_{i_\pm} = \left(a_{i_+}^{\nu^+} \cdot a_{i_-}^{\nu^-}\right)^{\frac{1}{\nu}} \tag{7.2}$$

where ν^+ and $\nu^-$are the amounts of positive and negative ions resulting from the dissociation of one formula unit of the salt, and $\nu = \nu^+ + \nu^-$. For example, for NaCl $a_{HCl_\pm} = \left(a_{H_+} \cdot a_{Cl_-}\right)^{\frac{1}{2}}$.

Using the mean ionic activity coefficient $\gamma_{i_\pm}$, defined similarly to the mean ionic activity, it results

$$a_{i_\pm} = \gamma_{i_\pm} \cdot \frac{b_i}{b^0} \tag{7.3}$$

According to the Debye-Hückel limiting law [7.1, 7.3], valid for diluted solutions (< 10^{-3} mol/kg) results

$$\log_{10} \gamma_{i_\pm} = -0.509 \cdot \left|z_{i_+} \cdot z_{i_-}\right| \cdot \sqrt{I} \tag{7.4}$$

where $T = 298\ K$, $b_i \to 0$, z_{i_+} and z_{i_-} are the charges of the positive and negative ions. The dimensionless *ionic strength* I is defined as

$$I = \frac{1}{2} \cdot \sum_i \frac{b_i}{b^0} \cdot z_i^2 \tag{7.5}$$

where b_i is the concentration in mol/kg of each ionic species i, z_i is the charge of each dissolved ionic species and Σ_i is the sum over all the ionic species i. Table 7.2-1 reports some examples on how to calculate the ionic strengths of 1 mol/kg solutions for various salts. The activity of a solid, e. g., insoluble salts or pure metals, is defined as 1.

Table 7.2-1: Examples of ionic-strength calculations of 1 mol/kg solutions of various salts.

Type of salt	I	*Type of salt*	I
1, 1 (NaCl)	$\frac{1}{2}(1 \cdot 1^2 + 1 \cdot 1^2) = 1$	1, 3 ($LaCl_3$)	$\frac{1}{2}(1 \cdot 3^2 + 3 \cdot 1^2) = 6$
1, 2 ($BaCl_2$)	$\frac{1}{2}(1 \cdot 2^2 + 2 \cdot 1^2) = 3$	1, 3 (K_3PO_4)	$\frac{1}{2}(3 \cdot 1^2 + 1 \cdot 3^2) = 6$
2, 2 ($ZnSO_4$)	$\frac{1}{2}(1 \cdot 2^2 + 1 \cdot 2^2) = 4$	2, 3 ($Mg_3(PO_4)_2$)	$\frac{1}{2}(3 \cdot 2^2 + 2 \cdot 3^2) = 15$

In the case of solutions having a concentration higher than 10^{-3} mol/kg (too high ionic strength), the Debye-Hückel limiting law does not fit the real trend anymore, and the activity coefficients can be estimated using a semi-empirical fit of that law, called the ***extended Debye-Hückel law***

$$\log_{10} \gamma_{i_\pm} = -\frac{\mathrm{A} \cdot \left|z_{i_+} \cdot z_{i_-}\right| \cdot \sqrt{I}}{1 + \mathrm{B} \cdot \sqrt{I}} + C \cdot I \tag{7.6}$$

where A, B and C are adjustable empiric parameters characteristic of each salt. This equation also fits the real values only for concentrations below 0.1 mol/kg. For higher concentrations, there is no widely accepted model, and values are determined experimentally or using thermodynamic state functions.

7.2.2 Electrochemical cells and emf

An electrochemical cell consists of two ***electrodes***, which must conduct electrons, in contact with an ionic conductive medium (***electrolyte***). If the two electrodes are in different compartments, an ionic contact between them (***a salt bridge) is required*** to run the cell. An electrochemical cell is called ***galvanic*** if its overall electrochemical reaction is spontaneous (exergonic, $\Delta G < 0$). In this case, an electronic current will flow between the electrodes if they are in electrical contact, and, at the same time, an ionic current will flow through the electrolyte to prevent the separation of ionic charges caused by the ionic species produced. On the contrary, an electrochemical cell is called ***electrolytic*** if its overall electrochemical reaction is non-spontaneous (endergonic, $\Delta G > 0$); in this case, the reaction occurs only if a power supply provides enough electrical work (electric current between the two electrodes) for the electrochemical reaction to proceed.

At each electrode, a ***half-cell reaction*** occurs involving the transfer of electrons, also called ***redox reaction***. If electrons are flowing to an electrode, there is a ***reduction reaction*** that happens, and the electrode is called the ***cathode*** (equation (7.7)). The electrons flowing to the cathode must come from the other electrode, where an ***oxidation reaction*** must occur; this electrode is called the ***anode*** (equation (7.8)). Using the common sign convention, the cathode is the positive electrode in a galvanic cell and the negative electrode in an electrolytic cell, while for the anode, the signs are the opposite.

Cathode: Galvanic cell: $\oplus$
Electrolytic cell: $\ominus$

$$Ox_1 + ne^- \rightleftarrows Red_1 \tag{7.7}$$

Anode: Galvanic cell: $\ominus$
Electrolytic cell: $\oplus$

$$Red_2 \rightleftarrows Ox_2 + ne^- \tag{7.8}$$

$$Ox_1 + Red_2 \rightleftarrows Red_1 + Ox_2 \tag{7.9}$$

If the two electrodes are not in electric contact, only the dynamic equilibria of the single half-cells are active, and no change will occur; this condition is called ***open circuit***. If the two half-cell reactions are not at equilibrium, as soon as the circuit is closed (i.e., the two electrodes are in electrical contact and electrons are flowing), the electrochemical cell can provide electrical work w_e. This quantity is related to the difference in (electrochemical) potential between the two electrodes, called cell voltage, measured in volts (V). The maximum possible electric work w_e^{max} that the cell can perform in

fully reversible conditions is the Gibbs free energy $\Delta G_{p,T}$ at constant pressure and temperature. This is directly related to the cell potential when zero current is flowing through the circuit, which is called the *thermodynamic* or *reversible cell potential* E, formerly called the *electromotive force* (emf). This quantity is measured with a voltmeter at open circuit and is commonly called the *open-circuit voltage* (OCV) of the particular electrochemical cell.

7.2.3 Thermodynamic Cell Potential and Nernst Equation

The relation between the thermodynamic cell potential E and the Gibbs free energy ΔG is:

$$\Delta G = -n \cdot F \cdot E \tag{7.10}$$

where n is the number of electrons exchanged in the electrochemical reaction (equations (7.7) and (7.8)) and F is the Faraday constant (product of the charge of an electron e and the Avogadro number N_A, $F = 96485\ C/mol$). From the sign in the equation, it is easy to infer that E is positive if the ΔG is negative (spontaneous reaction) and vice versa.

It is known that the Gibbs free energy is related to the reaction-mixture composition by

$$\Delta G = \Delta G^0 + R \cdot T \cdot \ln \prod_i a_i^{\nu_i} \tag{7.11}$$

where R is the ideal-gas constant, T is the temperature and $a_i$is the activity of each term i of a chemical reaction elevated to its stoichiometric coefficient ν_i (negative for the reactants). Dividing both sides by $-nF$ and using the equation (7.10) it results in:

$$E = -\frac{\Delta G^0}{n \cdot F} - \frac{R \cdot T}{n \cdot F} \cdot \ln \prod_i a_i^{\nu_i} \tag{7.12}$$

Using equation (7.10), the first term on the right of the equation (7.12) can be defined as the *standard thermodynamic cell potential* E^0 (at $T = 298.15$ K, $p = 1$ atm and $a_i = 1$). Thus, we can write

$$E = E^0 - \frac{R \cdot T}{n \cdot F} \cdot \ln \prod_i a_i^{\nu_i} \tag{7.13}$$

and equation (7.13) is called *Nernst equation*.

The term $\prod_i a_i^{\nu_i}$ is also called the reaction quotient, and it is calculated using the activities a_i at zero current, i. e., before letting the electrons flow through the circuit. Of course, after the electrochemical reaction reaches its equilibrium, its thermodynamic cell potential is zero, exactly like its Gibbs free energy.

7.2.4 Half-cell potentials, standard potentials, and reference electrodes

It is practically nonsense to think of measuring the single potential of only one electrode reaction (half-cell potential) completely separated from a second electrode, or, in other words, everything is relative. Nevertheless, it is possible to measure the potential difference of every possible electrode reaction relative to another, which is characterized by a well-defined potential, called the standard potential, as in all standard conditions used to define the value of the Gibbs free energy of a reaction.

The well-known electrode used as a standard to measure the potential of other electrodes is the *standard hydrogen electrode* (SHE). It is an *electrode of the fourth kind*, i.e., it consists of an inert metal (Pt) in the presence of H_2 gas (at a pressure $p_{H_2} = 1$ atm) immersed in an aqueous solution of the ionic species of the gas (H^+ from an acid, $a_{H^+} = 1$ or pH = 0). The electrochemical notation of the SHE is usually:

$$Pt \mid H_2(g) \mid H^+(aq) \qquad \text{with } a_{H^+} = 1 \text{ at pH = 0 and } p_{H_2} = 1 \text{ atm} \tag{7.14}$$

and the SHE half-cell reaction is:

$$2H^+ + 2e^- \rightleftarrows H_2 \tag{7.15}$$

The SHE potential E^0_{SHE} is, by definition, set to 0 V for all temperatures. Since the SHE is used to measure the potential of other electrodes, it is also called the ***reference electrode***. The ***standard reduction potential*** E^0 (at standard p_i = 1 atm, a_i = 1 and T = 298.15 K) of a different electrode can be obtained by the OCV of the cell consisting of this electrode and the SHE. In this way, a table of potentials for different electrodes was redacted (see Table 7.2-2) and called the electrochemical series [7.4, 7.5]. In this series, the more positive the potential, the more stable the metal/product of the reduction, and the more negative the potential, the more reactive it is. Furthermore, the reduction reaction with a higher potential allows spontaneous oxidation of anything with a lower standard reduction potential.

Table 7.2-2: Examples of some standard reduction potentials E^0 vs. E^0_{SHE} as reported in the electrochemical series [7.4, 7.5].

Electrode	*Reduction reaction*	$E^0\ [V]$
$Pt \mid O_2(g) \mid H^+(aq)$	$O_2 + 4H^+ + 4e^- \rightleftarrows 2H_2O$	1.229
$Pt(s) \mid Pt^{2+}(aq)$	$Pt^{2+} + 2e^- \rightleftarrows Pt$	1.180
$Ag(s) \mid Ag^+(aq)$	$Ag^+ + e^- \rightleftarrows Ag$	0.800
$Cu(s) \mid Cu^+(aq)$	$Cu^+ + e^- \rightleftarrows Cu$	0.521
$Cu(s) \mid Cu^{2+}(aq)$	$Cu^{2+} + 2e^- \rightleftarrows Cu$	0.342
SHE	$2H^+ + 2e^- \rightleftarrows H_2$	0.00000
$Fe(s) \mid Fe^{2+}(aq)$	$Fe^{2+} + 2e^- \rightleftarrows Fe$	-0.447
$Zn(s) \mid Zn^{2+}(aq)$	$Zn^{2+} + 2e^- \rightleftarrows Zn$	-0.762
$Li(s) \mid Li^+$	$Li^+ + e^- \rightleftarrows Li$	-3.040

Another common reference electrode is the ***silver-silver chloride electrode***, consisting of an Ag wire coated with a thin layer of AgCl and immersed in a solution of KCl and saturated AgCl. It is an ***electrode of the second kind***. Its electrochemical half-cell reaction is:

$$Ag \mid AgCl(s) \mid Cl^-(aq) \qquad AgCl + e^- \rightleftarrows Ag(s) + Cl^- \tag{7.16}$$

Applying the Nernst equation to the reaction above, we can derive:

$$E_{AgCl/Ag} = E^0_{AgCl/Ag} - \frac{R \cdot T}{F} \cdot \ln a_{Cl^-} \tag{7.17}$$

This reveals that the $E_{AgCl/Ag}$ is related to the $\ln a_{Cl^-}$.

Equation (7.16) can also be written as a combination of the two reactions:

$$Ag^+ + e^- \rightleftarrows Ag \tag{7.18}$$

$$AgCl \rightleftarrows Ag^+ + Cl^- \tag{7.19}$$

The derivation of the equation (7.17) from the Nernst equation of reaction (7.18) and the solubility equilibrium of the reaction (7.19) is left to the student.

An ***electrode of the third kind*** is an inert metal in a solution of two redox species of the same element.

A further common reference electrode is the ***calomel electrode***, consisting of a Pt wire in electrical contact with liquid mercury and mercury (I) chloride (calomel, Hg_2Cl_2), which, in turn, are in contact with a saturated solution of KCl in water. The electrochemical half-cell reaction is:

$$Pt \mid Hg(s) \mid Hg_2Cl_2(s) \mid Cl^-(aq) \qquad Hg_2Cl_2(s) + 2e^- \rightleftarrows 2Hg(s) + 2Cl^- \tag{7.20}$$

Applying the Nernst equation to the reaction above, we can derive:

$$E_{Hg_2Cl_2/Hg} = E^0_{Hg_2Cl_2/Hg} - \frac{R \cdot T}{2F} \cdot \ln a^2_{Cl^-} = E^0_{Hg_2Cl_2/Hg} - \frac{R \cdot T}{F} \cdot \ln a_{Cl^-} \tag{7.21}$$

7.2.5 The Daniell cell and its temperature dependence

The Daniell cell is a well-known example of a galvanic electrochemical cell. It is composed of a metallic zinc electrode immersed in a solution of Zn(II) sulfate and a metallic copper electrode immersed in a solution of Cu(II) sulfate. The two half-cells are placed in ionic contact with each other using a salt bridge (which contains a salt solution) or an ionically conductive membrane. The cell can be schematized as follows:

$$Zn(s) \mid ZnSO_4(aq) \;\; || \; CuSO_4(aq) \mid Cu(s) \tag{7.22}$$

The half-cell electrodes here are *electrodes of the first kind*.

To understand at which electrode the reduction and at which the oxidation can happen spontaneously, one can think that the reduction reaction with the higher standard potential takes place at the cathode. From Table 7.2-2 it is evident that the cathode is the Cu electrode and the anode is the Zn electrode for a spontaneous electrochemical reaction. This means that, if the two electrodes are in electrical contact, zinc dissolves while copper deposits as metal on the cathode and electrons spontaneously flow from Zn to Cu. If the electrodes are not in electric contact, the following equilibrium reactions occur:

Cathode: $$Cu^{2+} + 2e^- \rightleftarrows Cu \tag{7.23}$$

Anode: $$Zn \rightleftarrows Zn^{2+} + 2e^- \tag{7.24}$$

$$Cu^{2+} + Zn \rightleftarrows Cu + Zn^{2+} \tag{7.25}$$

The standard thermodynamic potential of the galvanic cell E^0 is the difference between the standard reduction potential of the cathode and that of the anode, $E^0 = E_c - E_a$, and can be calculated from Table 7.2-2. For the overall electrochemical reaction (7.25) the cell potential can be calculated using the Nernst equation to be

$$E = E^0 - \frac{R \cdot T}{2 \cdot F} \cdot \ln \frac{a_{Zn^{2+}} \cdot a_{Cu}}{a_{Cu^{2+}} \cdot a_{Zn}} \tag{7.26}$$

Cell potential can be measured with voltmeters, characterized by a high internal electrical resistance and designed to determine the voltage difference between two electrodes with negligible current flow between them, thereby minimizing perturbation and obtaining a true OCV (open-circuit voltage).

The temperature dependence of the cell potential is evident in the second term of the equation (7.26). Furthermore, the standard thermodynamic potential of the galvanic cell E^0 has an intrinsic temperature dependence. Since ΔG is directly proportional to E according to the equation (7.10), we can use the Gibbs-Helmholtz equation to get the dependence of ΔG with temperature at constant pressure:

$$\left(\frac{\partial \Delta G}{\partial T}\right)_p = -\Delta S = \frac{\Delta G - \Delta H}{T} \tag{7.27}$$

$$\Delta H = \Delta G - T \cdot \left(\frac{\partial \Delta G}{\partial T}\right)_p \tag{7.28}$$

By substituting the equation (7.10) in the previous, we obtain:

$$\Delta H = -n \cdot F \cdot \left[E - T \cdot \left(\frac{\partial E}{\partial T}\right)_p\right] \tag{7.29}$$

Using this equation, we can also derive the reaction enthalpy ΔH of the Daniell-cell reaction, knowing the derivative of E with temperature at constant pressure.

7.3 Experimental details and evaluation

7.3.1 Experimental execution

General Preparation

Adjust the filling level of the water bath to the lower mark (for the reference electrode measurements, **1**) as in Figure 7.1. Turn on the cooling for the water bath (**2**). Turn on the equipment for potential and temperature measurements: the Cobra4 Mobile-Link (**3**), the computer (for basic instructions on how to use the software, see Chapter 12) and the thermostat (**4**). Set the temperature to 25 °C by pressing the yellow button twice, adjusting it with the red and blue buttons, and locking the setting by pressing the yellow button once more. The glass sleeves for the temperature sensors (**5**, **5***) are filled to a height of ≈1 cm with deionized water, and the temperature sensors are inserted into the sleeves so that their tips are immersed in the liquid. Hereinafter, the term "temperature sensor" means its combination with the glass sleeve. **Always handle delicate equipment carefully, especially the glass cell and electrodes!**

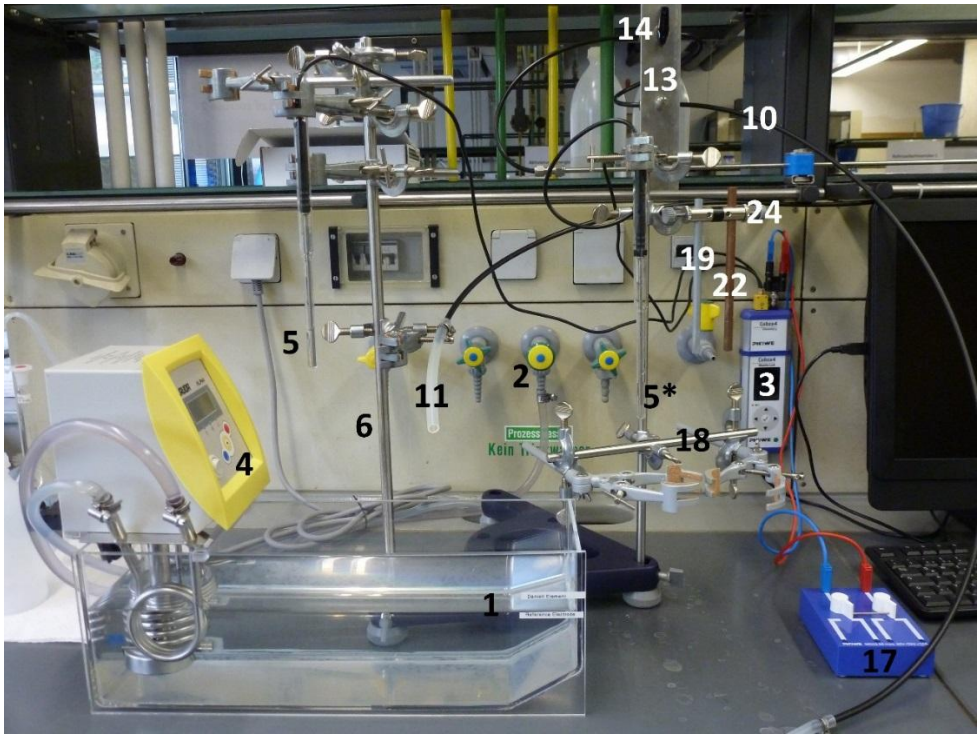

Figure 7.1: Workplace for electromotive-force experiments and its parts. (**1**) Water level marks, (**2**) cooling water, (**3**) Cobra4 Mobile-Link, (**4**) thermostat, (**5, 5***) temperature sensors, (**6**) left supporting rod, (**10**) hydrogen inlet tube, (**11**) hydrogen outlet tube, (**13**) needle valve, (**14**) hydrogen main plug, (**17**) switch, (**18**) stand arm, (**19**) Zn rod, (**22**) Cu rod and (**24**) electrode holder.

Standard Hydrogen Electrode and other reference electrodes

Move the stand to the right, so that the left support rod (**6**) is roughly in the middle of the water bath (Figure 7.1). Fill the 250 mL beaker (**25**) to the 200 mL mark with 1 m hydrochloric acid (for 1 m HCl $\gamma_{HCl_{\pm}} = 0.809$ [7.6, 7.7]) and place it in the water bath. Clamp the cell for the Standard Hydrogen Electrode (SHE, **7**) at the joint and position it so that the exit of the electrolyte bridge is roughly 2 cm above the HCl solution (Figure 7.2). Insert the **non-greased** glass plug into the electrolyte bridge (**8**) in the open position.

Think about why it is important to use a non-greased glass plug.

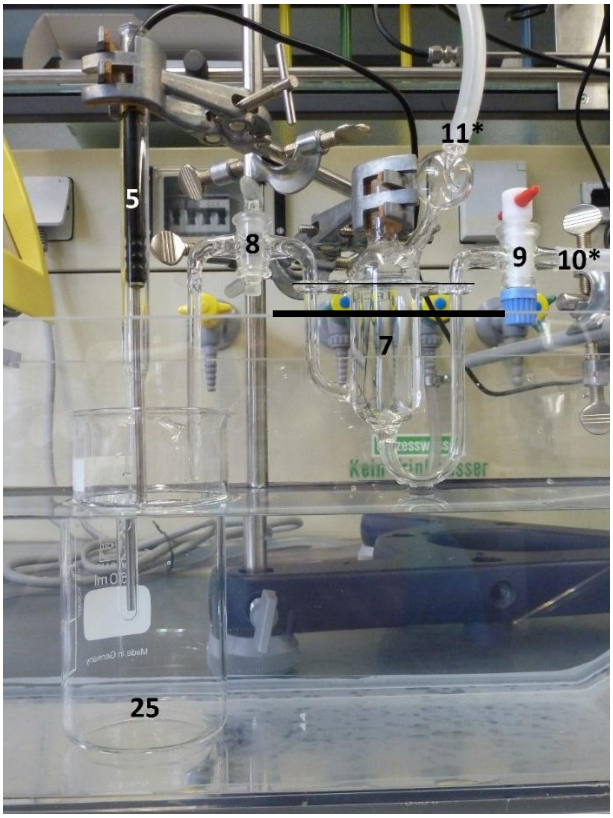

Figure 7.2: Preparation of the standard hydrogen electrode. (**5**) Temperature sensor 1, (**7**) standard hydrogen electrode cell, (**8**) electrolyte bridge/glass valve, (**9**) hydrogen inlet valve, (**10***) hydrogen intake, (**11***) hydrogen outlet, and (**25**) HCl beaker. The black line over the (**7**) SHE cell shows where the HCl level is supposed to be.

Insert the other plug in the hydrogen intake (**9**) in the closed position. Now fill the cell slowly with 1 m HCl using a funnel until the electrolyte runs through the electrolyte bridge. Turn the plug 2-3 times to create an electrolyte film, let the electrolyte leak until the level reaches the glass branches (black line), and close the plug. **Take care that no large bubbles (= no liquid connection) are present in the electrolyte bridge!** If the bridge is blocked, repeat the filling process. Now lower the cell until the plugs are just above the water. Use the "CLEANING" beaker (600 mL) and a washing water bottle to rinse the platinum electrode (**12**) with deionized water and insert it.

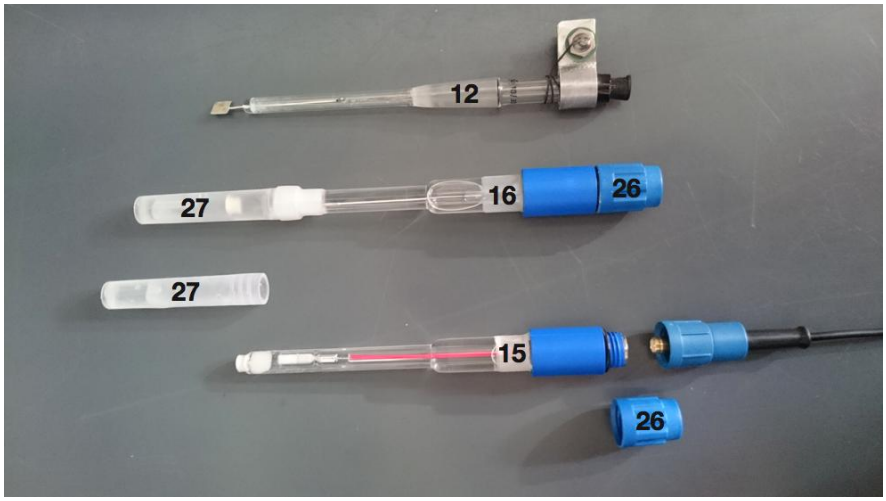

Figure 7.3: Electrodes. (**12**) Platinum electrode, (**15**) calomel electrode (with a red wire inside), (**16**) silver-silver chloride electrode, (**26**) blue cap, and (**27**) protective cap.

Screw off the blue caps (**26**) of the other electrodes and connect the cables. The protecting caps (**27**) from the saturated calomel electrode (**15**, in saturated KCl, $\gamma_{KCl_{\pm}} = 0.583$ [7.7]) and the silver-silver chloride (**16**, Ag/AgCl, in saturated KCl+AgCl) reference electrode are removed carefully, the electrodes are rinsed with deionized water, and inserted in the HCl-filled beaker (**25**). The temperature sensor number 1 (T1, **5**) is rinsed with deionized water, inserted into the protection glass cover (filled with 1 cm of water), and then put into the acid. No sensors or electrodes may come into contact with the beaker. Connect the hydrogen inlet tube (**10**) to the intake (**10***) and the outlet tube (**11**) to the outlet (**11***). First, open the valve at the cell (**9**), then the main valve (**14**) for hydrogen flow. **The needle valve (13) should not be touched**, as it is already set for the correct volume flow rate.

The hydrogen flow must be maintained for at least 5-10 minutes before measurements can begin. Think about possible reasons.

The configuration "ReferenceElectrode" is loaded on the software as described in Chapter 12. Three separate measurements (calomel vs. SHE; Ag/AgCl vs. SHE; Ag/AgCl vs. calomel) are performed. The electrodes are connected to the switch (**17**, Figure 7.4). The switch is connected to the Cobra4 Mobile-Link, which measures the potential difference between the working electrode (WE, red) and the reference electrode (RE, blue). The blue and black wires connect both switch branches to the SHE (platinum electrode). Measurements should start only once the potential is steady (± 0.2 mV). Each measurement stops automatically after 3 minutes.

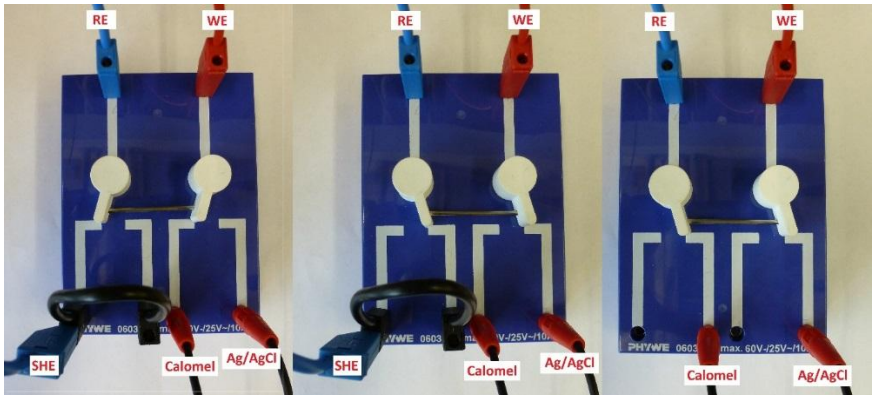

Figure 7.4: Connection of the cables and switch positions for the three reference electrode measurements: calomel electrode vs. SHE (left); Ag/AgCl vs. SHE (middle); Ag/AgCl vs. calomel electrode (right).

After all measurements are completed and the data are exported to an Excel file, the hydrogen flow is stopped by closing the main plug (**14**). Afterward, all electrodes are rinsed thoroughly with deionized water and stored as found. Make sure the white frits at the tips of the reference electrodes are in contact with the storage solution to prevent drying. Clean the other equipment carefully.

Daniell cell

After dismantling the reference electrode setup, all stand clamps must be moved high enough to move the stand to the left (Figure 7.5). The stand arm (**18**) is lowered as much as possible. Roughly 40 mL of 0.5 m $ZnSO_4$ ($\gamma_{ZnSO4_{\pm}} = 0.063$) and $CuSO_4$ solutions 0.5 m ($\gamma_{CuSO4_{\pm}} = 0.062$) [7.6], 0.05 m ($\gamma_{CuSO4_{\pm}} = 0.201$) and 0.005 m ($\gamma_{CuSO4_{\pm}} = 0.484$) [7.8] are filled in the corresponding 150 mL beaker. The $ZnSO_4$ beaker (**20**) is placed in the water bath and fixed with the left clamp. The beaker (**21**) with the lowest concentration, 0.005 m $CuSO_4$, is placed on the other side.

Rinse both temperature sensors with water and insert the first one (T1, **5**) in the $ZnSO_4$-containing beaker and the second one (T2, **5***) in the $CuSO_4$-containing beaker. The Zn (**19**) and Cu (**22**) rods are carefully sandpapered, rinsed with water,

inserted, and lowered until they are immersed to roughly 1 cm in their respective salt solutions. Set the temperature to 25°C and wait for its rough equilibration.

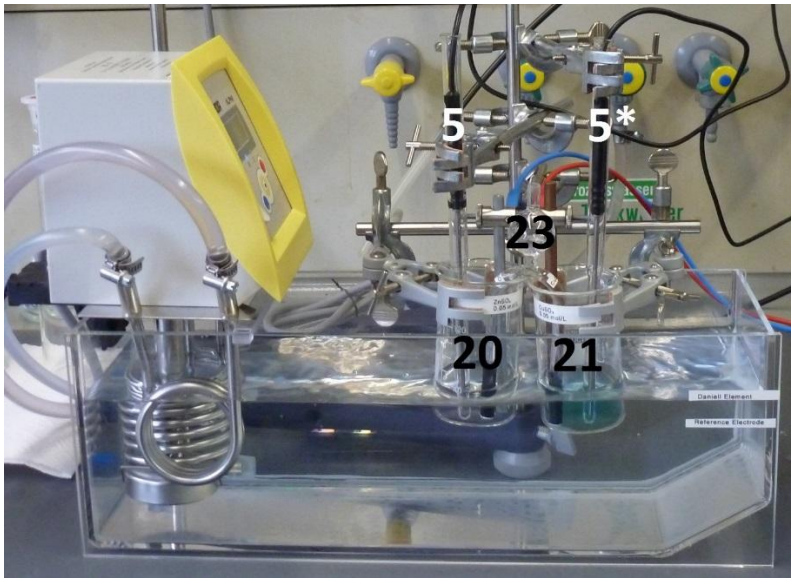

Figure 7.5: Setup for Daniell-cell measurements. Temperature sensors (**5**) T1 and (**5***) T2, (**20**) $ZnSO_4$ beaker, (**21**) $CuSO_4$ beaker, and (**23**) electrolyte bridge.

Connect the blue cable to the Zn side of the electrode holder (**24**) and the red cable to the Cu side. Move the switch in Figure 7.6 so that the electrodes are disconnected from the Cobra4 unit (open circuit), and both cables are connected to the switch.

Then the electrolyte bridge (**23**) is filled with 0.5 m NH_4Cl solution using a Pasteur pipette. **Make sure to remove all air bubbles by shaking and snapping against the glass**. Some electrolyte should be in the reservoir. Rinse the black side of the salt bridge with water, then insert one arm into each beaker. Immerse the salt bridge only after temperature equilibration and just before starting the voltage measurement. **To avoid contamination, always make sure that the $CuSO_4$ arm (blueish clay frit, labeled) is exclusively in contact with $CuSO_4$ solution and the $ZnSO_4$ arm (white clay frit, labeled) is exclusively in contact with $ZnSO_4$ solution**.

On the software, load the configuration “DaniellElement” as described in Chapter 12. Insert the salt bridge, close the circuit by acting on the switch, and start the measurement.

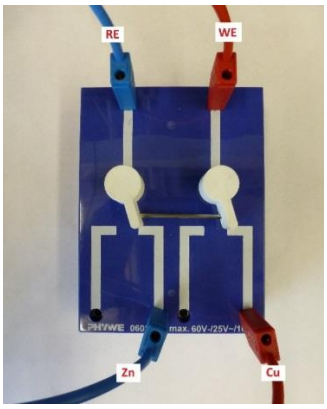

Figure 7.6: Connection of cables and switch positions for Daniell-cell measurements.

Check the electrolyte bridge if the potential is not stable. Empty and refill it, if necessary. Stop the measurement by clicking on the black square after you have enough data on the variability of the potential one minute should be enough) and open the circuit by acting on the switch. Transfer the data to an Excel sheet as described in Chapter 12.

Remove and rinse the electrolyte bridge and the second temperature sensor, and move up and rinse the Cu electrode too. Replace the $CuSO_4$-containing beaker and repeat the measurement first for the 0.05 m and then for the 0.5 m solution.

After investigating the variation of the thermodynamic potential with the concentration, its variation with temperature is considered. Before this, sandpaper the electrodes carefully and rinse them again. Then use the 1 m solutions for both the sulfates (the activity coefficients of the two solutions are very similar: $\gamma_{ZnSO4_{\pm}} = 0.0435$, $\gamma_{CuSO4_{\pm}} = 0.0423$ [7.6]). **Make sure to carefully remove any deposits that may have formed on Zn and Cu to avoid artifacts in the measured potential!**

After dipping the electrodes in the solutions, let the temperature of both the solutions stabilize to **roughly** 25 °C. Then insert the salt bridge and measure the potential until you have enough data on its variability (one minute should be enough). It is better to **remove the salt bridge and the electrodes while varying the temperature**. Set the water-bath temperature to 36, then to 47 °C to aim for reaction temperatures of **roughly** 35 and 45 °C. When the temperature is **roughly** reached (it takes 10–15 minutes), you can insert the salt bridge and the electrodes again and start measuring the cell voltage for 1 minute.

After transferring the data to Excel, set the temperature back to 25 °C, clean all equipment thoroughly, and wash the electrolyte bridge once with water.

Think about an explanation why a deposit can be formed on the electrodes and why we are disconnecting the cell while the temperature is stabilizing.

7.3.2 Data evaluation

- ☐ Evaluate the reference electrode potentials, comparing your measurements to the theoretical values that you can calculate starting from the electrochemical series [7.4, 7.5], using the Nernst equation and the activity coefficients reported in the experimental execution [7.6-7.8]. Discuss deviations.
- ☐ Consider the variation of the potential of the Daniell cell with the concentration of copper sulfate. Compare your measurements to the theoretical values that you can calculate starting from the electrochemical series [7.4, 7.5], using the Nernst equation and the activity coefficients reported in the experimental execution [7.6-7.8]. Discuss deviations. Plot the measured potential as a function of $\ln a_{Zn^{2+}}/a_{Cu^{2+}}$ and extract the standard cell potential E^0 and ΔG^0 by extrapolating to an activity ratio of 1.
- ☐ Consider the variation with temperature of the potential of the Daniell element measured at an activity ratio of 1 and plot the measured potentials as a function of temperature.
- ☐ Estimate the ΔH of the Daniell-cell reaction from $\left(\frac{\partial E}{\partial T}\right)_p$ using the equation (7.29) derived using the Gibbs-Helmholtz relation.
- ☐ Perform an error analysis for all calculations.

7.4 Applications of the experiment and its theory

- ☑ The cell potential and the Nernst equation allow us to predict the thermodynamic reversible potential of every electrochemical device, i.e., the maximum possible voltage in a galvanic cell and the minimum voltage required for an electrolytic cell.

- ☑ Examples of mature technologies that employ electrochemical cells are the old alkaline batteries for small portable devices and the lead-acid batteries that help to start the internal combustion engine of a vehicle. Do you know which electrochemical reactions are occurring in those devices, and what their reversible cell potentials are?
- ☑ The urge to reduce the human CO_2 footprint has led to the use of electrochemical devices for energy conversion across many applications. The transportation sector is of paramount importance, where Li batteries and fuel cells are possible substitutes for internal combustion engines. Li-ion batteries are characterized by the ability to store much more energy per unit mass than other past technologies, such as those cited above, also due to their much higher cell voltage. Do you know the functioning principle of a Li-ion battery? What are their cell voltage and reversible cell potential? How is it possible that such a high difference exists between the old technologies and this relatively new one?
- ☑ In a fuel cell, the chemical energy of a fuel is converted directly to electrical energy, with an energy efficiency much higher than that of an internal combustion engine. A possible fuel is H_2, and the cell reaction is that of a controlled electrochemical combustion, with O_2 from air reduced at the cathode. The students could calculate the reversible potential of a fuel cell from Table 7.2-2.

7.5 Literature

7.1 - P.W. Atkins, Physical Chemistry, 6th ed., Oxford University Press, Oxford (1998), pp. 243-270.

7.2 - P.W. Atkins and J. de Paula, Atkins' Physical Chemistry, 8th ed., Oxford University Press, Oxford (2006), pp. 216-224.

7.3 - P.W. Atkins and J. de Paula, Atkins' Physical Chemistry, 8th ed., Oxford University Press, Oxford (2006), pp.163-165.

7.4 - CRC Handbook of Chemistry and Physics., 91st edition, CRC Press,: Boca Raton, FL, (2009-2010); pp. 8-20,8-29. https://diverdi.colostate.edu/all_courses/CRC%20reference%20data/electrochemical%20series.pdf (Accessed on 25 October 2024).

7.5 - S.G.Bratsch, *J. Phys. Chem. Ref. Data*, **18** (1989), 1–21. https://www.nist.gov/sites/default/files/documents/srd/jpcrd355.pdf (Accessed on 25th October 2024).

7.6 - CRC Handbook of Chemistry and Physics, 95th edition, CRC Press, Boca Raton, FL, (2014-2015); p. 5-104.

7.7 - (Accessed on 25 October 2024).

7.8 - K. S. Pitzer, *J. Chem. Soc., Faraday Trans*. 2, **68** (1972), 101–113. https://pubs.rsc.org/en/content/articlelanding/1972/f2/f29726800101 (Accessed on 25 October 2024).

8 Activation Energy of a First-Order Reaction

8.1 Context and aim of the experiment

In this experiment, the activation energy of a first-order reaction is estimated. To do this, the activation energy is determined by measuring the temperature dependence of a reaction rate constant [8.1 - 8.5].

8.1.1 Important concepts to know

Reaction kinetics, reaction rate constant, rate-limiting step, reaction order, Arrhenius equation, activation energy, integration of the differential equation for first-order reactions, conductivity, reaction coordinate, half-life, elementary reactions, molecularity.

8.1.2 Most common questions to be answered

- How can you prove the existence of a first-order reaction graphically?
- Can the activation energy change with temperature? If so, consider an explanation.
- What indicates a non-linear Arrhenius behavior?
- Think about the pre-exponential factor of the Arrhenius equation. How does it change for different types of reactions?
- What is the unit of the measured conductivity? Try to explain it more familiarly. How can you derive the unit for the conductivity from the setting of the used electrode?

8.1.3 Further preparations before the experiment

Before performing the experiment, prepare a worksheet as follows:

Table 8.1-1: Example of the table to prepare for data collection and evaluation.

$T = \dots K$	*t (s)*	χ_C *(S cm^{-1})*	$\chi_{CE} - \chi_C$ *(S cm^{-1})*	$\frac{\chi_{CE}}{\chi_{CE} - \chi_C}$
	…	…	…	…
	…	…	…	…
	…	…	…	…
	…	…	…	…

8.2 Theory

In biology and chemistry, the analysis of reaction kinetics has two important impacts. On the one hand, it is possible to investigate reaction mechanisms; on the other hand, it is very interesting to know the rates, which are quite high for many reactions of interest.

8.2.1 Reaction rate, reaction order, and molecularity

For a reaction with i partners, the *reaction rate* v is defined as

$$v = \frac{1}{\nu_i}\frac{d[i]}{dt} \tag{8.1}$$

where the stoichiometric coefficients ν_i are negative for the educts and positive for the products. As an example, for the reaction

$$2A + B \rightarrow 3C + 2H^+ \tag{8.2}$$

the reaction rate is

$$v = \frac{1}{3}\frac{d[C]}{dt} = \frac{1}{2}\frac{d[H^+]}{dt} = -\frac{1}{2}\frac{d[A]}{dt} = -\frac{d[B]}{dt} \tag{8.3}$$

where $[C]$, $[H^+]$, $[A]$ and $[B]$ are the actual concentrations of the different species during the reaction. Often, an empirical time dependence of the following form is found

$$v = k \cdot [A]^x \cdot [B]^y \tag{8.4}$$

The parameter k is the proportionality constant and is called the *reaction rate constant*, while $x + y$ is the reaction order. Since equation (8.2) is an overall reaction, which can include totally different elementary reactions in its mechanism, x and y are usually not equal to one or two. The terms x and y can also be fractional numbers and must not be mixed up with molecularity. The latter is only defined for elementary reactions, of which there are only three types (Table 8.2-1).

Table 8.2-1: Overview of elementary reactions.

Molecularity	Reaction scheme	Example
Unimolecular	$A \rightarrow P$	Decay reactions
Bimolecular	$A + B \rightarrow P$ $2A \rightarrow P$	many chemical and bio-chemical reactions
Trimolecular	$A + B + C \rightarrow P$ $2A + B \rightarrow P$ $3A \rightarrow P$	quite rare, only in the gas phase e. g., $2NO + O_2 \rightarrow 2NO_2$

8.2.2 Differential equation and time course of an irreversible first-order reaction

Integration of the differential equations yields the time courses of the reactions and is relatively simple for even-numbered reaction orders. For an irreversible first-order reaction:

$$A \xrightarrow{k} B \tag{8.5}$$

The reaction rate v is proportional to the concentration of one of the reacting substances at each time t of the reaction.

$$v = -\frac{d[A]}{dt} = k[A] \tag{8.6}$$

with k in s^{-1}. Thus, the real reaction rate changes permanently during the reaction and equals the product of the reaction rate constant and the actual concentration. The reaction rate is highest at the beginning of the reaction and decreases as the reactant concentration decreases. Integration of the differential equation gives

$$\int_{[A]_0}^{[A]_t} \frac{d[A]}{[A]} = -\int_0^t k \cdot dt \tag{8.7}$$

and for $t = 0$

$$\ln\frac{[A]_0}{[A]} = k \cdot t \tag{8.8}$$

$$[A] = [A]_0 \cdot e^{-k \cdot t} \tag{8.9}$$

This reveals that a graph of $\ln[A]$ as a function of t gives a straight line with the slope $m = k$ and the intercept $b = \ln[A]_0$. The half-life of the reaction, where $[A] = [A]_0/2$ is

$$t_{1/2} = \frac{1}{k} \cdot \ln 2 \tag{8.10}$$

8.2.3 Temperature dependence of a reaction rate constant

Van't Hoff and Arrhenius empirically found that the temperature dependence of reaction rate constants often could be described using the following equation

$$k = A \cdot e^{-\frac{E_A}{R \cdot T}} \tag{8.11}$$

This relation is called the *Arrhenius equation*. A is the Arrhenius *pre-exponential factor*, which equals the rate constant in case all the collisions lead to reaction. Additionally, A includes a steric factor, which takes into account that the reactants have to be properly aligned during the collision for the reaction to occur. E_A is the Arrhenius *activation energy*, which can vary significantly across different reactions. In the Arrhenius equation, we can see a Boltzmann factor, which gives the fraction of molecules with energy higher than E_A (see Figure 8.1) and a constant, temperature-independent pre-exponential factor A. According to the Maxwell-Boltzmann equation, the number of molecules with kinetic energy higher than E_A is dependent on temperature.

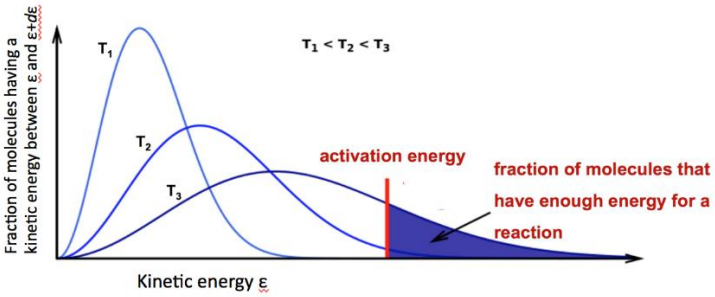

Figure 8.1: Molecular interpretation of the activation energy.

Equation (8.11) is only valid in a relatively small temperature region, therefore it is better to write

$$\frac{d(\ln k)}{dT} = \frac{E_A}{R \cdot T^2} \tag{8.12}$$

or

$$\frac{d(\ln k)}{d(1/T)} = -\frac{E_A}{R} \tag{8.13}$$

and

$$\ln \frac{k_1}{k_2} = \frac{E_A}{R}\left(\frac{1}{T_2} - \frac{1}{T_1}\right) \tag{8.14}$$

Thus, the activation energy can be determined graphically by plotting $\ln k$ versus $1/T$. This plot is called the Arrhenius plot (see Figure 8.2).

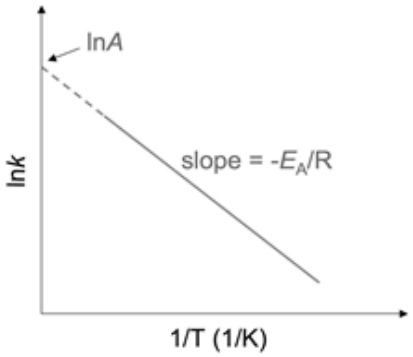

Figure 8.2: Schematic depiction of an Arrhenius plot.

8.2.4 Correlation between activation energy and reaction enthalpy

For the reversible reaction

$$A \underset{k_{back}}{\overset{k_{forw}}{\rightleftarrows}} B \tag{8.15}$$

with the equilibrium constant

$$K = \frac{k_{forw}}{k_{back}} \tag{8.16}$$

we obtain

$$\frac{d(\ln k_{forw})}{dT} - \frac{d(\ln k_{back})}{dT} = \frac{d(\ln K)}{dT} = \frac{\Delta H^0}{R \cdot T^2} \tag{8.17}$$

where ΔH^0 is the Van't Hoff enthalpy or *reaction enthalpy*. This shows that the activation energy is directly correlated to the reaction enthalpy (see Figure 8.3).

$$E_{A,back} - E_{A,forw} = \Delta H^0 \tag{8.18}$$

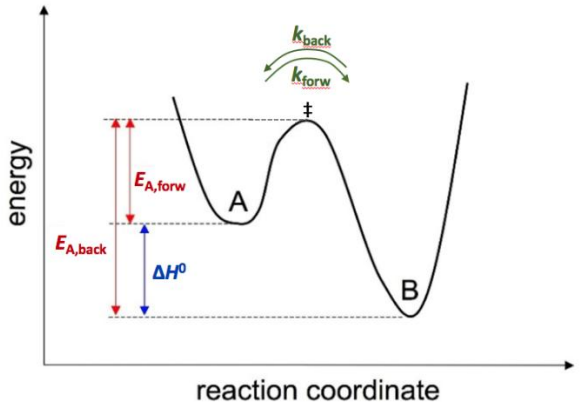

Figure 8.3: Correlation between the activation energy and the reaction enthalpy.

8.2.5 Decomposition of the tertiary amyl bromide

In this experiment, the decay of tertiary amyl bromide is considered

$$C_2H_5(CH_3)_2CBr \longrightarrow [C_2H_5(CH_3)_2C^+] + Br^- \quad \textit{slow} \tag{8.19}$$

$$[C_2H_5(CH_3)_2C^+] + H_2O \rightarrow C_2H_5(CH_3)_2COH + H^+ \quad \textit{fast} \tag{8.20}$$

Following a *S_N1* reaction mechanism, tertiary amyl bromide decomposes in solution into bromide ions and a tertiary amyl cation. The latter reacts instantaneously with water, forming a non-dissociated alcohol. The rate-determining step in the overall reaction is the decomposition of amyl bromide, which is a first-order reaction.

If x designates the reaction turnover (concentration of HBr produced), then the concentration c of amyl bromide is

$$c = c_0 - x \tag{8.21}$$

HBr is present in its dissociated form. Therefore, its concentration can be followed by conductivity measurements. The turnover is proportional to the conductivity χ_C in the measuring cell. The final conductivity χ_{CE}, reached when the reaction process is completed, is proportional to the initial concentration c_0 of amylbromide. Thus, measuring conductivity provides an easy way to monitor changes in concentration during the reaction.

The above approach yields

$$\frac{c_0}{c} = \frac{c_0}{c_0 - x} = \frac{\chi_{CE}}{\chi_{CE} - \chi_C} \tag{8.22}$$

and equation (8.8) can be converted to

$$\ln \frac{\chi_{CE}}{\chi_{CE} - \chi_C} = k \cdot t \tag{8.23}$$

8.3 Experimental details and evaluation

8.3.1 Experimental execution

The conductivity measurements are performed with special conductivity electrodes (**3**) (see Figure 8.4) that provide the temperature of the solution simultaneously.

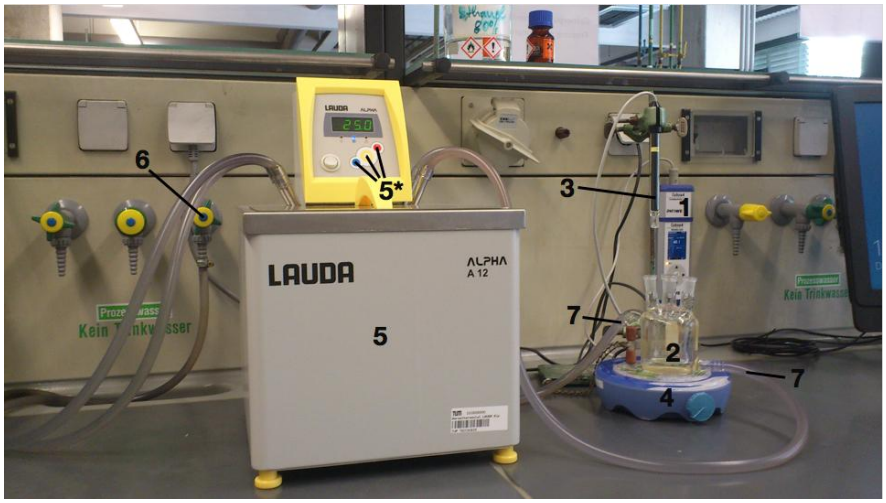

Figure 8.4: Experimental setup in all its parts. (**1**) Cobra 4 Mobile-Link, (**2**) measuring cell, (**3**) conductivity electrode, (**4**) magnetic stirrer, (**5**) thermostat, (**5***) buttons to regulate the set temperature, (**6**) valve to turn on and off the cooling water, (**7**) tubes connecting measuring cell and thermostat.

Turn on the equipment for conductivity measurement: the Cobra 4 Mobile-Link (**1**) and the computer (for basic instructions on how to use the software, see Chapter 12). Clean the measuring cell (**2**) thoroughly. **Always handle delicate equipment with care**. First, rinse the conductivity electrode (**3**) with ethanol. Then take the glass cell (**2**) from the holder and rinse it once with alcohol over a washbowl. For washing, use the ethanol provided in the plastic bottle, not the concentrated 80 vol% ethanol in the glass bottle. Furthermore, clean the stirring bar with alcohol and put it into the measuring cell (**2**).

Now, fill the cell with 80 mL of 80 vol% ethanol from the glass bottle and insert the electrode. The probe must be completely immersed in the solvent. Then, turn on the thermostat (**5**) and adjust the temperature to obtain $T = 25 \pm 0.5$ °C in the reaction solution. The set temperature of the thermostat can be adjusted by pressing the yellow button (**5***) of the thermostat twice. The display starts blinking, and the set temperature can be regulated using the red and blue buttons with the arrows pointing up and down (**5***). Finally, the yellow button (**5***) must be pressed once to confirm the set temperature. **Do not forget to turn on the cooling water! (6)**. Furthermore, turn on the magnetic stirrer (**4**), but take care that it does not touch the conductivity probe.

When the solvent has reached the desired temperature, add 0.5 mL of tertiary amyl bromide through one of the openings in the measuring cell using a clean, dry pipette. **It is important that the amount of amyl bromide be measured exactly**.

Measure the conductivity as a function of time at $T = 25(\pm 0.5)$ °C and then clean the cell and electrode, and repeat the same experiment at $T = 30(\pm 0.5)$ °C and $T = 35(\pm 0.5)$ °C as a function of time for each temperature. At $T = 25$ °C and $T = 30$ °C data collection must last 30 minutes. At $T = 35$ °C the conductivity measurement has to last until the reaction is finished.

Think about how you can ensure that the reaction process is finished and discuss it with your supervisor before you start the experiment.

As mentioned above, it is important to measure the amount of amyl bromide exactly. What happens if the initial concentration of amyl bromide varies for the three measurements?

Enter the collected data in the prepared table (see Table 8.1-1). At T = 25 °C and T = 30 °C, the final conductivity χ_{CE} is reached only after quite a long time. Therefore, χ_{CE} for all temperatures is measured using the solution after the last measurement at T = 35 °C, for which the reaction was completed. To do this, set the thermostat (**5**) to 20 °C, add ice into the water reservoir of the thermostat to speed up the cooling process while collecting conductivity data, and measure the final conductivity χ_{CE} also at T = 25 °C and T = 30 °C. **Take care that the water does not overflow**.

How can you explain that the final conductivity varies with different temperatures?

8.3.2 Data evaluation

- ☐ Plot $ln(\chi_{CE}/\chi_{CE} - \chi_C)$ as a function of time for the three temperatures, and determine the reaction-rate constant k from the slope of the straight line according to the equation (8.23). Use an adequate number of data points for this evaluation.
- ☐ Determine the half-life $t_{1/2}$ of the reaction for the three temperatures.
- ☐ Plot $ln\, k$ vs. $1/T$ and determine the activation energy E_A from the resulting straight line.
- ☐ Perform an error analysis for all calculations.

8.4 Applications of the experiment and its theory

- ☑ The effect of temperature on reaction rate constants is important in everyday life, e.g., for extending the shelf life of food by keeping it in your fridge.
- ☑ Activation energy for combustion reactions. E.g., in the petrol engine, the activation energy for the combustion of the present mixture of air and gaseous petrol is provided by an electrical ignition spark (heat energy). By comparison, in a diesel engine, the activation energy for diesel combustion is based solely on the compression of the air-diesel fuel mixture.
- ☑ Lighting a match: frictional heat and pressure provide the activation energy for the spontaneous ignition of chlorate and red phosphorus.
- ☑ Frictional heat provides the activation energy for the explosion of cap bombs.
- ☑ Characterization of the free energy barrier for chemical and biochemical reactions. Comparison with the general rate equation allows determination of the enthalpic (activation enthalpy) and entropic (activation entropy) contributions to the energy barrier.
- ☑ Investigation of the kinetic activity of catalysts.

8.5 Literature

8.1 - P.W. Atkins, Physical Chemistry, 6th ed., Oxford University Press, Oxford (1998), pp. 761-777.

8.2 - P.W. Atkins and J. de Paula, Atkins' Physical Chemistry, 8th ed., Oxford University Press, Oxford (2006), pp. 791-808.

8.3 - G. Wedler, *Lehrbuch der Physikalischen Chemie*, 6th ed., Wiley/VCH (2012).

8.4 - W.J. Moore, *Grundlagen der Physikalischen Chemie,* 1st ed., de Gruyter (1990).

8.5 - R. Brdicka, *Grundlagen der Physikalischen Chemie,* 15th ed., Willey/VCH (1981).

9 Kinetics of the Inversion of Sucrose

9.1 Context and aim of the experiment

The inversion of sucrose is a reaction that can be catalyzed in an acidic environment. In this experiment, polarimetric measurements are performed to investigate the reaction rate at different acid concentrations. The obtained data are used to define the reaction-rate constant [9.1 - 9.3].

9.1.1 Important concepts to know

Kinetics, reaction-rate constant, rate-determining step, thermodynamics, equilibrium constant, catalyst, activation energy, reaction enthalpy, reaction order, molecularity, integration of the differential equation for first-order reactions, reaction coordinates, polarimetry, polarization of light, optically-active molecules, Law of Biot, Law of Malus.

9.1.2 Most common questions to be answered

- How can you prove the existence of a first-order reaction or a pseudo-first-order reaction graphically?
- What are the requirements for a pseudo-first-order reaction?
- How can polarized light be produced?
- What is an optically active substance? Give some examples.
- How does a catalyst act on the kinetics and on the thermodynamics of a reaction?

9.1.3 Further preparations before the experiment

Before performing the experiment, prepare a worksheet as follows:

Table 9.1-1: Example of the table to prepare for data collection and evaluation. α_{exp} stands for the individual rotation angles that are determined experimentally.

sample	*t (s)*	α_{exp} (°)	$\frac{1}{n}\sum_{i=1}^{n}\alpha_{exp,i}$ (°)	$\ln\frac{\alpha(t)-\alpha_\infty}{\alpha_0-\alpha_\infty}$
	…	…	…	…
	…	…	…	…
	…	…	…	…
	…	…	…	…

9.2 Theory

9.2.1 Catalytic reactions

The function of a catalyst can be explained as its effect on decreasing the activation energy E_A of a reaction. This decrease can affect the reaction-rate constant k of a reaction dramatically, since E_A is at the exponent of the Arrhenius equation (see equation (8.11) in Chapter 8) [9.4]. During catalysis, the reactants and the catalyst form one or more intermediate states z, and the highest activation energy of this new mechanism is smaller than the activation energy of the reaction without a catalyst (Figure 9.1); for this reason, the reaction proceeds faster. The catalyst itself is not consumed, but rather regenerated after product formation, much like in a cycle. A single catalyst can thus run through several catalytic cycles. Since the forward

and backward reactions are accelerated equally, the catalyst does change the reaction kinetics but not its thermodynamics (enthalpy ΔH^0).

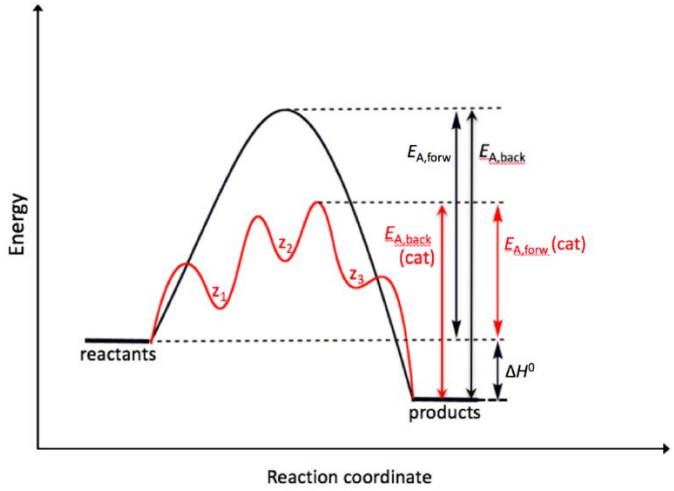

Figure 9.1: A catalyst provides a different reaction path with a lower activation energy. The energy profile of the reaction is shown in the absence (black line) and in the presence (red line) of a catalyst.

In catalysis, the most important reaction mechanism is a series of sequential reactions in which the first step is bimolecular:

$$Cat + S \underset{k_{21}}{\overset{k_{12}}{\rightleftarrows}} CatS \xrightarrow{k_{23}} CatP \longrightarrow Cat + P \tag{9.1}$$

where Cat stands for the catalyst, S for the substrate (the reactant which is bound to the catalyst) and P for the product. The general mathematical solution for this mechanism is complex; however, it can be simplified under certain assumptions.

9.2.2 Kinetics of first-order and pseudo-first-order reactions

Catalytic reaction mechanisms always contain bimolecular steps (Equation (9.1)) but the analysis of second-order kinetics is complex. The reaction rate v for an irreversible, heterogeneous, second-order reaction of the type

$$Cat + S \xrightarrow{k_{bimol}} CatS \tag{9.2}$$

is

$$v = -\frac{d[Cat]}{dt} = -\frac{d[S]}{dt} = k_{bimol} \cdot [Cat] \cdot [S] \tag{9.3}$$

Equation (9.3) can be simplified if one of the involved species is present in a large excess (at least a fivefold excess). For instance, if Cat is present in large excess, its concentration can be approximated to be constant throughout the reaction. Thus, $[Cat]$ can be approximated by $[Cat]_0$ and the rate law becomes apparent first-order. The reaction rate v is then proportional to the concentration of the reactant present at low concentration at each time point of the reaction.

$$v = -\frac{d[S]}{dt} = k' \cdot [S] \text{ with } k' = k_{bimol} \cdot [Cat] \tag{9.4}$$

Reactions in which the observed kinetics is first-order, but the mechanism is second order, are referred to as pseudo-first-order reactions. The integration of the differential equation

$$\int_{[S]_0}^{[S]_t} \frac{d[S]}{[S]} = \int_0^t k' \cdot dt \tag{9.5}$$

that for $t = 0$ gives

$$\ln \frac{[S]}{[S]_0} = -k' \cdot t \tag{9.6}$$

$$[S] = [S]_0 \cdot e^{-k' \cdot t} \tag{9.7}$$

This reveals that a graph of $\ln[S]$ vs. time gives a straight line with the slope $m = k'$. The half-life of the reaction, where $[S] = [S]_0/2$ is

$$t_{½} = \frac{1}{k'} \cdot \ln 2 \tag{9.8}$$

9.2.3 *Polarization of light*

Polarized light is an electromagnetic wave whose electric field vector $\vec{E}$ has a defined orientation relative to the direction of propagation of the wave. It has a transversal character, meaning that the electrical field vector and the magnetic field vector $\vec{B}$ are perpendicular to each other. By convention, the polarization plane of light refers to the direction of the electrical field vector. Natural light is non-polarized, meaning that it is a mixture of waves with polarization planes in all directions perpendicular to the direction of propagation $\vec{k}$. Furthermore, light can exist in different polarization states. In the simplest form of one plane wave in space, it is called linearly polarized light (Figure 9.2). Linearly polarized light can be produced by a polarizer, which acts as an optical filter that allows light of a specific polarization direction to pass and blocks electromagnetic waves of other polarization directions. A mechanical analogy for a polarizer would be a fence with poles in the y-direction. Transversal waves along a rope can only pass the fence without being attenuated if they oscillate in the direction of the y-axis. Passage of linearly polarized light through an optically active substance results in a rotation of the polarization plane.

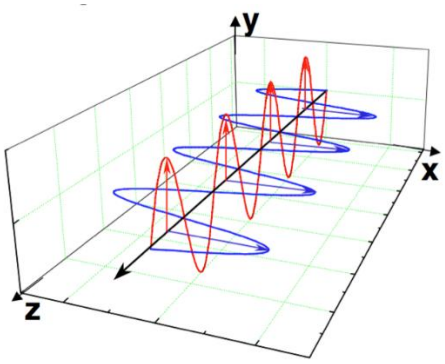

Figure 9.2: The electric (red) and magnetic (blue) components in linear polarized light.

9.2.4 *Optically active molecules*

Chiral molecules can exist in two different structures, which cannot be easily converted between each other with any rotation around a bond, but only by breaking 2 or more chemical bonds. The two structures have the same molecular formula but are not superimposable; they are mirror images of each other. To specify the configuration of a three-dimensional chiral molecule in a two-dimensional picture, the nomenclature introduced by Emil Fischer [9.5 - 9.7] is used (Figure 9.3). Here, the prefixes “D-“ and “L-“ are used to indicate the configuration of the molecule. A typical structural characteristic of chiral molecules is an asymmetrically substituted carbon atom. Chiral molecules are optically active, meaning that they can rotate the polarization plane of linearly polarized light. If such an optically active substance rotates the polarization plane of linearly polarized light to the right (clockwise), this is termed dextrorotation, and the compound is additionally prefixed with (+). If the polarization plane is rotated to the left (counterclockwise), this is termed levorotation, and the compound is additionally prefixed with (-).

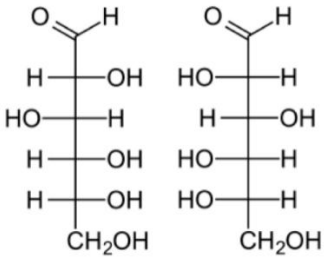

Figure 9.3: Fisher projection of D-glucose (left) and L-glucose (right).

9.2.5 Polarimetry

The rotatory dispersion observed when linearly polarized light passes through an optically active substance provides the basis for polarimetric measurements. The typical setup for a polarimetric experiment is sketched in Figure 9.4. It consists of a light source (often a sodium-vapor discharge lamp) that produces non-polarized light, a polarizer (Nicol prism), a measuring cell filled with the sample, and a second polarizer (called the analyzer, a rotatable Nicol prism) that probes the polarization state after the light passes through the sample.

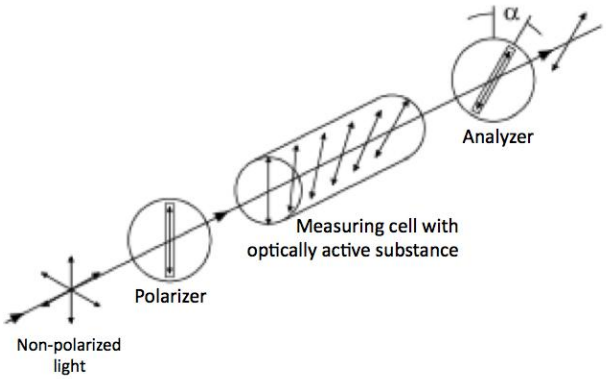

Figure 9.4: Sketch of the typical setup for a polarimetric experiment.

The angle α of rotation is given by

$$\alpha = [\alpha]_{\lambda}^{T} \cdot c \cdot l \tag{9.9}$$

where c denotes the concentration of the optically active substance in grams per milliliter (g/mL). The parameter l is the length of the measuring cell in dm. $[\alpha]_{\lambda}^{T}$ is the *specific rotation* of a substance at a certain wavelength λ and temperature T and it corresponds to the rotation angle detected for 1 g of the optically active substance in 1 mL solution along a path length l = 1 dm. To use the concentration in mol/L, being M the molar mass of the optically active substance, the following relationship needs to be used

$$c\left[\frac{g}{mL}\right] = \frac{1}{1000} \cdot M[\frac{g}{mol}] \cdot c[\frac{mol}{L}] \tag{9.10}$$

The *Malus' law* describes the intensity I of the passed light as a function of the initial light intensity I_0 and the angle α as

$$I = I_0 \cdot cos^2(\alpha) \tag{9.11}$$

9.2.6 Optical activity and decomposition of sucrose

Sucrose (also called saccharose) is the common crystalline sugar used in households. It is a disaccharide consisting of glucose and fructose. In acidic aqueous solution, sucrose is thermodynamically unstable and decomposes hydrolytically into α-D-Glucose and β-D-Fructose (Figure 9.5). The resulting mixture of glucose and fructose, with equal amounts of each, is called inverted sugar. Equilibrium is reached, which lies almost completely on the right side of the reaction; thus, the reaction can be viewed as irreversible. In the absence of acid, almost no sucrose is cleaved.

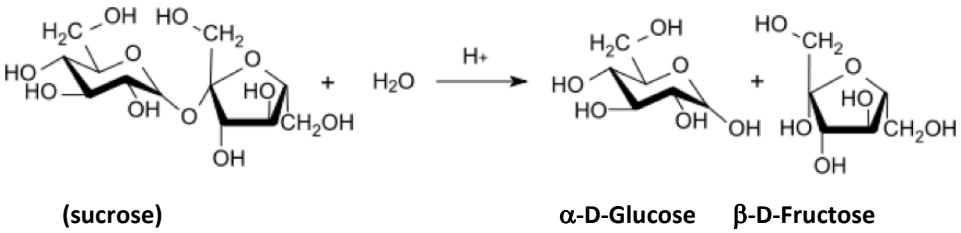

Figure 9.5: Hydrolytic decomposition of sucrose in acidic solution.

The overall reaction process (as shown in Figure 9.5) consists of different sub-reactions (Figure 9.6).

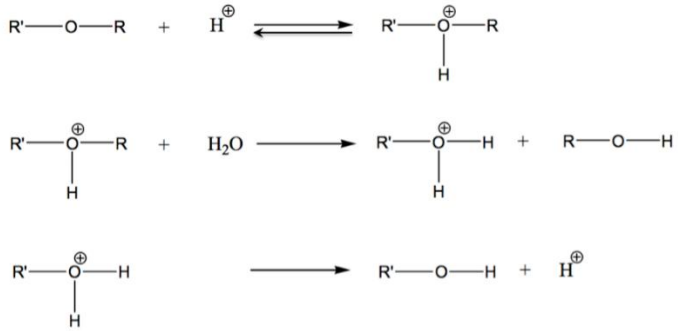

Figure 9.6: Role of H^+ during cleavage of sucrose. Note that protons are not consumed but released at the end of the process, thus acting as catalysts for the hydrolytic decomposition.

The addition of acid leads to the protonation of the oxygen atom that binds glucose and fructose in the disaccharide. The protonation reaction reaches equilibrium very quickly. Thereby, the positive partial charge of the neighboring carbon atoms is increased, allowing the attack of the free electron pairs of the oxygen atom in water at this site. This leads to cleavage of the disaccharide and to subsequent deprotonation. Since protons are not consumed but released at the end of the process, they act as catalysts.

Formally, inversion of sucrose is thus a third-order reaction. Note that the reaction order can only be determined experimentally, and the inversion of sucrose data reveal a first-order reaction. This can be explained by the fact that a trimolecular elementary reaction is extremely unlikely (see Table 8.2-1), since in this case, three molecules must collide simultaneously. Such reactions usually occur in two consecutive bimolecular steps, as is also the case for the inversion of sucrose (see Figure 9.6). Take care that you are familiar with the terms elementary reaction, molecularity, and reaction order; for these, see paragraph 8.2.1.

In the case of the inversion of sucrose, the second bimolecular step is significantly slower compared to the first one ($k_{12} \gg k_{23}$) and thus represents the rate-limiting step. Therefore, the protonation step is described as a fast pre-equilibrium, which depends on the degree of dissociation of the available acid.

$$S(aq) + H^+(aq) \underset{k_{21}}{\overset{k_{12}}{\rightleftharpoons}} SH^+(aq) \xrightarrow{k_{23}} G(aq) + F(aq) + H^+(aq) \tag{9.12}$$

Here S, G and F denote sucrose, glucose, and fructose, respectively. Note that this mechanism agrees with the mechanism usually found for catalyzed reactions (Equation (9.2)). For the kinetics of the decomposition of sucrose and for the formation of the product, we can write:

$$-\frac{d[S]}{dt} = \frac{d[G]}{dt} = \frac{d[F]}{dt} = k_{23} \cdot [SH^+] \cdot [H_2O] \tag{9.13}$$

The concentration $[SH^+]$ of protonated sucrose is determined by the pre-equilibrium:

$$S + H^+ \underset{k_{21}}{\overset{k_{12}}{\rightleftarrows}} SH^+ \tag{9.14}$$

and it is thus given by

$$[SH^+] = K \cdot [S] \cdot [H^+] \tag{9.15}$$

where

$$K = \frac{k_{12}}{k_{21}} = \frac{[SH^+]}{[S] \cdot [H^+]} \tag{9.16}$$

According to the equation (9.15), Equation (9.13) becomes

$$-\frac{d[S]}{dt} = k_{23} \cdot K \cdot [S] \cdot [H^+] \cdot [H_2O] \tag{9.17}$$

Considering that the concentration of protons stays constant, allows the inclusion of $[H^+]$ into the effective reaction-rate constant

$$k' = k_{23} \cdot K \cdot [H^+] \tag{9.18}$$

This leads to

$$-\frac{d[S]}{dt} = k' \cdot [S] \cdot [H_2O] \tag{9.19}$$

The amount of water hardly changes during the reaction since it is present in large excess (pseudo-first-order conditions) and thus, $[H_2O]$ can also be added to the rate constant, and one obtains the pseudo-first-order rate constant k''

$$k'' = k' \cdot [H_2O] \tag{9.20}$$

This explains the experimentally observed first-order reaction. A second-order reaction that can be approximated to a first-order reaction since one of the reactants is present in large excess is called a pseudo-first-order reaction (see paragraph 9.2.2). The decomposition of sucrose can now be written as

$$-\frac{d[S]}{dt} = k'' \cdot [S] \tag{9.21}$$

By solving the differential equation for the concentration of sucrose as in Equation (9.5), we can obtain the relation with time of the decomposition of sucrose as in Equations (9.6) and (9.7)

All three sugars that are involved in the reaction under investigation are optically active due to their asymmetrical carbon atom (Table 9.2-1). This allows determination of the reaction rate from polarimetric measurements.

Table 9.2-1: Specific rotations α at T = 20 °C and λ = 598.3 nm for the species involved in the inversion of sucrose. Data taken from [2.9].

Substance	α (°)
Sucrose	+66.5
D-Glucose	+52.7
D-Fructose	-92.4
1/1 mol/mol D-Glucose/D-Fructose	-19.8

Based on the equation (9.9) and using the concentration given in mol/L, the rotation angle α_0 at the beginning of the reaction is

$$\alpha_0 = l \cdot 1000 \cdot M_S \cdot \alpha_{\lambda,S}^T \cdot [S]_0 \tag{9.22}$$

where M_S is the molecular weight of the sucrose.

At any point in the reaction, the actual total rotation angle $\alpha(t)$ corresponds to the sum of the contributions of the existing species.

$$\alpha(t) = \alpha_S + \alpha_G + \alpha_F = \tag{9.23}$$

$$= l \cdot 1000 \cdot \{M_S \cdot \alpha_{\lambda,S}^T \cdot [S] + M_G \cdot \alpha_{\lambda,G}^T \cdot [G] + M_F \cdot \alpha_{\lambda,F}^T \cdot [F]\}$$

Considering that $[G] = [F] = [S]_0 - [S]$ (from Equation (9.12)) we can write:

$$\begin{aligned} &\alpha(t) = \\ &= l \cdot 1000 \cdot \{M_S \cdot \alpha_{\lambda,S}^T \cdot [S] + M_G \cdot \alpha_{\lambda,G}^T \cdot [G] + M_F \cdot \alpha_{\lambda,F}^T \cdot [F]\} = \\ &= l \cdot 1000 \cdot \{M_S \cdot \alpha_{\lambda,S}^T \cdot [S] + (M_G \cdot \alpha_{\lambda,G}^T + M_F \cdot \alpha_{\lambda,F}^T) \cdot ([S]_0 - [S])\} = \\ &\quad = l \cdot 1000 \cdot \{(M_G \cdot \alpha_{\lambda,G}^T + M_F \cdot \alpha_{\lambda,F}^T) \cdot [S]_0 + (M_S \cdot \alpha_{\lambda,S}^T - M_G \cdot \alpha_{\lambda,G}^T - M_F \cdot \alpha_{\lambda,F}^T) \cdot [S]\} \end{aligned} \tag{9.24}$$

The reactant sucrose turns the polarization plane of linearly polarized light to the right, while the equimolar mixture of glucose and fructose that is formed during the inversion reaction, turns it to the left (Table 9.2-1). As a result, the polarization plane of linearly polarized light turns more to the left, and the overall rotation angle becomes smaller as the inversion reaction proceeds. At the end, the overall rotation angle becomes even negative. This is the reason for the name of the produced inverted sugar. When the reaction is completed, the final rotation angle α_∞ (with $t \to \infty$) is

$$\alpha_\infty = l \cdot 1000 \cdot (M_G \cdot \alpha_{\lambda,G}^T + M_F \cdot \alpha_{\lambda,F}^T) \cdot [S]_0 \tag{9.25}$$

Combining Equations from (9.22) to (9.25) results in the following expressions

$$\alpha(t) - \alpha_\infty = l \cdot 1000 \cdot (M_S \cdot \alpha_{\lambda,S}^T - M_G \cdot \alpha_{\lambda,G}^T - M_F \cdot \alpha_{\lambda,F}^T) \cdot [S] \tag{9.26}$$

$$\alpha_0 - \alpha_\infty = l \cdot 1000 \cdot (M_S \cdot \alpha_{\lambda,S}^T - M_G \cdot \alpha_{\lambda,G}^T - M_F \cdot \alpha_{\lambda,F}^T) \cdot [S]_0 \tag{9.27}$$

This shows that $\alpha(t) - \alpha_\infty$ is proportional to $[S]$ and $\alpha_0 - \alpha_\infty$ is proportional to $[S]_0$, both through the same constant. Inserting this into the equation (9.6) enables getting rid of the specific rotation angles:

$$ln \frac{\alpha(t) - \alpha_\infty}{\alpha_0 - \alpha_\infty} = -k' \cdot t \tag{9.28}$$

Thus, the rate constant for the inversion of sucrose can be determined from the slope of the straight line obtained by plotting $\ln \frac{\alpha(t)-\alpha_\infty}{\alpha_0-\alpha_\infty}$ vs. time.

9.3 Experimental details and evaluation

9.3.1 Experimental execution

Figure 9.7 shows the experimental setup used to follow the inversion of sucrose in all its components. **To use the polarizer (5), refer to its operating manual, which is located on the laboratory bench.** It is a Lippich half-shade polariser; to know the big advantage of its use, you can read the Appendix 9.5.2. **The rotation angle for pure water should be approximately zero degrees. You should never rotate past 20 degrees.**

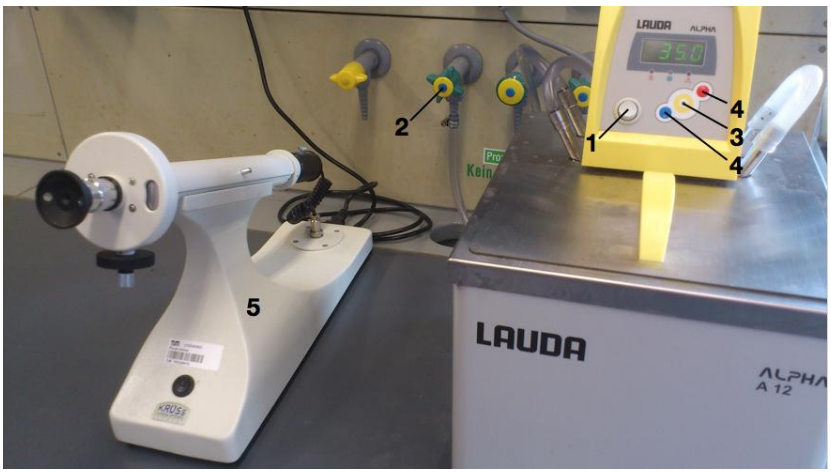

Figure 9.7: Experimental setup used to investigate the inversion of sucrose; **(1)** main switch to turn on and off the thermostat, **(2)** valve to turn on and off the cooling water, **(3 and 4)** buttons to regulate the set temperature, **(5)** polarizer.

Switch on the thermostat (**1**) and the cooling water (**2**). Set the temperature to T = 35 °C by pressing the yellow button (**3**) twice and subsequent use of the up/down buttons (**4**) to adjust the temperature. To confirm the set temperature, pressed the yellow button once again. Now you need to prepare the required samples and solutions (A, B, C, D, and E) in 50 ml volumetric flasks:

Solution A: 5 g of sucrose in 50 mL of solution in deionized water

Solution B: 10 g of sucrose in 50 mL of solution in deionized water

Solution C: 10 g of sucrose in 50 mL of solution in deionized water

Solution D: 50 mL of a 1 N solution of HCl in deionized water

Solution E: 50 mL of a 2 N solution of HCl in deionized water

To prepare solutions A to C: weigh the sucrose directly into the flask. Then, fill the flask with deionized water to approximately 80% of the total volume (total volume = 50 ml). After dissolving the sucrose by swirling the flask, fill the flask to 50 ml and ensure the solution is homogeneous.

Close all five flasks with their caps and place them in the water bath to temper. Take care that the flasks do not tip over in the water bath. To ensure a homogeneous temperature of T = 35 °C in the flasks, let them temper for 20 minutes.

Now, each student should determine the zero point of the polarizer (5) using deionized water as a reference. Overall, the zero point needs to be determined ten times. For all subsequent data, enter the results into the prepared Excel table and calculate the average value for further analysis. Comparing the average to the individual values, each student can determine their own reading accuracy, which is required for error calculation.

Then, determine the initial rotation angle α_0 by measuring solution A three times. Afterward, mix

a) 50 mL of solution B with 50 mL of solution D in a 100 mL volumetric flask (**sample 1**)

b) 50 mL of solution C with 50 mL of solution E in a 100 mL volumetric flask (**sample 2**)

Start the chronograph right after mixing the solutions. This is the starting time ($t = 0$) of the reactions. Fill one cuvette with sample 1 and the other with sample 2. **Start the measurement immediately after filling the cuvettes.** Before putting the cuvettes in the polarizer, dry them on the outside with a paper towel. Place sample 1 in the polarizer, perform three individual measurements efficiently, and then calculate the corresponding average. Place the cuvette back in the water bath and repeat the procedure for sample 2. Record the rotation angle of both samples every 5 minutes until t = 90 min. Now, heat the water bath to T = 60 °C and let the temperature of both cuvettes equilibrate for 10 minutes. Then cool down the water bath to a temperature of T = 35 °C, let the cuvettes equilibrate for another 10 minutes, and then use them to determine the final rotation angle α_∞. Finally, clean the cuvettes thoroughly with deionized water.

Think about why it is possible to determine the final rotation angle α_∞ by temporarily heating the samples to T = 60 °C and subsequent cooling to the actual measuring temperature.

9.3.2 Data evaluation

- ☐ Determine the rate constant k'' for the inversion of sucrose graphically according to the equation (9.28) or based on a weighted linear regression.
- ☐ Calculate k' and $k_{23}^{H^+} \cdot K_{12}^{H^+}$ as reported in the appendix 9.5.1.
- ☐ Perform an error analysis for all calculations.

9.4 Applications of the experiment and its theory

- ☑ Invert sugar is further processed into invert sugar syrup, which is applied in the food industry, in apiaries, and as an additive in tobacco.

- ☑ Catalysis plays an important role in technology, e.g., in the Haber process (the main industrial process for producing ammonia), the Ostwald process (a chemical process for the production of nitric acid), and the Contact process (the current method for producing sulfuric acid at high concentrations).
- ☑ Biocatalysts (enzymes) regulate the metabolism in animals and plants, without being consumed. An example is the enzyme *Ptyalin*, which is essential for initiating the reaction that cleaves starch into sugar molecules. Furthermore, the enzyme *Papain* from papaya fruit is used to tenderize protein-rich fibers in meat. During alcoholic fermentation, *Saccharomyces albicans* acts as an enzyme that converts glucose into ethanol and carbon dioxide.
- ☑ Polarimetry allows the determination of the concentration of optically active substances. Therefore, the kinetics of reactions involving optically active substances can be analyzed with this method. This is especially useful for substances whose concentration cannot be determined by other techniques.
- ☑ The specific rotation of an optically active substance is an intensive property of that substance. Thus, in analytical studies, it can be used to prove identity and purity, as well as to determine concentrations. For example, it is used to determine the sugar content of jams, fruit juices, fruits, wines, etc.
- ☑ The reaction of the inversion of sucrose has been analyzed intensively for a long time [9.10]. It is well understood and therefore often serves as a model reaction.

9.5 Appendixes

9.5.1 General acid catalysis

In special cases, the pseudo-first-order rate constant (the k' above) can include contributions of reactions in which the first reaction step (reaction with the catalyst) is rate-limiting ($k_{12} \ll k_{23}$). In this case, the equation (9.17) would become

$$-\frac{d[S]}{dt} = k_{12} \cdot [HA] \cdot [S] \cdot [H_2O] \tag{9.29}$$

In the presence of numerous acids, each acid has its individual rate constant k_{12}^{i} and this leads to

$$-\frac{d[S]}{dt} = [S] \cdot [H_2O] \cdot \sum_i \left(k_{12}^{i} \cdot [HA^i]\right) \tag{9.30}$$

In this case, the rate of substrate decomposition depends on the concentrations of the individual non-dissociated acids, but not on the concentration of H^+. This is called *general acid catalysis*.

Analogously, contributions from a specific or general base catalysis can play a role. The rate constant for the general case can be formulated as in [9.2]

$$k' = \underbrace{k_0}_{\text{without catalyst}} + \underbrace{k_{23}^{H^+} \cdot K^{H^+} \cdot [H^+]}_{\text{specific acid catalysis}} + \underbrace{\sum_i k_{12}^{HA_i} \cdot [HA_i]}_{\text{general acid catalysis}} + \underbrace{k_{23}^{OH^-} \cdot K^{OH^-} \cdot [OH^-]}_{\text{specific base catalysis}} + \underbrace{\sum_i k_{12}^{B_i} \cdot [B_i]}_{\text{general base catalysis}} \tag{9.31}$$

9.5.2 Lippich half-shade polarizer

Two crossbred polarizers can detect rotation of the polarization plane by an optically active substance. In this case, and in the absence of an optically active substance, the analyzer measures the maximum darkness. By introducing a certain optically active substance, the corresponding rotatory dispersion is the angle by which the analyzer must be turned to achieve maximum darkness again. It is difficult to adjust the analyzer to the maximum darkness, so small rotation angles can

only be measured with imprecision. A better criterion for adjusting the analyzer is provided by the Lippich half-shade polarizer, a frequently used measuring device for the determination of the rotatory dispersion of optically active substances (Figure 9.8) [9.8].

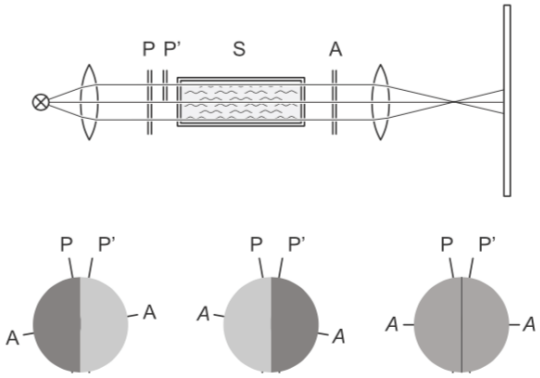

Figure 9.8: Chemical potential of a pure solvent *A* (black) and a solution made with it (red) as a function of temperature.

Here, an additional auxiliary prism is introduced between the common polarization prism and the sample under investigation. The polarization plane of the auxiliary prism is turned by a small angle compared to the polarization plane of the common polarization prism. After the light beam passes the sample and encounters the analyzer, it is reproduced by a telescope. The auxiliary prism covers half of the visual field of the telescope. If the analyzer is positioned perpendicular to the polarizer, the free half of the visual field is dark; if the analyzer is positioned perpendicular to the auxiliary prism, the covered half of the visual field is dark. In an average position of the analyzer, both halves of the visual field are equally bright. This zero position can be adjusted with high precision, as deviations from it due to opposing changes in brightness can be measured with great accuracy. By reading the angle of the analyzer in the presence and in the absence of the investigated substance, the rotatory dispersion of the substance can be determined.

9.6 Literature

9.1 - J.I. Steinfeld, J.S. Francisco and W.L. Hase, *Chemical kinetics and dynamics*, 2nd ed., Prentice Hall (1998).

9.2 - G. Wedler, *Lehrbuch der Physikalischen Chemie*, 6th ed., Willey/VCH (2012).

9.3 - L. Bergmann and C. Schaefer, *Lehrbuch der Experimentalphysik,* Vol. 3: Optik, 10th ed., rel. by H. Niedrig, De Gruyter (2004).

9.4 - R.L. Schowen, How does an enzyme surmount the activation energy barrier, *Proc. Nat. Acad. Sci*, **100** (2003) 11931-11932.

9.5 - E. Fischer, Ueber die Configuration des Traubenzuckers und seiner Isomeren, *Ber. Dtsch. Chem. Ges.*, **24**, (1891)0 1836. DOI: 10.1002/cber.189102401311 (accessed on 25 October 2024).

9.6 - E. Fischer, Ueber die Configuration des Traubenzuckers und seiner Isomeren. II, *Ber. Dtsch. Chem. Ges.*, **24**, (1891) 2683. DOI: 10.1002/cber.18910240278 (accessed on 25 October 2024).

9.7 - L. F. Moreno, *J. Chem. Educ.*, **89** (1), (2012) 175. DOI:10.1021/ed101011c (accessed on 16 September 2016).

9.8 - LD Handblätter Physik P5.4.3.3 Optik, LD DIDACTIC GmbH.

9.9 - H.-D. Belitz and W. Grosch, *Lehrbuch der Lebensmittelchemie,* Vol. 1, Springer-Verlag (1982).

9.10 - K.B. Storey and J.M. Storey, Natural Freezing Survival in Animals*, Ann. Rev. of Ecology and Systematics*, **27** (1996) 365-386.

9.11 - S. Arrhenius, Über die Reaktionsgeschwindigkeit bei der Inversion von Rohrzucker durch Säuren, *Z. Phys. Chem.* **4**, (1889) 226-248.

10 Primary Kinetic Salt Effect

10.1 Context and aim of the experiment

The primary kinetic salt effect [10.1, 10.2] describes the effect of the ionic strength on the rate constant of a reaction in solution, i.e., the change in reaction kinetics by the addition of a salt that does not take part in the reaction. In this experiment, this effect is investigated by studying the kinetics of a reaction in the presence of different electrolyte (salt) concentrations. The reaction kinetics in the absence of this supporting electrolyte are also determined and serve as a reference.

10.1.1 Important concepts to know

Reaction kinetics, reaction rate constant, relaxation time, pseudo-first-order reaction, hypothesis of the activated complex, ionic reaction, electrolyte, ionic strength, Debye-Hückel theory, absorption spectroscopy, absorption, transmission, Lambert-Beer's law, single and dual beam spectrophotometer, Brønsted equation.

10.1.2 Most common questions to be answered

- What is described by the kinetic primary salt effect?
- How can you prove the existence of a first-order reaction graphically?
- Consider a reaction between charged reactants A and B. Explain the kinetic primary salt effect for different z_A and z_B. How can the product $z_A \cdot z_B$ be determined experimentally?
- What is the meaning of the activity of a molecule in solution?
- What is the ionic strength, and how can it be adjusted?
- What is an inert electrolyte?

10.1.3 Further preparations before the experiment

Before performing the experiment, prepare a few worksheets as follows for each of the five measurements:

Table 10.1-1: Example of the table to prepare for data collection and evaluation.

Conditions:	*t (s)*	*Transmittance T (%)*	*Absorbance A*	$\ln A$
	…	…	…	…
	…	…	…	…

10.2 Theory

10.2.1 Activity of ions in solution

In solution, ions prefer to be surrounded by a cloud of ions with opposite sign. This ion cloud stabilizes the central ion, thereby reducing its chemical reactivity. This effect is quantified by the so-called *activity* a_i. The activity is an effective quantity, which is only a fraction γ_i (called *activity coefficient*) of the *molal concentration* b_i in mol/kg, made dimensionless by dividing it by $b_0 = 1$ mol/kg, similarly to the activity of gases

$$a_i = \gamma_i \cdot \frac{b_i}{b^0} \tag{10.1}$$

The activity coefficient γ_i describes the deviation from the ideal behavior. In infinitely diluted solutions, the interionic interactions disappear, leading to

$$\lim_{b_i \to 0} \gamma_i = 1 \tag{10.2}$$

In the case of the solution of an ionic compound, the individual activities a_i are not accessible experimentally. Therefore, a *mean ionic activity coefficient* $\gamma_\pm$ is defined, and obtained by the geometrical mean of the individual activity coefficients. For an electrolyte that decays in x cations and y anions, it is given by

$$\gamma_\pm = \left(\gamma_{i_+}^{x} \cdot \gamma_{i_-}^{y}\right)^{\frac{1}{x+y}} \tag{10.3}$$

10.2.2 Hypothesis of the activated complex and effect of ionic strength on reaction kinetics

In 1922, J. N. Brønsted described the effect of salts on the kinetics of ionic reactions [10.1, 10.2]. This was a long time before the Debye-Hückel theory was introduced [10.3 - 10.5]. The studies of Brønsted represent the first applications of the hypothesis of an activated complex on the quantitative interpretation of reaction rates.

We consider a reaction between ions A and ions B with the charges z_A and z_B, introducing the activated complex $X^\ddagger$

$$A + B \leftrightharpoons X^\ddagger \rightarrow products \tag{10.4}$$

The activated complex is assumed to be in equilibrium with the reactants and thus

$$K^\ddagger = \frac{a_{X^\ddagger}}{a_A \cdot a_B} \tag{10.5}$$

where $K^\ddagger$ is the equilibrium constant of the reaction (10.4) and $a_{X^\ddagger}$, a_A and a_B are the activities of the activated complex and the ions A and B, respectively. Using equation (10.1) to replace the activities in the equation (10.5), we can derive

$$K^\ddagger = \frac{b_{X^\ddagger} \cdot b^0}{b_A \cdot b_B} \cdot \frac{\gamma^\ddagger}{\gamma_A \cdot \gamma_B} \tag{10.6}$$

Using the transition state theory of Eyring [10.6] and inserting the equation (10.6), we can deduce the following relationship for the rate constant k

$$-\frac{db_A}{dt} = -\frac{db_B}{dt} = \frac{k_B \cdot T}{h} \cdot b_{X^\ddagger} = k \cdot b_A \cdot b_B \tag{10.7}$$

k_B is the Boltzmann constant and h is the Planck constant. $(k_B \cdot T)/h$ reflects the maximum rate constant k_0 for elementary reactions in organic chemistry, where covalent bonds are formed and broken. At room temperature, this corresponds to $6 \cdot 10^{12}$ s^{-1}, reflecting the vibration frequency of a covalent bond. Combination of equations (10.6) and (10.7) yields

$$k = \frac{k_B \cdot T}{h} \cdot \frac{K^\ddagger}{b^0} \cdot \frac{\gamma_A \cdot \gamma_B}{\gamma^\ddagger} \tag{10.8}$$

The Debye-Hückel limiting law indicates that, in general, the activity coefficient of an ion in diluted aqueous solutions (< 10^{-3} mol/kg) can be approximated with

$$\log_{10} \gamma_i = -0.509 \cdot z_i^2 \cdot \sqrt{I} \tag{10.9}$$

where $T = 298\ K$, $b_i \rightarrow 0$, z_i is the charge of the ion. The *ionic strength* I is defined as

$$I = \frac{1}{2} \cdot \sum_i \frac{b_i}{b^0} \cdot z_i^2 \tag{10.10}$$

where b_i is the concentration in mol/kg of each ionic species i, z_i is the charge of each dissolved ionic species and Σ_i is the sum over all the ionic species i. Table 10.2-1 reports some examples on how to calculate the ionic strengths of 1 mol/kg solutions for various salts.

Taking the logarithm of the equation (10.8) results

$$\log_{10} k = \log_{10}\left(\frac{k_B \cdot T}{h} \cdot \frac{K^\ddagger}{b^0}\right) + \log_{10} \frac{\gamma_A \cdot \gamma_B}{\gamma^\ddagger} = \log_{10} k_0 + \log_{10} \frac{\gamma_A \cdot \gamma_B}{\gamma^\ddagger} \tag{10.11}$$

Substituting equation (10.9) in (10.11) and using the assumption that $z^\ddagger = z_A + z_B$ we get

$$\log_{10} k = \log_{10} k_0 + 0.509\sqrt{I} \cdot [-z_A^2 - z_B^2 + (z_A + z_B)^2] \tag{10.12}$$

And

$$\log_{10} k = \log_{10} k_0 + 1.018 \cdot z_A \cdot z_B\sqrt{I} \tag{10.13}$$

or

$$\log_{10} \frac{k}{k_0} = 1.018 \cdot z_A \cdot z_B\sqrt{I} \tag{10.14}$$

Equation (10.14) is called the ***Brønsted equation*** and predicts that $\log_{10} k$ is proportional to the square root of the ionic strength. Written in the form of the equation (10.13) it shows that a plot of $\log_{10} k$ vs. the square root of the ionic strength should yield a straight line with the slope $m = 1.018 \cdot z_A \cdot z_B$. The variation of the reaction rate constant k with the ionic strength (according to equations (10.13) and (10.14)) is also called the ***kinetic primary salt effect***.

Table 10.2-1: Examples of ionic-strength calculations of 1 mol/kg solutions of various salts.

Type of salt	I	*Type of salt*	I
1, 1 (NaCl)	$\frac{1}{2}(1 \cdot 1^2 + 1 \cdot 1^2) = 1$	1, 3 ($LaCl_3$)	$\frac{1}{2}(1 \cdot 3^2 + 3 \cdot 1^2) = 6$
1, 2 ($BaCl_2$)	$\frac{1}{2}(1 \cdot 2^2 + 2 \cdot 1^2) = 3$	1, 3 (K_3PO_4)	$\frac{1}{2}(3 \cdot 1^2 + 1 \cdot 3^2) = 6$
2, 2 ($ZnSO_4$)	$\frac{1}{2}(1 \cdot 2^2 + 1 \cdot 2^2) = 4$	2, 3 ($Mg_3(PO_4)_2$)	$\frac{1}{2}(3 \cdot 2^2 + 2 \cdot 3^2) = 15$

Please bear in mind that solvated ions, which do not take part in the reaction, also contribute to the ionic strength! The ionic charges of the reactants A and B are responsible for the strength and the direction of the effect. In principle, there are three possible cases for different values of z_A and z_B (Figure 10.1).

a) If z_A and z_B have the same signs, the product of the ionic charges $z_A \cdot z_B$ is positive, and the rate constant is directly proportional to the ionic strength.

b) If z_A and z_B have opposite signs, the product of the ionic charges $z_A \cdot z_B$ is negative, and the rate constant is inversely proportional to the ionic strength.

c) If one of the reactants is uncharged ($z = 0$), the product of the ionic charges $z_A \cdot z_B$ is zero, and the rate constant is independent of the ionic strength.

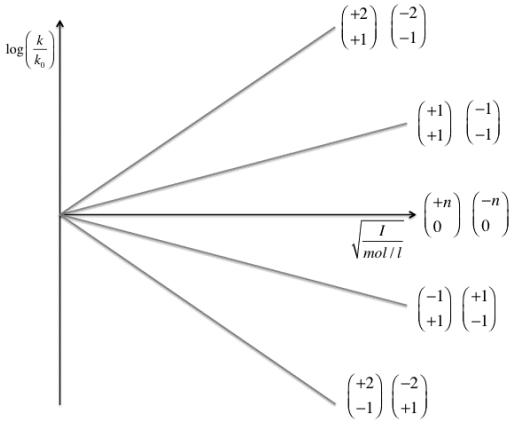

Figure 10.1: Theoretical trend of the kinetic primary salt effect for different z_A and z_B.

Thus, the slope of the straight line in a plot of $\log_{10} k$ vs. the square root of ionic strength provides information on the charges of the species involved in the activated complex. In general, a multiply charged activated complex formed from ions

with equally signed charges prefers an environment of high ionic strength. On the other side, if ions of opposite charge do react (e.g., z_A = 1 and z_B = -1), then these charges cancel each other in the activated complex ($z^{\ddagger}$ = 0); it follows that at high ionic strength the separated ions are preferred compared to the uncharged complex. These theoretical conclusions can be proved by many experiments.

10.2.3 Decomposition of murexide and its reaction rate

In this experiment, the decomposition of murexide in an acidic solution is investigated. Murexide is the ammonium salt of purpuric acid. In acidic solution, the anion of the salt decomposes irreversibly into uramil and alloxan (Figure 10.2)

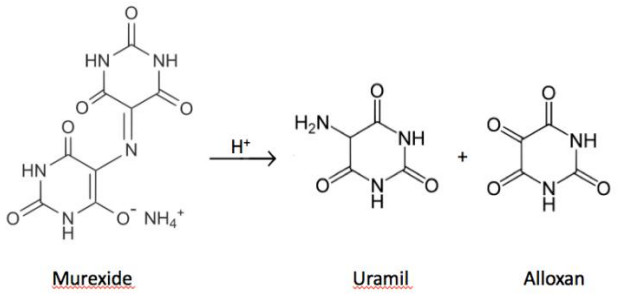

Figure 10.2: Decomposition reaction of murexide in acidic solution.

The progression of the decomposition reaction can be followed using UV-Vis spectroscopy (see Chapter 6) since the red/violet coloured murexide anion has an absorption maximum at 520 nm. The decay products uramil and alloxan are colorless and absorb only in the UV range (100 – 400 nm) of the electromagnetic spectrum. The decomposition of murexide proceeds according to the following mechanism

$$Mu^- + H^+ \underset{k_{21}}{\overset{k_{12}}{\rightleftharpoons}} MuH \xrightarrow{k_{23}} U + A \tag{10.15}$$

where Mu^- is the murexide anion, MuH is the purpuric acid, U is uramil and A is alloxan. The dissociation constant K_D (first equilibrium in the reaction (10.15)) is defined as

$$K_D = \frac{\gamma_{\pm} \cdot {}^{b_{Mu^-}}/_{b^0} \cdot \gamma_{\pm} \cdot {}^{b_{H^+}}/_{b^0}}{\gamma_{MuH} \cdot {}^{b_{MuH}}/_{b^0}} = \frac{b_{Mu^-} \cdot b_{H^+}}{b_{MuH} \cdot b^0} \cdot \gamma_{\pm}^2 \tag{10.16}$$

where $\gamma_{\pm}$ is the mean ionic activity coefficient of Mu^- and H^+, assuming that the activity coefficient of MuH (γ_{MuH}) is 1. From the mass balance, we obtain the total concentration b_{tot}

$$b_{tot} = b_{Mu^-} + b_U + b_{MuH} \tag{10.17}$$

The purpuric acid MuH is the intermediate product, and its concentration is very small compared to the concentrations of the reactants and the products (for purpuric acid, $pK_a \approx 0$). The fact that $b_{MuH} \ll b_{Mu^-} + b_U$ allows us to neglect b_{MuH} in equation (10.17) and thus

$$b_{tot} = b_{Mu^-} + b_U \tag{10.18}$$

The equation that describes the rate of formation of uramil and alloxan is

$$\frac{db_U}{dt} = \frac{db_A}{dt} = k_{23} b_{MuH} \tag{10.19}$$

Compared to the decomposition reaction, the equilibrium in the reaction (10.15) is reached very fast (10^{-8} s), thus the decomposition reaction becomes the rate-determining step (see chapter 8). b_{MuH} in equation (10.19) can be replaced using the equation (10.16) leading to

$$\frac{db_U}{dt} = \frac{db_A}{dt} = \frac{k_{23}}{K_D \cdot b^0} \cdot \gamma_{\pm}^2 \cdot b_{Mu^-} \cdot b_{H^+} \tag{10.20}$$

Furthermore, using the equation (10.18), we obtain

$$\frac{d(b_{tot} - b_{Mu^-})}{dt} = \frac{k_{23}}{K_D \cdot b^0} \cdot \gamma_{\pm}^2 \cdot b_{Mu^-} \cdot b_{H^+} \tag{10.21}$$

At the experimental conditions used here, the protons are present in large excess compared to the murexide ($b_{H^+} \gg b_{Mu^-}$), thus b_{H^+} stays almost constant. Under these conditions, the decay of murexide is thus a pseudo first-order reaction (see chapter 8). The individual activity coefficients vary with the ionic strength. However, since we adjust the ionic strength by the addition of inert electrolytes that do not take part in the reaction, the mean activity coefficient $\gamma_{\pm}$ is constant during the reaction, and so it is $\gamma_{\pm}^2$. All these considerations allow summing up all constant parameters to a new reaction rate constant

$$k' = \frac{k_{23}}{K_D \cdot b^0} \cdot \gamma_{\pm}^2 \cdot b_{H^+} \tag{10.22}$$

The rate of decomposition of murexide equals the rate of formation of uramil or alloxan (equation (10.20)) and can now be written as

$$-\frac{db_{Mu^-}}{dt} = k' \cdot b_{Mu^-} \tag{10.23}$$

Solving the differential equation for the concentration of murexide, we obtain

$$\int_{b^0_{Mu^-}}^{b^t_{Mu^-}} \frac{db_{Mu^-}}{b_{Mu^-}} = -\int_0^t k' \cdot dt \tag{10.24}$$

This allows us to obtain the following time law for the decomposition of murexide

$$\ln \frac{b^t_{Mu^-}}{b^0_{Mu^-}} = -k' \cdot t \quad \text{or} \quad b^t_{Mu^-} = b^0_{Mu^-} \cdot e^{-k' \cdot t} \tag{10.25}$$

where $b^0_{Mu^-}$ is the concentration of murexide at the time t = 0. The corresponding relaxation time τ is

$$\tau = -\frac{1}{k'} = -\frac{K_D \cdot b^0}{k_{23}} \cdot \frac{1}{\gamma_{\pm}^2 \cdot b_{H^+}} = -\frac{1}{k \cdot b_{H^+}} \tag{10.26}$$

10.3 Experimental details and evaluation

10.3.1 Experimental execution

The experimental setup (Figure 10.3) used to study the decomposition of murexide consists of a spectrophotometer connected to a computer. Usually, the computer and the spectrophotometer are already turned on. For the measurements, you must select a wavelength of 520 nm. At this wavelength the murexide [10.7] absorbs, but not uramil [10.8] and alloxan [10.9].

Figure 10.3: The UV-Vis spectrophotometer.

You need the following solutions:

Murexide solution: Prepare a 100 mL solution of 36,6 mg of murexide in deionized water (molar mass M = 284.19 g/mol).

Hydrochloric acid solution: 0,05 M, available in the laboratory

Ammonium chloride solution: 0.5 M, molar mass M = 53.49 g/mol, available in the laboratory

Deionized water

In the experiment, concentrations are expressed in molarity (mol/L), not molality (mol/kg). Estimate the difference between the two values and decide whether it is negligible.

The first column in Table 10.3-1 corresponds to the reference used to calibrate, the spectrophotometer. First, add the corresponding volumes of murexide solution, H_2O, and NH_4Cl solution to the cuvette using a pipette. Finally, add the acid and mix by briefly pipetting up and down. Then, put the cuvette into the cuvette holder and start the measurement immediately.

Table 10.3-1: Scheme of the composition of each solution to test. The numbers given are in mL of solution.

Solution	*Reference*	*Solution 1*	*Solution 2*	*Solution 3*	*Solution 4*	*Solution 5*
Murexide	–	0,5	0,5	0,5	0,5	0,5
H_2O	2,5	2,0	1,5	1,0	0,5	–
NH_4Cl	–	–	0,5	1,0	1,5	2,0
HCl	1,0	1,0	1,0	1,0	1,0	1,0

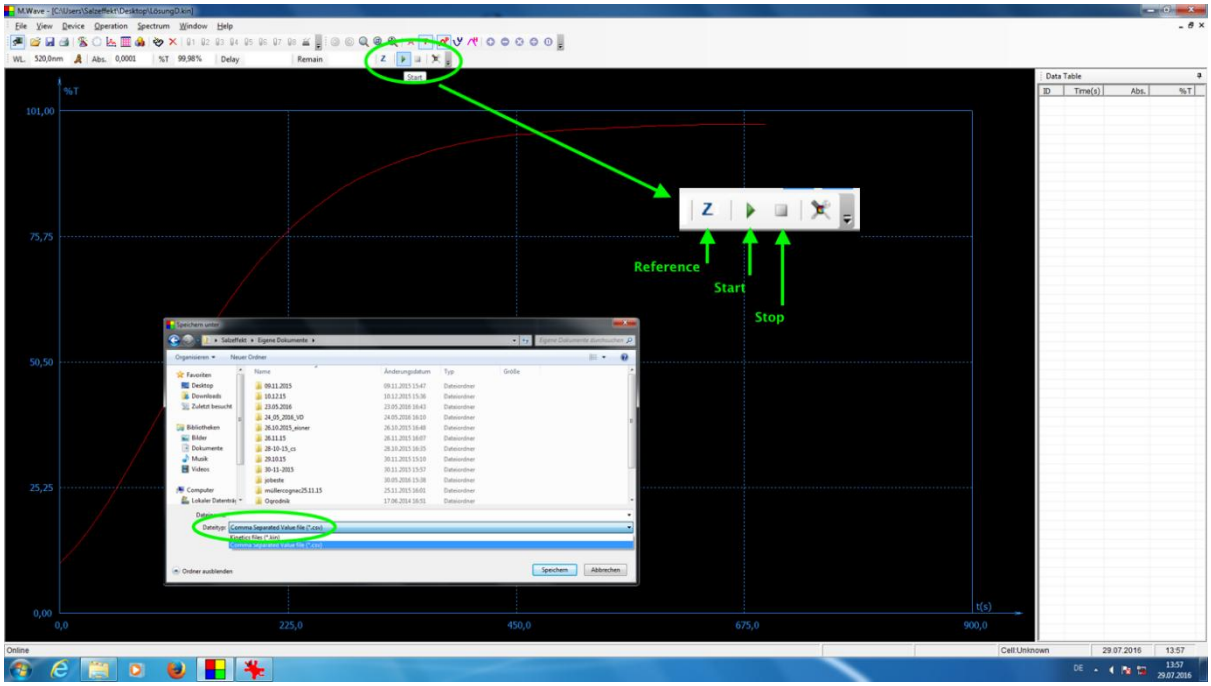

Figure 10.4: The measuring program M.Wave.

The measuring program (Figure 10.4) records the transmittance T vs. time t in seconds.

The measurements will stop automatically after t = 900 s. To save your data, choose “Save” in the “File” menu. For the file type, use a Comma-Separated-Value file (*.csv) (Figure 10.4).

10.3.2 Data evaluation

- ☐ From the transmittance T vs. time t in seconds. Calculate the absorbance A from that, in time intervals of minutes.
- ☐ Plot $\ln A$ vs. time t for each solution and determine the rate constant k' from the slope of the straight line, according to the equation (10.25) and (10.26).
- ☐ Use the rate constant k' to calculate the relaxation time τ for the different conditions, by using the equation (10.26).
- ☐ Verify the Brønsted equation (10.14).
- ☐ Perform an error analysis for all calculations. For the used spectrophotometer $\delta T = 0.012 \cdot T$

10.4 Applications of the experiment and its theory

- ☑ In reactions between large molecules (e.g., proteins), not all charges on the interacting molecules typically influence reaction kinetics. Then, studying the effect of ionic strength on the kinetics may reveal information on the charges that influence the reaction rate.
- ☑ Murexide is the final product of the murexide reaction, an analytical reaction to detect uric acid, xanthine, and other related substances.
- ☑ Murexide can be used as an indicator since it undergoes a color change in the presence of calcium ions and other specific metal ions.

10.5 Literature

10.1 - P.W. Atkins, Physical Chemistry, 6th ed., Oxford University Press, Oxford (1998), pp. 819-837.

10.2 - P.W. Atkins and J. de Paula, Atkins' Physical Chemistry, 8th ed., Oxford University Press, Oxford (2006), pp. 880-885.

10.3 - P.W. Atkins, Physical Chemistry, 6th ed., Oxford University Press, Oxford (1998), pp. 249-253.

10.4 - P.W. Atkins and J. de Paula, Atkins' Physical Chemistry, 8th ed., Oxford University Press, Oxford (2006), pp. 163-165.

10.5 - P. Debye, and E. Hückel, Zur Theorie der Elektrolyte. I. Gefrierpunktserniedrigung und verwandte Erscheinungen, *Phys. Z.* 24 (1923) 185-206.

10.6 - Eyring, H., The activated complex in chemical reactions. *J. Chem. Phys.* 3 (1935) 107-115.

10.7 - National Center for Biotechnology Information. PubChem Compound Database; CID=14453351, https://pubchem.ncbi.nlm.nih.gov/compound/14453351 (accessed on 25 October 2024).

10.8 - National Center for Biotechnology Information. PubChem Compound Database; CID=67051, https://pubchem.ncbi.nlm.nih.gov/compound/67051 (accessed on 25 October 2024).

10.9 - National Center for Biotechnology Information. PubChem Compound Database; CID=5781, https://pubchem.ncbi.nlm.nih.gov/compound/5781 (accessed on 25 October 2024).

11 Estimation and Propagation of Measurement Uncertainties

11.1 Basics and types of measurement uncertainties

Any measurement of a physical quantity is flawed by a measurement uncertainty (or error), no matter how sophisticated the measurement procedure is. Since experimental data cannot be determined with unlimited accuracy, *a measurement lacking information about its precision is essentially useless*. Therefore, in any publication or report, it is necessary to specify the uncertainty of the acquired result. This uncertainty is also called measurement error and can either be given as an *absolute* error:

$$E_A = 110 \pm 1.2 \frac{\text{kJ}}{\text{mol}} \tag{11.1}$$

or as a *relative* error:

$$E_A = 110 \pm 1.1\% \frac{\text{kJ}}{\text{mol}} \tag{11.2}$$

Here, 110 kJ/mol corresponds to an average value of the activation energy $\overline{E_A}$ determined from a series of measurements. 1.2 kJ/mole is the absolute error δE_A while 1.1% is the relative error $\delta E_A / \overline{E_A}$. Units are essential, and you must not forget them.

Keep in mind the following meaning of any experimentally obtained result, like $\overline{E_A}$:

a) Usually, it is the arithmetic mean of a series of measurements and merely represents an approximation of the true value (E_A^{true}).

b) With a certain probability, the true value E_A^{true} lies within the interval $[\overline{E_A} - \delta E_A, \overline{E_A} + \delta E_A]$. This probability is called the confidence level or level of significance, and usually is 68% (see below). The width of the interval is determined by the size of the error δE_A.

The **significant digits** in the measured value are the digits larger than or similar to the uncertainty. As a matter of principle, the uncertainty of the error is of the same magnitude as the error itself, thus it must not indicate more than two significant digits. Accordingly, the experimental value must not indicate digits smaller than the error (non-significant):

$$E_A = 110.\underbrace{\sout{493826397}}_{non-significant\ digits} \pm 1.2\sout{263} \frac{\text{kJ}}{\text{mol}}$$

If the error is not given explicitly, it is assumed that only significant digits are given and that its magnitude is half of the last significant digit:

$$E_A = 110 = 110 \pm 0.5 \ \frac{kJ}{mol}$$

In the following paragraphs (11.1.1 to 11.1.3), the three main types of error (coarse, statistical, and systematic errors) are discussed.

11.1.1 Coarse errors

Coarse errors appear if the experiment exhibits fundamental uncertainties. Examples for sources of coarse errors are:

- Unsuitable experimental setup, e.g., characterized by uncontrolled parameters (not keeping the measuring conditions like temperature and pressure constant).
- Unsuitable technique of measurement, e.g., trying to determine the temperature in a very small sample (1cm^3 of a liquid or a small amount of gas) using a thermometer having a large heat capacity.

- Wrong calibration.
- Wrong reading of the experimental data.
- Deteriorated samples.

Rigorous planning of the experiment will avoid coarse errors:

- ✓ Be familiar with the theoretical background and literature relative to the experiment.
- ✓ Estimate the expected magnitude of collected data and compare it with the precision of your equipment before starting the experiment.
- ✓ Perform control measurements with reference samples.
- ✓ Be sure to have full control of every step of the experimental procedure.

11.1.2 Statistical errors

Increasing the measurement precision of any physical quantity will progressively reveal fluctuations. Sophisticated instruments and experimental setups may reduce such fluctuations. However, they ultimately rest on the nature of thermodynamics (the Boltzmann distribution) and are thus inevitable. Mainly, they lead to randomly distributed measurements with positive and negative deviations from the real value, which, due to their statistical nature, have equal probability. Therefore, if the number of measurements is increased, they cancel each other cumulatively. Thus, the statistical error of the average of a measured variable can be reduced, but not infinitely, by increasing the amount of acquired data.

To determine the *size of the statistical error*, the mean of the square of the error needs to be considered, since this leads to a summation of just positive values that do not eliminate each other (see paragraph 11.2.1 for the theory of statistical errors). Various possible sources of statistical errors are:

- **Reading error**: the signal of an analog measuring instrument usually can only be determined with an accuracy of half or quarter of the smallest separation of marks on the scale (think about a ruler with millimeter graduation or an analog thermometer). A *Vernier scale* (German: Nonius-Skala, see Figure 11.1) may provide a significant improvement in this interpolation problem.

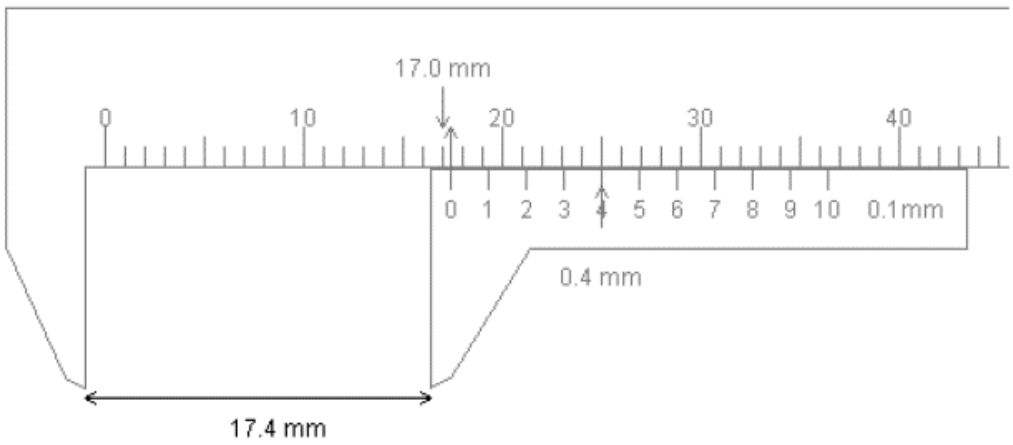

Figure 11.1: A vernier scale.

- **Error of digitalization**: trivially, a digital measuring device can only be accurate up to the last specified digit. However, beware: the error could be much larger than the last digit due to the intrinsic noise of the instrument or of the setup.
- **Environmental influences:** vibrations, fluctuations of temperature (feedback fluctuations of a thermostat), alternating electrical field (pick-up).

- **Shot noise:** (German: Schrotrauschen): Some physical properties are "quantized", i.e., the minimal unit electrical charge is the electron charge, or the smallest unit of light energy is that of a photon $\frac{h \cdot c}{\lambda}$. Single charges can be detected by an electron multiplier (as in a mass spectrometer), and single photons can be counted using a Geiger counter (for measuring radioactive decay) or a photomultiplier (e.g., in a fluorimeter). Therefore, such quantities can only be detected as an integer multiple of the unit quantity.
- **Intrinsic noise** (*fluctuations*): based on the quantum nature of charge, any electronic component (e.g., a resistor) exhibits an unavoidable basic noise current (Nyquist noise, Figure 11.2A). Any amplification of the signal will also amplify this noise (like for the sizzling noise in an audio amplifier that is completely turned up in the absence of an input signal). Usually, the intrinsic noise has a characteristic frequency response: the larger the frequency, the smaller the amplitude of the noise (1/f noise, Figure 11.2B).

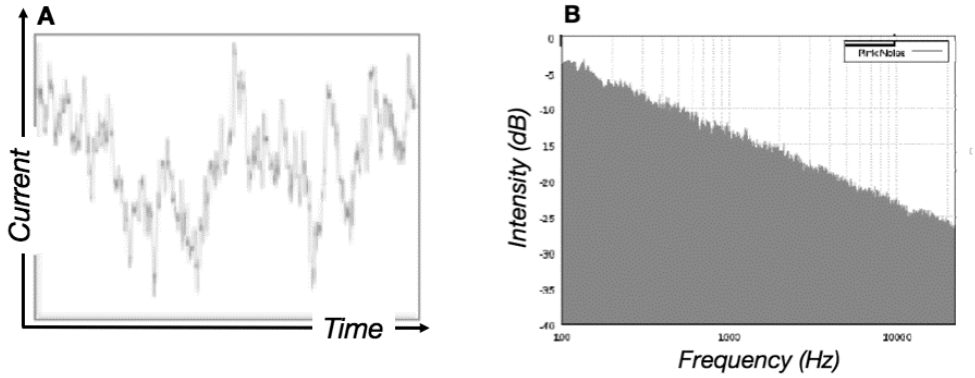

Figure 11.2: A) Noise current as a function of time; B) Intensity of the noise current as a function of frequency.

As mentioned above, any physical quantity exhibits statistical errors due to the thermal agitation of particles, reflected in the Boltzmann distribution (or the Fermi- and Bose-Einstein distributions). The higher the temperature, the broader the distribution. An exciting example of maximum reduction of thermal noise by cooling down electronic amplifiers to a temperature of 4.2 K is given in Figure 11.3.

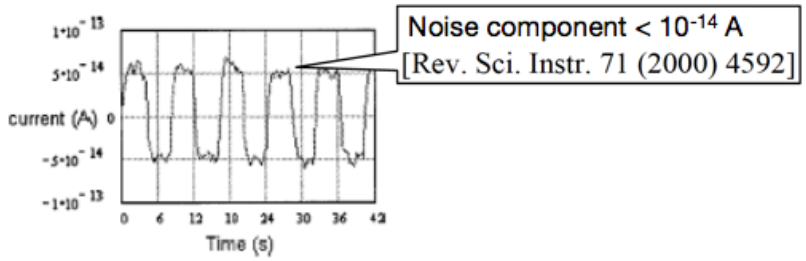

Figure 11.3: Output signal of an amplifier of the receiving earth station in Raisting (Bavaria, Germany). The receiving station is cooled down to 4.2 K and exhibits a noise amplitude of 10^{-14} A. This noise can be further reduced to $5 \cdot 10^{-17}$ A by averaging the signal over one hour (this noise current corresponds to a fluctuation of 300 electrons per second).

In summary: to minimize statistical errors, it is necessary to perform measurements repeatedly and to obtain average values of these data (see paragraph 11.2).

11.1.3Systematic errors

Under identical measurement conditions, systematic errors always impair measurements in a similar manner. On repeating the measurement, the value and sign of a systematic error remain the same, and therefore, it cannot be reduced by averaging.

Possible origins of systematic errors are:

- Air buoyancy on weight.
- Temperature dependence of practically all physical quantities (e.g., expansion of a ruler with increasing temperature).
- External electrical d.c. fields.
- Instability of samples and measuring setups due to aging.
- Wrong zero point: many measuring devices do not report the exact zero point, and therefore all measured data are shifted by a certain value, e.g., in balances, shifted scales, parallax errors.
- Friction and Hysteresis effects: when measurement series at increasing pressure and decreasing pressure reveal different data.
- Non-linearity: most measuring sensors are based on idealized *linear* physical laws. However, on closer inspection, one usually finds deviations from linearity, especially if the measuring parameters become large. Examples are: Hooke's law in a spring balance, ideal gas law in gas thermometers, and non-linear distortions in analog-digital converters.

Strategies to minimize systematic errors are:

- Providing a reliable and accurate experimental setup. Counteracting systematic deviations can be utilized for mutual compensation.
- Experimental and theoretical calibration functions can be utilized for numerical corrections.
- Different measuring methods could be compared.

In summary, it is generally not possible to account for systematic errors within the context of a practical course. However, a discussion of possible sources of systematic error can proceed.

11.1.4 Precision and accuracy

The statistical error reflects the *precision* of a measurement, meaning its reproducibility. Only if the systematic error is small as well, the result of a measurement will be close to the corresponding real value and is thus *accurate* (Figure 11.1.4).

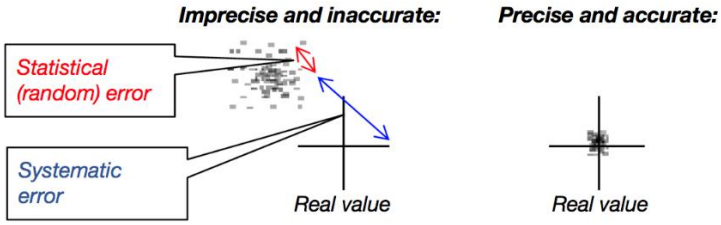

Figure 11.4: Precision and accuracy of a determined measuring parameter.

The following paragraph 11.2 describes the statistical methods that are used to quantify the precision of a measurement.

11.2 Quantification of the precision of a measurement

11.2.1 Mean value and statistical error

An example of data collection is the following: using a stopwatch with a display accuracy of 0.01 s, we measure the time t_i required for a steel bullet to fall from the lowest viewing platform of Munich's Olympia tower (height: 172 m). Table 11.2-1 shows 20 individual measurements.

Table 11.2-1: Data sheet for 20 individual measurements of the falling time taken from a steel bullet falling from the Munich Olympia tower.

No. of measurement (= index i)	t_i *(s)*	*Deviation from the mean value:* $t_i - \bar{t}$ *(s)*	$(t_i - \bar{t})^2$ *(s²)*
1	5.51	-0.02	0.0006
2	5.26	-0.28	0.0761
3	5.04	-0.49	0.2430
4	5.63	0.10	0.0095
5	5.39	-0.14	0.0204
6	5.83	0.30	0.0902
7	6.01	0.48	0.2282
8	5.64	0.11	0.0124
9	5.06	-0.47	0.2205
10	5.18	-0.35	0.1222
11	5.75	0.22	0.0467
12	5.72	0.19	0.0367
13	5.94	0.40	0.1633
14	5.69	0.16	0.0244
15	5.49	-0.04	0.0014
16	5.74	0.2	0.0445
17	5.70	0.17	0.0287
18	5.32	-0.22	0.0466
19	5.42	-0.11	0.0125
20	5.32	-0.22	0.0463
Sum:	**110.62**	**-0.0000000000000133**	**1.4742**

The *arithmetic mean value* $\bar{t}$ of the falling time is calculated according to

$$\bar{t} = \frac{1}{n} \cdot \sum_{i=1}^{n} t_i = \frac{110.62\ s}{20} = 5.53\ s \tag{11.3}$$

Calculating the average of the deviation of the individual falling times from its mean value, positive and negative terms (in the third column of Table 11.2-1) cancel each other, the small value that remains (-0.0000000000000133) results from rounding errors of the software program:

$$\frac{1}{n} \cdot \sum_{i=1}^{n} (t_i - \bar{t}) = 0.0000000000000133 \approx 0 \tag{11.4}$$

As one can easily prove, the deviation is exactly zero:

$$\overline{(t_i - \bar{t})} = \frac{1}{n} \cdot \sum_{i=1}^{n} (t_i - \bar{t}) = \frac{1}{n} \cdot \sum_{i=1}^{n} (t_i) - \frac{1}{n} \cdot \sum_{i=1}^{n} (\bar{t}) = \bar{t} - \frac{1}{n} \cdot n \cdot \bar{t} = 0 \tag{11.5}$$

To determine the size of the statistical error (i.e., to quantify the average magnitude of deviation), Gauss (and Legendre) suggested averaging the *squares of the deviations* $(t_i - \bar{t})^2$ (fourth column of Table 11.2-1). In this way, the *standard deviation σ* of the individual measurement is calculated by averaging the squares of the errors. This leads to a summation of only positive values that do not cancel each other out.

$$\sigma = \sqrt{\frac{1}{n-1} \cdot \sum_{i=1}^{n} (t_i - \bar{t})^2} = 0.278\ s \tag{11.6}$$

The square of the equation (11.6) σ^2, is called **variance**.

Note: In the equation (11.6), the mean value $\bar{t}$ is assumed to be known, and by this, it determines one of the n terms $(t_i - \bar{t})^2$. Thus, there exist only $n-1$ independent terms. Therefore, the sum is divided by $n-1$ (however, in general, $n - 1 \approx n$).

11.2.1.1 Gauss's least-squares method

In principle, there are various ways of averaging data; the most natural and simple is the arithmetic mean, as in the equation (11.3). Carl Friedrich Gauss noted that the arithmetic mean has a unique and important property. If you look at the square of the deviations of all the data points x_i from any mean value: $(\bar{x} - x_i)^2$ one finds that the sum of all these squares $\sum_{i=1}^{n}(\bar{x} - x_i)^2$ is minimal only if $\bar{x}$ is an arithmetic mean according to the equation (11.3).

11.2.2 Probability distribution

The distribution of individual measurement values can be captured in a probability distribution and depicted as a histogram (bar plot). To construct a histogram, the first step is to define the range of values, i.e., divide the entire range of values into a series of intervals $\left[t_k - \frac{1}{2}\Delta t, t_k + \frac{1}{2}\Delta t\right]$ (called *classes*) and then count how many values fall into each interval (called *frequency of occurrence* n_k). Here, the horizontal axis (abscissa) shows the falling time t, the vertical axis (ordinate) gives n_k. Figure 11.5 shows the probability distribution derived from the data of Table 11.2-1 (with n = 20 and an interval width of Dt = 0.2 s).

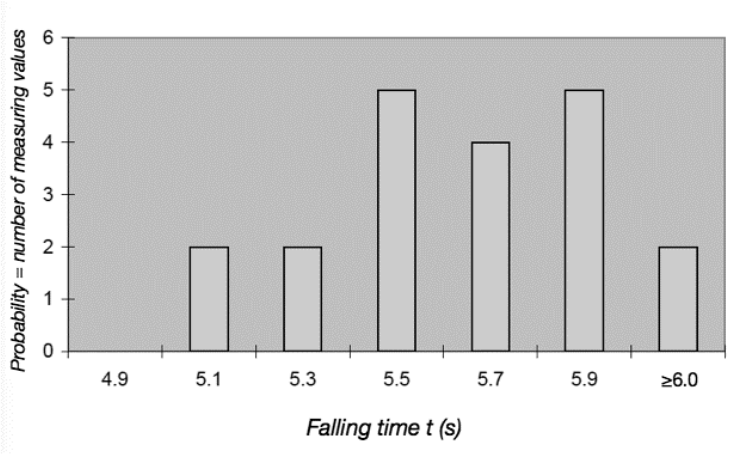

Figure 11.5: Histogram of the data given in Table 11.2-1 using an interval width of Dt = 0.2 s, leading to six individual classes.

This distribution has a *centroid* exactly at the arithmetic mean value $\bar{t}$ = 5.53 s. However, due to the small amount of data, the distribution is ill-defined. The *width of the distribution* is a measure of the scatter of the data points and is given by the standard deviation s = 0.278s. If we increase the number of data points, we observe that the distribution becomes smoother and better defined (see Figure 11.6), while both centroid and width are independent of the number of measurements; s depicts the quality of each individual measurement. On the other hand, it is obvious that the distribution would become imperceptible if the number of data points were considerably smaller than n = 20.

Usually, it makes sense to normalize distributions to make them easier to handle and to compare them. For normalization, the *frequency* f_k (*relative probability* or *probability density*) is introduced; it corresponds to the probability of finding a measuring value in a certain interval $\left[t_k - \frac{1}{2}\Delta t, t_k + \frac{1}{2}\Delta t\right]$ and it is given by

$$f_k = \frac{absolute\ probability\ n_k}{number\ of\ measurements\ n} = \frac{n_k}{\sum_{k=1}^{K} n_k} \tag{11.7}$$

This normalization provides that the sum of all f_k is 1 (=100%)

To make the depicted distribution independent of the interval width Δt, the relative probability f_k is further divided by Δt to reveal the *probability density* r_k (see Figure 11.6)

$$r_k = \frac{f_k}{\Delta t} \tag{11.8}$$

Applying the equation (11.8) to a given probability density makes possible to calculate back the frequency of finding a measuring result in an arbitrary interval $\left[t_k - \frac{1}{2}\Delta t, t_k + \frac{1}{2}\Delta t\right]$

$$f_k = r_k \cdot \Delta t \tag{11.9}$$

In a histogram, the number of classes K depends on the interval size Δt and on the length of the horizontal axis $t_{max} - t_{min} = K \cdot \Delta t$. Here K = 15. The proper choice of K is not trivial and depends on the number of data points n, which are available. If K is chosen too large, the noise in each interval will be too large, if K is too small, the diagram will be too coarse. It is good practice to choose

$$K \approx \sqrt{n} \quad \text{for } n \leq 1000 \tag{11.10}$$

$$K \approx 10 \log n \quad \text{for } n > 1000 \tag{11.11}$$

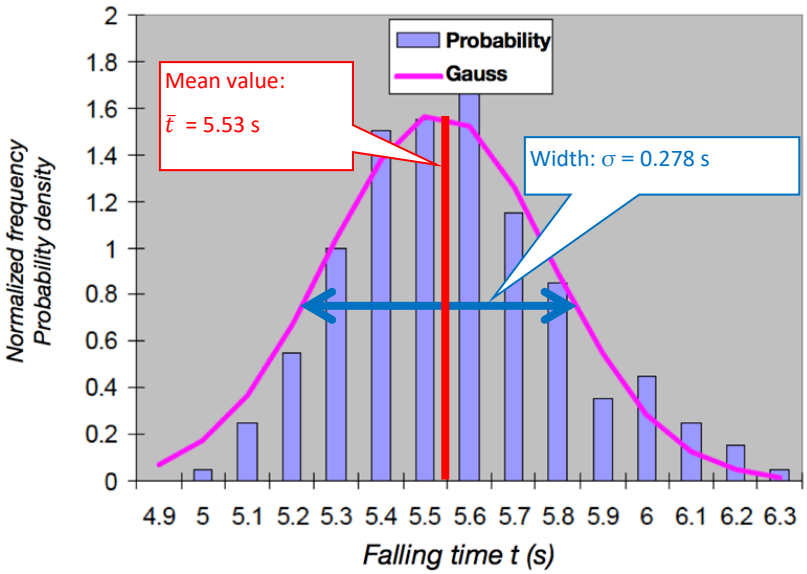

Figure 11.6: Normalized frequency (probability density) for 200 measuring values of the falling time of a steel bullet from Munich's Olympia tower using Dt = 0.1s leading to K = 15. The pink line represents the corresponding continuous Gaussian distribution $r(t)$ (see paragraph 11.2.3).

Moving on to the limiting case of an infinite number of measurements leads to infinitesimal intervals Δt and the discrete distribution becomes a continuous function, called the *limiting distribution* $r(t)$.

11.2.3 Gaussian (or normal) distribution

There are various discrete distributions based on statistical considerations that can describe fluctuations resulting from randomly occurring events; among them, the binomial distribution is particularly important. Increasing the number of events to infinity, Gauss derived an expression for the limiting continuous distribution, called the *Gaussian distribution* (or *normal distribution*) $G(t)$:

$$r(t) = G(t) = \sqrt{\frac{1}{2 \cdot \pi \cdot \hat{\sigma}^2}} \cdot e^{-\frac{(t-t_0)^2}{2 \cdot \hat{\sigma}^2}} \tag{11.12}$$

In the case of a sufficient number of individual measurements, i.e., in the case of good statistics, all distributions turn into a Gaussian distribution (Figure 11.7).

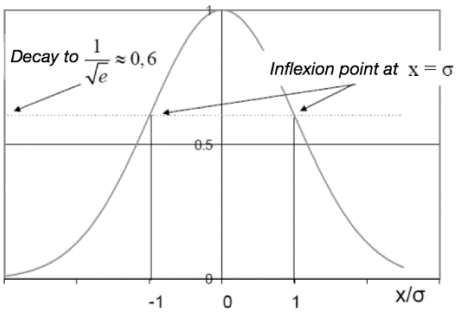

Figure 11.7: Gaussian distribution for which the x-axis is normalized to σ and the y-axis to $\sqrt{\frac{1}{2\cdot\pi\cdot\hat{\sigma}^2}}$.

The Gaussian distribution is characterized by two parameters:

- $\boldsymbol{t_0}$, which is the position of the *maximum* and of its *center* (since $G(t)$ is symmetrical).
- $\boldsymbol{t = \pm\hat{\sigma}}$ is the position of the two *inflection points*. The distance between these two points $\boldsymbol{2\hat{\sigma}}$ is regarded as the *width of the distribution*. Indeed, the value of the Gaussian at the inflection point $t = \hat{\sigma}$ is

$$G(t = \hat{\sigma}) = \sqrt{\frac{1}{2 \cdot \pi \cdot \hat{\sigma}^2}} \cdot e^{-\frac{1}{2}} \tag{11.13}$$

The pre-factor $\sqrt{\frac{1}{2\cdot\pi\cdot\hat{\sigma}^2}}$ normalizes the distribution, so that the area under the bell-shaped curve always equals $\int_{-\infty}^{\infty} G(t) \cdot dt = 1$. This means that the total probability of finding an event within the interval [-∞, +∞] equals one.

11.2.3.1 Central moments of the Gaussian distribution

Since we are dealing with a continuous probability density ρ(*t*), we need to redefine the mean value. Since for a discrete distribution, the arithmetic mean and the centroid were identical, we define the **mean value** of the continuous distribution as its centroid:

$$\bar{t} = \int_{-\infty}^{\infty} t \cdot \rho(t) \cdot dt \tag{11.14}$$

Mathematically, this integral is called the **first central moment** of the distribution. One can easily show that $\bar{t} = t_0$. Since t_0 is the maximum of the Gaussian, the mean value, and the maximum coincide. This is not surprising, since $G(t)$ is a symmetrical distribution.

The **second central moment** of the Gaussian distribution corresponds to the **variance** and characterizes its width; analogously to (11.6) it is defined as

$$\sigma^2 = \int_{-\infty}^{\infty} (t - \bar{t})^2 \cdot \rho(t) \cdot dt \tag{11.15}$$

Another feature of the Gaussian distribution is its *mean value of the square* $\overline{t^2}$, defined as

$$\overline{t^2} = \int_{-\infty}^{\infty} t^2 \cdot \rho(t) \cdot dt \tag{11.16}$$

An integration of the Gaussian yields:

$$\overline{t^2} = \hat{\sigma}^2 - \bar{t}^2 \tag{11.17}$$

It is also possible to demonstrate that the variance corresponds to

$$\sigma^2 = \overline{t^2} - \bar{t}^2 \tag{11.18}$$

Comparing (11.17) and (11.18), it is evident that $\sigma^2 = \hat{\sigma}^2$ or the variance corresponds to the square of the Gaussian parameter $\hat{\sigma}$, i.e. half of the full width of the distribution $2\hat{\sigma}$.

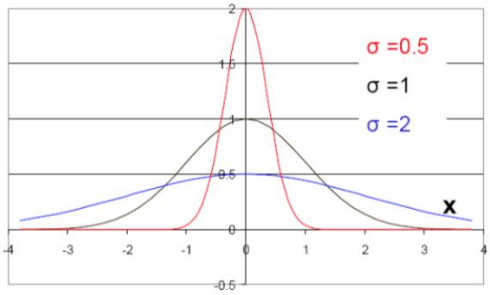

Figure 11.8: Influence of the Gaussian parameter $\hat{\sigma}$ on the shape of the distribution.

Figure 11.8 clearly shows that the distribution becomes broader with increasing $\hat{\sigma}$. Simultaneously, the amplitude of the distribution must decrease according to $\sqrt{\frac{1}{2\cdot\pi\cdot\hat{\sigma}^2}}$, to provide a constant area under the distribution (normalization).

11.2.3.2 Gauss error function and confidence integral

To estimate the statistics of your measurement, it is important to know how likely it is to find statistical events in an interval of width $\pm\sigma$ around the center of the Gaussian distribution. The probability w of finding a certain measuring value in any interval $[t_1, t_2]$ is given by

$$w = \int_{t_2}^{t_1} G(t) \cdot dt \tag{11.19}$$

This probability corresponds to the shaded area F in Figure 11.9A.

The *Gauss error function* gives the probability of finding a value in the interval $[-\infty, t]$ (see Figure 11.9B)

$$\phi(t) = \int_{-\infty}^{t} G(t') \cdot dt' \tag{11.20}$$

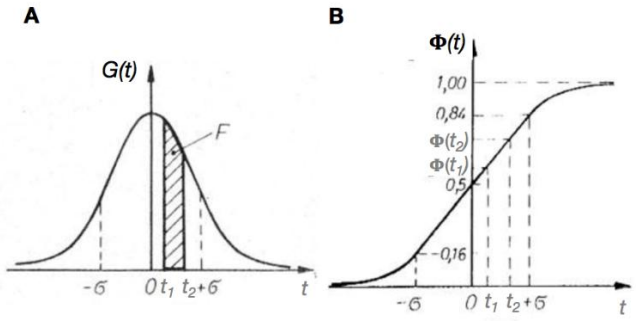

Figure 11.9: A) Gaussian distribution $G(t)$ and B) corresponding Gauss error function $\phi(t)$.

Since $\phi(t)$ is the primitive function of $G(t)$, the probability w in (11.19) can be easily calculated from the difference $\phi(t_2) - \phi(t_1)$. Unfortunately, $\phi(t)$ cannot be integrated analytically, and we need to use the tables given in mathematical formularies. The probability w_σ of finding a measuring value within the interval $[t_0 - \sigma, t_0 + \sigma]$ can be quantified as

$$w_\sigma = \int_{t_0-\sigma}^{t_0+\sigma} \cdot G(t) \cdot dt = \phi(\sigma) - \phi(-\sigma) = 0.841 - 0.159 = 0.683 = 68.3\% \tag{11.21}$$

In physics, the above-mentioned interval of a single standard deviation from the maximum of the distribution $[t_0 - \sigma, t_0 + \sigma]$ is generally accepted as the **confidence interval**.

In the technical field, a higher safety is required; therefore, the confidence interval is extended to ± the doubled standard deviation $[t_0 - 2\sigma, t_0 + 2\sigma]$. The probability of finding the measuring values in this region increases to 95.5%. In biology and medicine, the criterion of confidence is further enhanced to a probability of 97.7%, which is reached in the interval $[t_0 - 3\sigma, t_0 + 3\sigma]$.

11.3 **Error propagation**

In most experiments, multiple measurements are required, and we must calculate the desired result using a physical formula. For example, to determine the gravitational constant from $g = \frac{2 \cdot \bar{h}}{\bar{t}^2}$, we need to measure both the falling time t and the height h. From both measurements, we get average values $\bar{t}$ and $\bar{h}$ with different accuracies, defined by the standard deviations σ_t and σ_h.

The crucial question now is: how can we determine the best value for g, and what is the accuracy and precision of the obtained result? Generally speaking, we want to determine the value of a physical quantity f, which is a function of the measurable parameters $f(x_1, x_2, x_3 \dots)$, having uncertainties $(\Delta x_1, \Delta x_2, \Delta x_3 \dots)$. Our task is to obtain a meaningful result from the function $f(x_1, x_2, x_3 \dots)$ and to track the propagation of the measurement uncertaities, $(\Delta x_1, \Delta x_2, \Delta x_3 \dots)$ on the accuracy and precision of the result. To do so, it is necessary to discriminate between systematic errors and statistical errors.

11.3.1 Propagation of systematic errors

The systematic uncertainty of a measurement is not random, i.e., it has a distinct tendency. If we make a Taylor expansion of our function f:

$$f(x_1 + \Delta x_1, x_2 + \Delta x_2, \dots) = f(x_1, x_2, \dots) + \sum_{i=1}^{N} \left(\frac{\partial f}{\partial x_i}\right) \cdot \Delta x_i + \sum_{i,k=1}^{N} \left(\frac{\partial f}{\partial x_i}\right)\left(\frac{\partial f}{\partial x_k}\right) \cdot \Delta x_i \cdot \Delta x_k + \cdots \quad (11.22)$$

the systematic error Δf_{syst} can be calculated as

$$\Delta f_{syst}(x_1, x_2, \dots) = f(x_1 + \Delta x_1, x_2 + \Delta x_2, \dots) - f(x_1, x_2, \dots) = \sum_{i=1}^{N} \left(\frac{\partial f}{\partial x_i}\right) \cdot \Delta x_i \quad (11.23)$$

Since usually the errors are small, the expansion in the equation (11.22) is truncated at the linear term. For this reason, *systematic errors* contribute to the final error Δf_{syst} in a *linear* way.

11.3.2 Gaussian propagation of statistical errors

11.3.2.1 Functions of a single variable

For simplicity, we first discuss a simple example with only a single measured parameter and a quadratic function $f(x) = a \cdot x^2$. In Figure 11.10, a Gaussian distribution of x is depicted on the horizontal axis with a mean value $\bar{x}$ and an error Δx (i.e., standard deviation σ), corresponding to the width of the distribution. From each value of x we can calculate a result $f(x)$ and construct a distribution of results (depicted on the vertical axis). Note that the new distribution is not symmetric anymore, because of the rising slope of the function $f(x)$. With this distribution of f_i values, it is possible to calculate the average value $\overline{f(x)}$. Having more than one parameter x, this procedure becomes tedious and impractical.

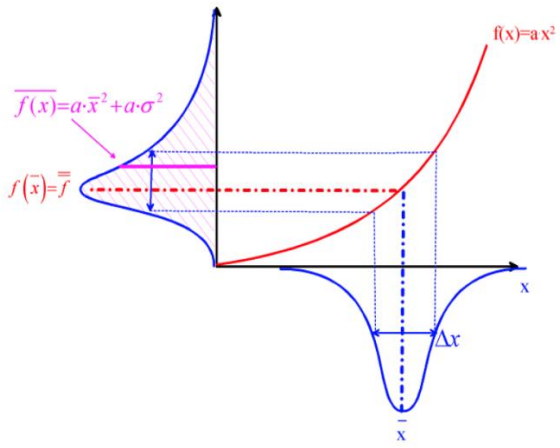

Figure 11.10: Formation of the real mean value $\overline{f(x)}$ in the case of strong non-linearity. The mean value $\overline{f(x)}$ is shifted towards higher values since the distribution of the f_i values is asymmetric. Furthermore, the width of the distribution of the f_i values becomes larger.

Obviously, it would be much simpler to average over the x_i values first, obtaining $\bar{x}$, and to calculate $f(\bar{x})$ in a second step. The question will be whether such a procedure is appropriate, and, in particular, how large the error will be.

To investigate this issue, we construct a linear approximation of the function $f(x) = a \cdot x^2$ by making a Taylor expansion in terms of a deviation Δx around the mean value of $\bar{x}$, as we did in paragraph 11.3.1:

$$f(\bar{x}+\Delta x) = f(\bar{x}) + \sum_{i=1}^{N}\left(\frac{\partial f}{\partial x_i}\right)\cdot\Delta x_i + \sum_{i,k=1}^{N}\left(\frac{\partial f}{\partial x_i}\right)\left(\frac{\partial f}{\partial x_k}\right)\cdot\Delta x_i\cdot\Delta x_k + \cdots \tag{11.24}$$

Neglecting the higher-order terms, and in the case of the quadratic function $f(x) = a \cdot x^2$ we can derive:

$$f(\bar{x}+\Delta x) = f(\bar{x}) + \sum_{i=1}^{N}\left(\frac{\partial f}{\partial x_i}\right)\cdot\Delta x_i = a\cdot\bar{x}^2 + 2a\cdot\bar{x}\cdot\Delta x \tag{11.25}$$

This approximation of $\overline{f(x)}$ as a linear function of Δx is shown in Figure 11.11 as a dashed red line touching the correct function $f(x)$ as a tangent at $\bar{x}$. To construct the distribution of f_i values, we simply must mirror the Gaussian distribution of the x values at the dashed red tangent and obtain a Gaussian distribution of f_i values. Due to the symmetry of both distributions, the mean values $\overline{f(x)}$ and $f(\bar{x})$ coincide. Furthermore, we see how the width of the distribution of x_i affects the width of the $f(x)$ distribution: the larger the slope of the linear approximation is, the larger the width of the $f(x)$ distribution will be.

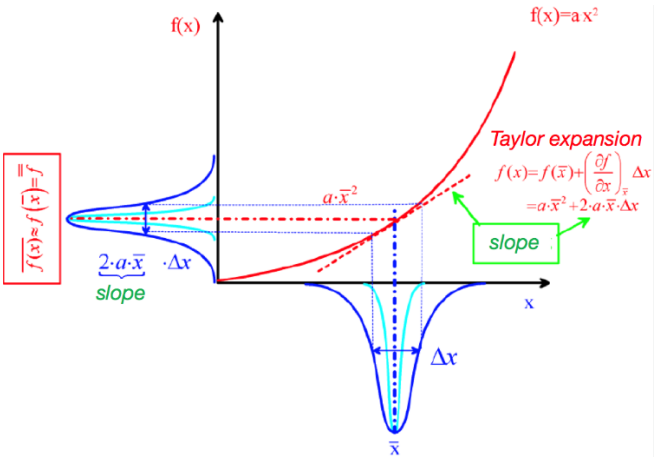

Figure 11.11: Construction of the distribution of $f(x)$ based on a linear approximation of $f(x) = a \cdot x^2$.

Frequently, we are confronted with functions $f(x_1, x_2, x_3 \ldots)$ of more than one independent variable x_1, x_2, x_3 …. In the appendix, it is shown that:

1. The mean values $\overline{f(x_1, x_2, x_3 \ldots)}$ and $f(\overline{x_i}) = f(\overline{x_1}, \overline{x_2}, \ldots, \overline{x_N})$ coincide (see Appendix 11.5.1).
2. The *Gaussian law of error propagation* gives the statistical error of the result $\overline{f(x_1, x_2, x_3 \ldots)}$ (see Appendix 11.5.2) as in:

$$\sigma_f = \sqrt{\left(\frac{\partial f}{\partial x_1}\right)^2 \cdot \sigma_1^2 + \left(\frac{\partial f}{\partial x_2}\right)^2 \cdot \sigma_2^2 + \cdots} \tag{11.26}$$

Note:

i. Equation (11.26) is valid for *statistical errors* only.

ii. the error contributions of the individual measuring variables $\Delta f_1 = \left(\frac{\partial f}{\partial x_1}\right)^2 \cdot \sigma_1^2$, $\Delta f_2 = \left(\frac{\partial f}{\partial x_2}\right)^2 \cdot \sigma_2^2$,… do not sum up linearly but partially compensate each other. This is considered in the orthogonal addition (refer to the Pythagorean theorem, Figure 11.12).

iii. Only contributions that are similar in size are important, meaning that small contributions can be neglected.

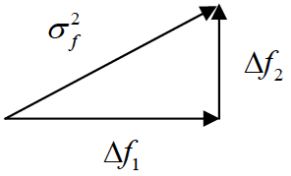

Figure 11.12: Pythagorean Theorem applied to the combination of the errors of two variables.

11.3.3 Useful rules for Gaussian error propagation

We now determine the derivatives for some frequently occurring functions and derive the Gaussian error propagation.

11.3.3.1 Sum or difference of variables: $f = x_1 + x_2$ or $f = x_1 - x_2$

$$\sigma_f = \sqrt{\left(\frac{\partial(x_1 \pm x_2)}{\partial x_1}\right)^2 \cdot \sigma_1^2 + \left(\frac{\partial(x_1 \pm x_2)}{\partial x_2}\right)^2 \cdot \sigma_2^2} \Rightarrow \sigma_f = \sqrt{\sigma_1^2 + \sigma_2^2} \tag{11.27}$$

since $\left(\frac{\partial(x_1 \pm x_2)}{\partial x_1}\right)^2 = \left(\frac{\partial(x_1 \pm x_2)}{\partial x_2}\right)^2 = 1$

The error square of a sum or a difference equals the sum of the error squares of all summands.

11.3.3.2 Product or quotient of variables: $f = x_1 \cdot x_2$ or $f = \frac{x_1}{x_2}$

$$\sigma_f = \sqrt{\left(\frac{\partial(x_1 \cdot x_2)}{\partial x_1}\right)^2 \cdot \sigma_1^2 + \left(\frac{\partial(x_1 \cdot x_2)}{\partial x_2}\right)^2 \cdot \sigma_2^2} \Rightarrow \sigma_f = \sqrt{x_2^2 \cdot \sigma_1^2 + x_1^2 \cdot \sigma_2^2} \tag{11.28}$$

since $\left(\frac{\partial(x_1 \cdot x_2)}{\partial x_1}\right)^2 = x_2^2$ and $\left(\frac{\partial(x_1 \cdot x_2)}{\partial x_2}\right)^2 = x_1^2$.

Dividing by $\mathbf{f = x_1 \cdot x_2}$ reveals the relative error

$$\frac{\sigma_f}{f} = \sqrt{\left(\frac{x_2}{x_1 \cdot x_2}\right)^2 \cdot \sigma_1^2 + \left(\frac{x_1}{x_1 \cdot x_2}\right)^2 \cdot \sigma_2^2} = \sqrt{\left(\frac{\sigma_1}{x_1}\right)^2 + \left(\frac{\sigma_2}{x_2}\right)^2} \tag{11.29}$$

It is easy to demonstrate that the equation (11.29) is valid also in the case of $\mathbf{f = \frac{x_1}{x_2}}$

The square of the relative error of a product or quotient equals the sum of the relative error squares of all factors.

11.3.3.3 Exponential function: $f = x^n$

$$\sigma_f = \sqrt{\left(\frac{\partial x^n}{\partial x}\right)^2 \cdot \sigma_x^2} \tag{11.30}$$

Here $\frac{\partial x^n}{\partial x} = n \cdot x^{n-1}$. Dividing by $\mathbf{f = x^n}$ reveals the relative error:

$$\frac{\sigma_f}{f} = \sqrt{\left(\frac{n \cdot x^{n-1}}{\mathbf{x^n}}\right)^2 \cdot \sigma_x^2} = n \cdot \frac{\sigma_x}{x} \tag{11.31}$$

The relative error of an exponential function equals the product of the relative error of the basis x multiplied by the exponent n

11.3.3.4 Natural exponential function: $f = e^{a \cdot x}$

$$\sigma_f = \sqrt{\left(\frac{\partial \mathbf{e^{a \cdot x}}}{\partial x}\right)^2 \cdot \sigma_x^2} \tag{11.32}$$

Here $\frac{\partial \mathbf{e^{a \cdot x}}}{\partial x} = a \cdot \mathbf{e^{a \cdot x}}$. Dividing by $\mathbf{f = e^{a \cdot x}}$ reveals the relative error:

$$\frac{\sigma_f}{f} = \sqrt{\left(\frac{a \cdot \boldsymbol{e^{a \cdot x}}}{\boldsymbol{e^{a \cdot x}}}\right)^2 \cdot \sigma_x^2} = a \cdot \sigma_x \tag{11.33}$$

The relative error of a natural exponential function equals the product of the absolute error of the basis x multiplied by the coefficient at the exponent a.

11.3.3.5 General and natural logarithms: $f = \log_b x$ and $f = \ln x$

$$\sigma_f = \sqrt{\left(\frac{\partial \log_{\boldsymbol{b}} \boldsymbol{x}}{\partial x}\right)^2 \cdot \sigma_x^2} = \sqrt{\left(\frac{1}{x \cdot \ln b}\right)^2 \cdot \sigma_x^2} = \frac{1}{\ln b} \cdot \frac{\sigma_x}{x} \tag{11.34}$$

It is easy to demonstrate that $\mathbf{f = \ln x}$ is a particular case of the equation (11.34):

$$\sigma_f = \sqrt{\left(\frac{\partial \ln x}{\partial x}\right)^2 \cdot \sigma_x^2} = \sqrt{\left(\frac{1}{x}\right)^2 \cdot \sigma_x^2} = \frac{\sigma_x}{x} \tag{11.35}$$

The absolute error of the logarithm of x in base b equals the relative error of x multiplied by $\frac{1}{ln\, b}$.

11.3.4 Standard deviation of the mean value

Table 11.2-1 provides the data for the time t_i of a steel bullet falling a certain distance. The experiment was repeated n times and from the n t_i values the corresponding mean value $\bar{t}$ (Equation (11.3)) and the standard deviation σ of the individual measurements (Equation (11.6)) were determined. Comparing different data sets would yield slightly different mean values $\bar{t}$. This leads to the question of how the mean values (also called optimal values) of different data sets differ from each other, and in particular, how much they differ from the "real value". Though the real value is not known, it would be at the center of an idealized Gaussian distribution: $t_{real} = t_0$. We can formulate the **standard deviation of the mean value** σ_m (or the variance σ_m^2 of $\bar{t}$ with respect to t_0) by its second moment:

$$\sigma_m^2 = \int_{-\infty}^{\infty} (\bar{t} - t_0)^2 \cdot \rho(t) \cdot dt \tag{11.36}$$

We can insert the equation (11.3) in (11.36): $\sigma_m^2 = \int_{-\infty}^{\infty} (\frac{1}{n} \sum_{i=1}^{n} t_i - t_0)^2 \cdot \rho(t) \cdot dt$

$$\sigma_m^2 = \int_{-\infty}^{\infty} \left(\frac{1}{n} \sum_{i=1}^{n} t_i - t_0\right)^2 \cdot \rho(t) \cdot dt \tag{11.37}$$

Considering $\bar{t}$ as a function of the individual measuring values t_i, each of which is affected by the error σ. The error of $\bar{t}$, can be calculated according to Gaussian error propagation, obtaining:

$$\sigma_m^2 = \sum_{k=1}^{N} \left(\frac{\partial \bar{t}}{\partial t_k}\right)^2 \cdot \sigma_k^2 \text{ where } \frac{\partial \bar{t}}{\partial t_k} = \frac{\partial}{\partial t_k}\left(\frac{1}{n} \cdot \sum_{i=1}^{n} t_i\right) = \frac{1}{n} \cdot \sum_{i=1}^{n} \frac{\partial}{\partial t_k} t_i \tag{11.38}$$

Since the derivative of independent variables is: $\frac{\partial t_i}{\partial t_k} = 1$ for $i = k$ and $\frac{\partial t_i}{\partial t_k} = 0$ for $i \neq k$, the sum reduces to $\sum_{i=1}^{n} \frac{\partial}{\partial t_k} t_i = 1$, and we obtain: $\frac{\partial \bar{t}}{\partial t_k} = \frac{1}{n}$.

Since the standard deviation of each individual measurement remains constant, i.e. $\sigma_k = \sigma$ we finally obtain:

$$\sigma_m^2 = \sum_{k=1}^{n} \left(\frac{1}{n}\right)^2 \cdot \sigma^2 = \frac{1}{n} \cdot \sigma^2 \tag{11.39}$$

Taking the square root of (11.39), we get the simple but important result for the **standard deviation of the mean value**:

$$\sigma_m == \frac{\sigma}{\sqrt{n}} \tag{11.40}$$

Equation (11.40) clearly shows that the larger the data set (the larger n) is, the smaller the standard deviation of the mean value. For example, for $n = 10 \Rightarrow \sigma_m = \frac{\sigma}{3.16}$ and for $n = 100 \Rightarrow \sigma_m = \frac{\sigma}{10}$.

11.4 Least-square fitting

We want to discuss now whether the measuring values do obey a particular physical law or, if there´s no physical model yet obtainable, whether the data can be reasonably described empirically by an analytical function and how the parameters of the particular law can be optimized (search for the "best" curve = line of best fit or regression line).

Let us describe the physical law by a function: $y = f(\,{}^1x,\ {}^2x, \ldots \alpha_1, \alpha_2, \ldots)$. Here, the dependent variable y is expressed by the variables ${}^1x,\ {}^2x, \ldots$. Both y and ${}^kx$ can be measured while the unknown parameters of the theory $\alpha_1 \ldots \alpha_j \ldots \alpha_n$ are to be determined by matching theory and experiment as closely as possible. To test the course of a model function, the experiment is performed at different "settings" of each variable ${}^1x_i$ (index $i = 1 \rightarrow m$) and for each variable set ${}^kx_i$ the corresponding value y_i of the function is measured. As an example, the Van-der-Waals equation in the case of real gases is considered:

$$\left(p + \frac{n^2 \cdot a}{V^2}\right) \cdot (V - n \cdot b) = n \cdot R \cdot T \tag{11.41}$$

where $n = \frac{m}{M}$ (mass m divided by the molar mass M, i.e., the number of moles). The pressure p is measured as a function of the volume V and the temperature T and we can summarize the relations among the variables as follows:

- ✓ p is the dependent variable and can be measured:

$$y = p(V, T, a, b, R) = \frac{n \cdot R \cdot T}{V - n \cdot b} - \frac{n^2 \cdot a}{V^2} \tag{11.42}$$

- ✓ V, T are the independent variables ${}^kx$ and can be measured:

$$\begin{aligned} {}^1x &\rightarrow V \\ {}^2x &\rightarrow T \end{aligned} \tag{11.43}$$

- ✓ a, b, R are the parameters of the theory α_j, which are not directly accessible by measurement, and which should be determined (fitting parameters):

$$\begin{aligned} \alpha_1 &\rightarrow a \\ \alpha_2 &\rightarrow b \\ \alpha_3 &\rightarrow R \end{aligned} \tag{11.44}$$

During the measurement, the variables V and T are varied (and labelled with the index i):

$$
\begin{aligned}
&i = 1 \rightarrow V_1, T_1 \\
&i = 2 \rightarrow V_2, T_1 \\
&i = 3 \rightarrow V_3, T_1 \ldots etc \\
&i = 10 \rightarrow V_{10}, T_1 \\
&i = 11 \rightarrow V_1, T_2 \\
&i = 12 \rightarrow V_2, T_2 \\
&i = 13 \rightarrow V_3, T_2
\end{aligned}
\qquad (11.45)
$$

Figure 11.13 shows the corresponding van-der-Waals isotherms. At each grid point, a measurement is performed and labeled with the corresponding counting index i. The grid is composed of 4 isotherms at different temperatures, and each individual isotherm (p, V curve) consists of 20 points that lead in total to $m = 80$. For each theoretical value $p(T_i, V_i)$ there is a measured value y_i. The latter is positioned slightly below or above the theoretical grid point, meaning that it deviates from the model function $f(\,{}^1x_i,\ {}^2x_i, \ldots)$ by a certain amount r_i, called residual (see paragraph 11.4.1). For a suitable model function, this deviation is of similar magnitude to the measuring error σ_p. Since the error in y_i can be considered now, the error bars for the variables V and T are added to the σ_p (see also paragraph 11.4.1). The calculation of best fit tries to fit the theoretical curve as well as possible to all measuring values by minimizing the sum of all squares of the residuals, and therefore this method is called the least-squares method.

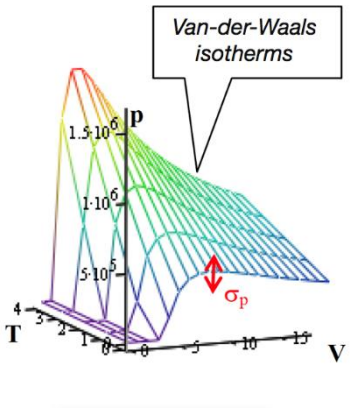

Figure 11.13: A series of Van-der-Waals isotherms.

11.4.1 Residuals

Usually, the accuracy of the measured values y and ${}^kx$ can be quantified with the help of their standard deviations σ_y and ${}^k\sigma_x$, respectively. For the sake of simplification, we shall only consider the inaccuracy σ_y of the dependent variable y. The errors of the independent variables ${}^k\sigma_x$ can be added to σ_y using the functional relationship $f(\,{}^1x,\ {}^2x, \ldots \alpha_1, \alpha_2, \ldots)$ and the Gaussian law of error propagation (Equation (11.26)).

Let us first assume that $f(\,{}^1x,\ {}^2x, \ldots \alpha_1, \alpha_2, \ldots)$ is exactly equal to the expected value of y in case the parameters $\alpha_1, \alpha_2, \ldots \alpha_n$ are correct. Next, let us quantify the deviation of a measuring point y_i, from the theoretical function $f(\,{}^1x,\ {}^2x, \ldots \alpha_1, \alpha_2, \ldots)$, if the parameters $\alpha_1, \alpha_2, \ldots \alpha_n$ are not correct by the **residual**:

$$r_i = y_i - f(\,{}^1x_i,\ {}^2x_i, \ldots) \qquad (11.46)$$

or the **weighted residual**:

$$r_{i(w)} = \frac{y_i - f(\,{}^1x_i,\ {}^2x_i, \ldots)}{\sigma_{y,i}} \qquad (11.47)$$

For the example given in the previous paragraph (Equation (11.41)) this would mean

$$r_i = p_i - \frac{n \cdot R \cdot T_i}{V_i - n \cdot b} - \frac{n^2 \cdot a}{V_i^2} \tag{11.48}$$

Usually, the number of measurements m is more than one order of magnitude larger than the number p of fitting parameters α_j. Since in general p equations are necessary for the determination of p unknowns, the problem is mathematically overdetermined. This gives us the chance to test the suitability of the model function f and to compare it with other model functions. If the number of measurements m would be identical to the number of parameters p, then the problem would be solvable as well, but there would be no way to determine whether a given model fits better than another. According to the principle of "*maximum likelihood*", we quantify the probability of obtaining a certain set of measuring results and must search for that set of parameters $\alpha_1, \alpha_2, \ldots$ for which this probability becomes maximal. In the Appendix 11.5.3 it is shown that this is the case when chi-square χ^2:

$$\chi^2 \equiv \sum_{i=1}^{N} \frac{\left(y_i - f\left({}^1x_2,\ {}^2x_2 \ldots, \alpha_1, \alpha_2 \ldots \alpha_p\right)\right)^2}{\sigma_i^2} \tag{11.49}$$

becomes minimal. This method is called "least-square principle". The weighting term $\frac{1}{\sigma_i^2}$ makes sure that each measuring value y_i contributes to the sum of the error squares according to its measuring accuracy. Thereby, the absolute value of $\frac{1}{\sigma_i^2}$ is not crucial, but only the relative weighting needs to be correct. At this point, it is important to note that in standard software for linear regression (e.g., Excel), it is assumed implicitly that all $\frac{1}{\sigma_i^2} = 1$. This can provide wrong fit results (see below, paragraph 11.4.3 page 110).

Figure 11.14 illustrates the least-squares principle by depicting χ^2 as a function of the parameters α_j. This function $\left(\chi^2(\alpha_1, \alpha_2, \ldots)\right)$ represents a multidimensional hypersurface. The task is now to find the lowest point in the valleys of this "landscape". We then need a suitable procedure for varying the parameters $\alpha_1, \alpha_2, \ldots$ until the minimum of χ^2 is found. There are several strategies to quickly and reliably find the global minimum on a multidimensional hypersurface. These are implemented in special software packages. In paragraphs 11.4.4 and 11.4.5 a standard method is derived, which provides an exact solution for the case of a linear dependence on α_i (linear regression). This method is available in many standard software packages, e.g., Excel.

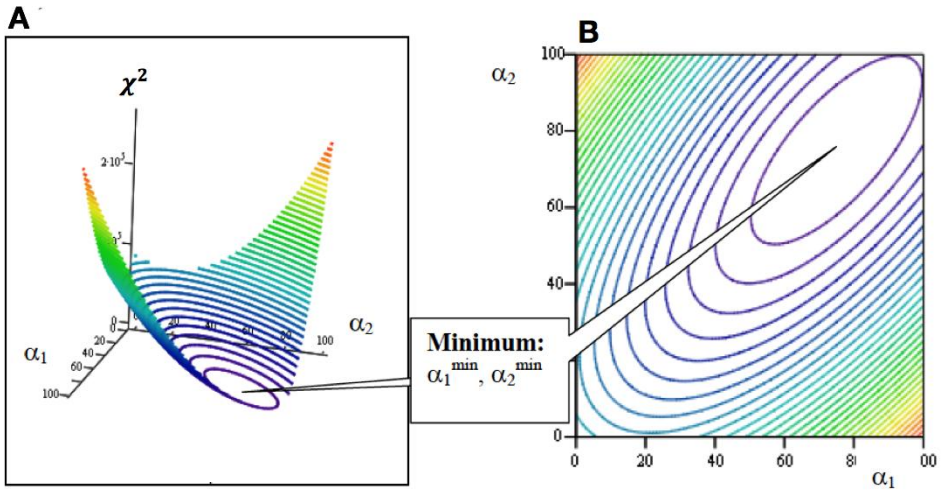

Figure 11.14: Error square as a function of the parameters α_j. In Figure A, χ^2 is plotted along the z-axis. The x-axis and the y-axis correspond to the parameter α_1 and α_2, respectively. Figure B represents a profile of the level curves of χ^2.

11.4.2 Linearization

Nonlinear functions are often linearized by transforming one of the coordinates. For example, in the case of a *natural exponential function*, we can get:

$$f(x) = a \cdot e^{\alpha \cdot x} \xrightarrow{take\ the\ \ln\ of\ the\ y-axis} g(x) = \ln y = \ln a + \alpha \cdot x \tag{11.50}$$

where $\ln a$ corresponds to the intercept and α to the slope of a line, respectively.

In the case of a general *exponential function*:

$$y(x) = a \cdot x^n \xrightarrow{take\ the\ \ln\ of\ the\ x-axis\ and\ the\ y-axis} \ln y = \ln a + n \cdot \ln x \tag{11.51}$$

where $\ln a$ corresponds to the intercept and n to the slope, respectively. Note that the error bars of $\ln y$ and $\ln x$, respectively, need to be calculated according to the Gaussian law of error propagation. *The smaller ln y, the larger gets the error bar.*

11.4.3 Linear regression

The function for the special case of a straight line with the slope α_2 and the intercept α_1 is

$$f(x, \alpha_1, \alpha_2) = \alpha_1 + \alpha_2 \cdot x \tag{11.52}$$

In this case can be demonstrated that we can derive the two parameters defining the regression line α_1, α_1 as:

$$\alpha_1 = \frac{S_y \cdot S_{x^2} - S_{xy} \cdot S_x}{\Delta} \tag{11.53}$$

$$\alpha_2 = \frac{S_{xy} \cdot S - S_y \cdot S_x}{\Delta} \tag{11.54}$$

with

$$S \equiv \sum_{i=1}^{N} \frac{1}{\sigma_i^2} \tag{11.55}$$

$$S_x \equiv \sum_{i=1}^{N} \frac{x_i}{\sigma_i^2} \tag{11.56}$$

$$S_y \equiv \sum_{i=1}^{N} \frac{y_i}{\sigma_i^2} \tag{11.57}$$

$$S_{x^2} \equiv \sum_{i=1}^{N} \frac{x_i^2}{\sigma_i^2} \tag{11.58}$$

$$S_{xy} \equiv \sum_{i=1}^{N} \frac{x_i \cdot y_i}{\sigma_i^2} \tag{11.59}$$

$$\Delta = S \cdot S_{x^2} - S_x \cdot S_x \tag{11.60}$$

Excel and other software provide automatic linear regression calculations. In these software, the measuring values x_i, y_i etc. are not automatically weighted with σ_i^2, meaning with the variances of y_i. Therefore, the regression should be directly performed with the help of equations (11.53) and (11.54).

11.4.4 Estimation of the errors of the regression parameters

The influence of the error Δy_i on the errors $\Delta\alpha_1$ and $\Delta\alpha_2$ can be determined with the help of the law of error propagation (see paragraph 11.3.2)

$$\Delta\alpha_k^2 = \sum_{i=1}^{n} \left(\frac{\partial \alpha_k}{\partial y_i}\right)^2 \cdot \Delta y_i^2 \tag{11.61}$$

Using the equations (11.53) to (11.60), we can derive (see the Appendix 11.5.4)

$$\Delta\alpha_1^2 = \frac{S_{x^2}}{\Delta} \tag{11.62}$$

$$\Delta\alpha_2^2 = \frac{S}{\Delta} \tag{11.63}$$

Note that the evaluation of a fit (goodness of fit χ^2) and the comparison of different models is actually very complex and demands some experience. Equations (11.62) and (11.63), respectively, give only a rough indication.

11.4.5 Important example

Here, we consider the law of gravitation

$$t = \sqrt{\frac{2 \cdot H}{g}} \tag{11.64}$$

where H, t and g denote the falling height, the falling time, and the acceleration of gravity, respectively. The aim of this example is to prove this law and to determine the gravitational acceleration. For this purpose, a set of measured falling times $t_{j,i}$ is collected for different falling heights H_j. The falling times are averaged according to $\overline{t_j} = \frac{1}{n_j}\sum_{i=1}^{n_j} t_{j,i}$ (analogously to the equation (11.3)) and the corresponding standard deviation σ_{t_j} can be calculated (see equation (11.6)). The falling height is also measured several times and is registered with the mean value $\overline{H_j}$ and the corresponding σ_{h_j}. Linearization by double logarithmic plotting (according to (11.50)) yields a straight line with the slope $\alpha_2 = 1/2$

$$\log\left(\frac{t}{s}\right) = \log\left(\left(\frac{2 \cdot H}{g}\right)^{\frac{1}{2}}\right) = -\frac{1}{2} \cdot \log\left(\frac{g}{m/s^2}\right) + \frac{1}{2} \cdot \log\left(\frac{2 \cdot H}{m}\right) \tag{11.65}$$

where $\log\left(\frac{t}{s}\right)$ corresponds to the *y*-axis, $-\frac{1}{2} \cdot \log\left(\frac{g}{m/s^2}\right)$ to the intercept α_1, $\frac{1}{2}$ to the slope α_2 and $\log\left(\frac{2 \cdot H}{m}\right)$ to the x-axis, like in

$$y_i = \alpha_1 + \alpha_2 \cdot x_i \tag{11.66}$$

Note that the numbers need to be dimensionless in their logarithm, since the logarithm of a unit does not make physical sense. Therefore, each value is divided by its own dimension, e.g., t is divided by s, H by m and g by $\frac{m}{s^2}$, respectively. However, it is important to take care that the dimensions are consistent with the physical quantity. This means that it is not allowed to mix up *t*/min, *H*/cm, and *g*/(km/h²). The measuring data and the corresponding evaluation are summarized in Table 11.4-1. Before plotting the data in a graph (Figure 11.15), it is important to account for measurement errors when determining the error bars. First, *errors in the abscissa direction* are considered. For this, it is assumed that the height is determined with an accuracy of $\Delta H = \pm 0.2\ m$. The x-axis plots $\log\ (2 \cdot H)$ and the corresponding errors are calculated according to the Gaussian error propagation

$$\Delta \log H = \left(\frac{\partial \log(2 \cdot H)}{\partial H}\right) \cdot \Delta H = 2 \cdot \frac{\Delta H}{H} \tag{11.67}$$

Determination of the errors in the direction of the ordinate (y-axis): Table 11.2-1 shows data from 20 individual measurements at a given falling height. The mean value obtained by averaging is $\bar{t} = 5.53\ s$ and the corresponding statistical error of an individual measurement $\sigma_t = 0.278\ s$ (see paragraph 11.2). Compared to this, Table 11.4-1 shows the falling times for different falling heights, and the falling time for a given height was obtained by averaging only three individual measurements to limit the number of measurements. For the calculations, it is assumed that the time is determined with an accuracy of $\Delta t = \pm 0.075\ s$.

Table 11.4-1: Data and their evaluation on the experiment about the law of gravitation.

height H/m	**time** t/s	$\log\left(\frac{2\cdot H}{m}\right)$	$\log\left(\frac{t}{s}\right)$	$\Delta\log(2\cdot H)=2\cdot\frac{\Delta H}{H}$	$\Delta\log(t)=\frac{\Delta t}{t}$	$1/\sigma^2=1/[(\Delta\log(2\cdot H))^2+(\Delta\log(t))^2]$	$\frac{x_i}{\sigma_i^2}$	$\frac{y_i}{\sigma_i^2}$	$\frac{x_i^2}{\sigma_i^2}$	$\frac{x_i\cdot y_i}{\sigma_i^2}$
1	0.60	0.301	-0.223	0.400	0.125	5.693E+00	1.71E+0	-1.27E+0	5.16E-1	-3.82E-1
4	1.02	0.903	0.009	0.100	0.073	6.505E+01	5.87E+1	5.8E-1	5.31E+1	5.24E-1
9	1.02	1.255	0.007	0.044	0.074	1.351E+02	1.7E+2	9.15E-1	2.13E+2	1.15E+0
16	1.95	1.505	0.289	0.025	0.038	4.758E+02	7.16E+2	1.38E+2	1.08E+3	2.07E+2
25	2.47	1.699	0.393	0.016	0.030	8.529E+02	1.45E+3	3.35E+2	2.46E+3	5.69E+2
36	2.93	1.857	0.468	0.011	0.025	1.293E+03	2.4E+3	6.04E+2	4.46E+3	1.12E+3
49	3.46	1.991	0.539	0.008	0.022	1.874E+03	3.73E+3	1.01E+3	7.43E+3	2.01E+3
64	3.37	2.107	0.527	0.006	0.022	1.876E+03	3.95E+3	9.89E+2	8.33E+3	2.08E+3
81	3.83	2.210	0.584	0.005	0.020	2.467E+03	5.45E+3	1.44E+3	1.2E+4	3.18E+3
100	4.83	2.301	0.684	0.004	0.015	3.910E+03	9.E+3	2.67E+3	2.07E+4	6.16E+3
121	4.78	2.384	0.680	0.003	0.016	3.910E+03	9.32E+3	2.66E+3	2.22E+4	6.33E+3
144	5.54	2.459	0.743	0.003	0.014	5.259E+03	1.29E+4	3.91E+3	3.18E+4	9.62E+3
169	5.94	2.529	0.774	0.002	0.013	6.088E+03	1.54E+4	4.71E+3	3.89E+4	1.19E+4
196	6.30	2.593	0.799	0.002	0.012	6.876E+03	1.78E+4	5.49E+3	4.62E+4	1.42E+4
225	6.74	2.653	0.828	0.002	0.011	7.905E+03	2.1E+4	6.55E+3	5.56E+4	1.74E+4
256	7.51	2.709	0.876	0.002	0.010	9.830E+03	2.66E+4	8.61E+3	7.22E+4	2.33E+4
289	7.66	2.762	0.884	0.0014	0.010	1.026E+04	2.83E+4	9.07E+3	7.83E+4	2.51E+4
324	8.17	2.812	0.912	0.0012	0.009	1.171E+04	3.29E+4	1.07E+4	9.25E+4	3.E+4
361	8.50	2.859	0.929	0.0011	0.009	1.270E+04	3.63E+4	1.18E+4	1.04E+5	3.38E+4
400	9.15	2.903	0.962	0.0010	0.008	1.475E+04	4.28E+4	1.42E+4	1.24E+5	4.12E+4
						1.02E+5 $S\equiv\sum_{i=1}^{N}\frac{1}{\sigma_i^2}$	**2.7E+5** $S_x\equiv\sum_{i=1}^{N}\frac{x_i}{\sigma_i^2}$	**8.49E+4** $S_y\equiv\sum_{i=1}^{N}\frac{y_i}{\sigma_i^2}$	**7.23E+5** $S_{x^2}\equiv\sum_{i=1}^{N}\frac{x_i^2}{\sigma_i^2}$	**2.28E+5** $S_{xy}\equiv\sum_{i=1}^{N}\frac{x_i\cdot y_i}{\sigma_i^2}$

Intercept:	$\alpha_1=\frac{S_y\cdot S_{x^2}-S_{xy}\cdot S_x}{\Delta}$	-0.468		
	$\Delta\alpha_1=\sqrt{\frac{S_{x^2}}{\Delta}}$	0.031		
Slope:	$\alpha_2=\frac{S_{xy}\cdot S-S_y\cdot S_x}{\Delta}$	0.491	$\Delta\alpha_2=\sqrt{\frac{S}{\Delta}}$	0.011

$S_y\cdot S_{x^2}-S_{xy}\cdot S_x$	$S_{xy}\cdot S-S_y\cdot S_x$	$\Delta=S\cdot S_{x^2}-S_x\cdot S_x$
-3.619E+08	**3.795E+08**	**7.732E+08**

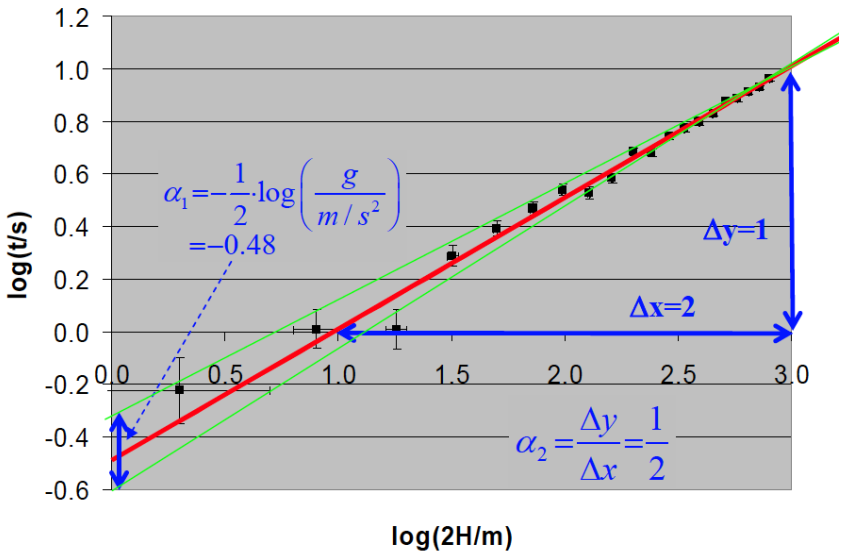

Figure 11.15: Double logarithmic plot of the data given in Table 11.4-1.

Thus, for the 20 measurements in Table 11.2-1 one obtains a mean deviation of the mean value of $\sigma_{\bar{t},20}=\frac{\sigma}{\sqrt{20}}$ and analogously, for the falling times in Table 11.4-1 $\sigma_{\bar{t},3}=\frac{\sigma}{\sqrt{3}}=0.15$. Since log(*t*) is plotted on the y-axis, the error bars in this direction are given by

$$\Delta\log t=\left(\frac{\partial\log(t)}{\partial t}\right)\cdot\sigma_{\bar{t},3}=\frac{\sigma_{\bar{t},3}}{t} \tag{11.68}$$

Besides the logarithmic conversion of the measuring data, Table 11.4-1 also reports the length of the error bars.

11.5 Appendixes

11.5.1 Function of several independent variables

In general, the N measuring parameters x_k and their respective errors are independent. Based on a measuring series, the measuring value is determined n times (index i) and from this the mean value $\overline{x_k}$ and the corresponding standard deviation σ_k can be determined by

$$\overline{x_k} = \frac{1}{n} \cdot \sum_{i=1}^{n} x_{i,k} \tag{11.69}$$

$$\sigma_k = \sqrt{\frac{1}{n-1} \cdot \sum_{i=1}^{n} \left(x_{i,k} - \overline{x_k}\right)^2} \tag{11.70}$$

From the ith measurement, one obtains the result $f_{i,k} = f(x_{i,1}, x_{i,2}, \dots)$. To obtain the most reliable result, one may calculate the arithmetic mean of the individual results $\bar{f} = \overline{f_{i,k}(x_{i,1}, x_{i,2}, \dots)}$ according to the Equation (11.69):

$$\bar{f} = \frac{1}{n} \cdot \sum_{i=1}^{n} f_{i,k} \tag{11.71}$$

Alternatively, one can first calculate the arithmetic mean of the individual arguments $\overline{x_k}$ from the same Equation (11.69) and then calculate the result function:

$$\bar{\bar{f}} = f_{i,k}(\overline{x_1}, \overline{x_2}, \dots, \overline{x_N}) \tag{11.72}$$

To compare $\bar{f}$ and $\bar{\bar{f}}$, we consider the deviation of each individual measurement f_i from the mean value $\bar{\bar{f}}$ by writing f_i as a Taylor expansion around $\bar{\bar{f}}$:

$$f_{i,k} = f(\overline{x_1}, \overline{x_2}, \dots, \overline{x_N}) + \sum_{k=1}^{N} \left(\frac{\partial f}{\partial x_k}\right) \cdot \Delta x_{i,k} + \cdots \tag{11.73}$$

where the first term $f(\overline{x_1}, \overline{x_2}, \dots, \overline{x_N}) = \bar{\bar{f}}$ while the following terms correspond to the deviation from $\bar{\bar{f}}$. The mean value $\bar{f}$ is now calculated by inserting Equation (11.71) into (11.72):

$$\bar{f} = \frac{1}{n} \cdot \sum_{i-1}^{n} \bar{\bar{f}} + \frac{1}{n} \cdot \sum_{i=1}^{n} \sum_{k=1}^{N} \left(\frac{\partial f}{\partial x_k}\right) \cdot \Delta x_{i,k} + quadratic\ terms\ etc. \tag{11.74}$$

Here, the first term equals $\frac{1}{n} \cdot \sum_{i-1}^{n} \bar{\bar{f}} = \bar{\bar{f}}$. The second term $\frac{1}{n} \cdot \sum_{i=1}^{n} \sum_{k=1}^{N} \left(\frac{\partial f}{\partial x_k}\right) \cdot \Delta x_{i,k}$ is zero, since reversing the order of summation reveals $\sum_{k=1}^{N} \left(\frac{\partial f}{\partial x_k}\right) \sum_{i=1}^{n} \Delta x_{i,k}$ with $\sum_{i=1}^{n} \Delta x_{i,k} = 0$. Consequently, as we already showed for a single variable, mean values $\overline{f(x_{i,1}, x_{i,2}, x_{i,3} \dots)}$ and $\bar{\bar{f}} = (\overline{x_1}, \overline{x_2}, \dots, \overline{x_N})$ coincide.

11.5.2 Standard deviation as a function of the variance

Here, we derive the *variance* σ_f^2 (or its square root, the *standard deviation* σ_f) of the result function $f(x)$

$$\sigma_f^2 \approx \frac{1}{n-1} \sum_{i=1}^{n} (f_i - \bar{f})^2 = \frac{1}{n-1} \sum_{i=1}^{n} \left(\sum_{k=1}^{N} \left(\frac{\partial f}{\partial x_k}\right) \Delta x_{i,k} \right)^2 \tag{11.75}$$

where

$$\left(\sum_{k=1}^{N} \left(\frac{\partial f}{\partial x_k}\right) \Delta x_{i,k} \right)^2 == \sum_{k=1}^{N} \left(\frac{\partial f}{\partial x_k}\right)^2 \Delta x_{i,k}^2 + \sum_{\substack{k,l=1 \\ l \neq m}}^{N} \left(\frac{\partial f}{\partial x_k}\right) \cdot \left(\frac{\partial f}{\partial x_i}\right) \Delta x_{i,k} \cdot \Delta x_{i,l} \tag{11.76}$$

Inverting the sigma signs reveals

$$\sigma_f^2 = \sum_{k=1}^{N}\left(\frac{\partial f}{\partial x_k}\right)^2 \frac{1}{n-1}\cdot\sum_{i=1}^{n}\Delta x_{i,k}^2 + \frac{1}{n-1}\cdot\sum_{\substack{k,l=1\\ l\neq m}}^{N}\left(\frac{\partial f}{\partial x_k}\right)\cdot\left(\frac{\partial f}{\partial x_i}\right) \cdot\sum_{i=1}^{n}\Delta x_{i,k}\cdot\Delta x_{i,l} \tag{11.77}$$

and finally, this yields the Gaussian law of error propagation

$$\sigma_f^2 \approx \frac{1}{n-1}\sum_{i=1}^{n}(f_i-\bar{f})^2 = \frac{1}{n-1}\sum\nolimits_{i=1}^{n}\left(\sum_{k=1}^{N}\left(\frac{\partial f}{\partial x_k}\right)\Delta x_{i,k}\right)^2 \tag{11.78}$$

or analogously

$$\sigma_f = \sqrt{\left(\frac{\partial f}{\partial x_1}\right)^2\cdot\sigma_1^2 + \left(\frac{\partial f}{\partial x_2}\right)^2\cdot\sigma_2^2 + \cdots} \tag{11.79}$$

11.5.3 The principle of "maximum likelihood"

We assume that the values y_i are normally distributed in a Gaussian. Having the right parameter set $\alpha_1 \ldots \alpha_j \ldots \alpha_n$, the expectation value of y is given by $f({}^1x,\ {}^2x, \ldots \alpha_1, \alpha_2, \ldots)$. In this case, the probability w_i to obtain the value y_i in an individual measurement, would be

$$w_i = \frac{1}{\sigma_i}\sqrt{\frac{1}{2\cdot\pi}}\cdot e^{-\frac{\left(y_i - f({}^1x_i,\ {}^2x_i \ldots, \alpha_1, \alpha_2 \ldots \alpha_p)\right)^2}{2\cdot\sigma_i^2}} \tag{11.80}$$

The total probability W for the whole set of measurements is then given by the product of the probabilities of each individual measurement

$$W = w_1\cdot w_2\cdot w_3\cdot \ldots = = \frac{1}{\sigma_1\cdot\sigma_2\cdot\ldots}\left(\sqrt{\frac{1}{2\cdot\pi}}\right)^N \cdot e^{-\frac{\left(y_1 - f({}^1x_1,\ {}^2x_1 \ldots, \alpha_1, \alpha_2 \ldots \alpha_p)\right)^2}{2\cdot\sigma_1^2}} \cdot e^{-\frac{\left(y_2 - f({}^1x_2,\ {}^2x_2 \ldots, \alpha_1, \alpha_2 \ldots \alpha_p)\right)^2}{2\cdot\sigma_2^2}}\cdot\ldots \tag{11.81}$$

where

$$e^{-\frac{\left(y_1 - f({}^1x_1,\ {}^2x_1 \ldots, \alpha_1, \alpha_2 \ldots \alpha_p)\right)^2}{2\cdot\sigma_1^2}}\cdot e^{-\frac{\left(y_2 - f({}^1x_2,\ {}^2x_2 \ldots, \alpha_1, \alpha_2 \ldots \alpha_p)\right)^2}{2\cdot\sigma_2^2}} == e^{-\sum_{i=1}^{N}\frac{\left(y_i - f({}^1x_2,\ {}^2x_2 \ldots, \alpha_1, \alpha_2 \ldots \alpha_p)\right)^2}{2\cdot\sigma_i^2}} \tag{11.82}$$

If the parameter set is correct, then the probability W becomes maximal. This occurs if the negative exponent ($\equiv \frac{1}{2}\cdot\chi^2$) in the equation (11.82) is minimal. Thus equation (11.49) (χ^2) needs to be minimal.

11.5.4 Deriving the errors of the regression parameters

The influence of the error Δy_i on the errors $\Delta\alpha_1$ and $\Delta\alpha_2$ can be determined with the help of the law of error propagation (see paragraph 11.3.2)

Equations (11.62) can be derived by substituting the equation (11.53) in (11.61), obtaining:

$$\Delta\alpha_1^2 = \sum_{i=1}^{n}\left(\frac{\partial\left(\frac{S_y\cdot S_{x^2} - S_{xy}\cdot S_x}{\Delta}\right)}{\partial y_i}\right)^2\cdot\Delta y_i^2 == \sum_{i=1}^{n}\left(\frac{\frac{\partial S_y}{\partial y_i}\cdot S_{x^2} - \frac{\partial S_{xy}}{\partial y_i}\cdot S_x}{\Delta}\right)^2\cdot\Delta y_i^2 \tag{11.83}$$

where $\frac{\partial S_y}{\partial y_i} = \frac{1}{\sigma_i^2}$, $\frac{\partial S_{xy}}{\partial y_i} = \frac{x_i}{\sigma_i^2}$ and $\Delta y_i^2 = \sigma_i^2$. Squaring out the bracket yields

$$\Delta\alpha_1^2 = \sum_{i=1}^{n}\left(\frac{S_{x^2}\cdot\frac{1}{\sigma_i^2} - S_x\cdot\frac{x_i}{\sigma_i^2}}{\Delta}\right)^2\cdot\sigma_i^2 = \\ = \frac{1}{\Delta^2}\sum_{i=1}^{n}\left(S_{x^2}^2\cdot\frac{\sigma_i^2}{\sigma_i^4} - 2\cdot S_x\cdot S_{x^2}\cdot\frac{x_i\cdot\sigma_i^2}{\sigma_i^4} + S_x^2\cdot\frac{x_i^2\cdot\sigma_i^2}{\sigma_i^4}\right) \tag{11.84}$$

and further using $\sum_{i=1}^{n}\frac{1}{\sigma_i^2} = S$, $\sum_{i=1}^{n}\frac{x_i}{\sigma_i^2} = S_x$ and $\sum_{i=1}^{n}\frac{x_i^2}{\sigma_i^2} = S_x^2$

$$\Delta\alpha_1^2 = \frac{1}{\Delta^2}\cdot\left(S_{x^2}^2\cdot\sum_{i=1}^{n}\frac{1}{\sigma_i^2} - 2\cdot S_x\cdot S_{x^2}\cdot\sum_{i=1}^{n}\frac{x_i}{\sigma_i^2} + S_x^2\cdot\sum_{i=1}^{n}\frac{x_i^2}{\sigma_i^2}\right) == S_{x^2}\cdot\frac{S\cdot S_{x^2} - S_x\cdot S_x}{\Delta^2} \tag{11.85}$$

Using equation (11.60) $S\cdot S_{x^2} - S_x\cdot S_x = \Delta$ finally yields (11.62). Equation (11.63) can be analogously derived.

12 Basic instructions to use the software “measure”

☐ Open the Phywe software “***measure***” that you can find at “Start” > “Alle Apps” > “Mathematische Software” > “measure”. 

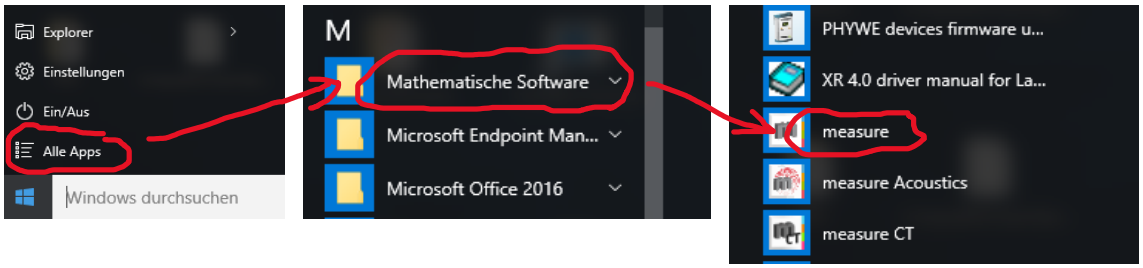

Figure 12.1: Path on the Windows Start Menu to reach and open the software “*measure*”.

☐ Click on “Experiment” followed by “Load configuration” to open the load configuration window. You find the configurations under “C:\Benutzer\Öffentlich”. Select the configuration needed for the experiment you are working on.

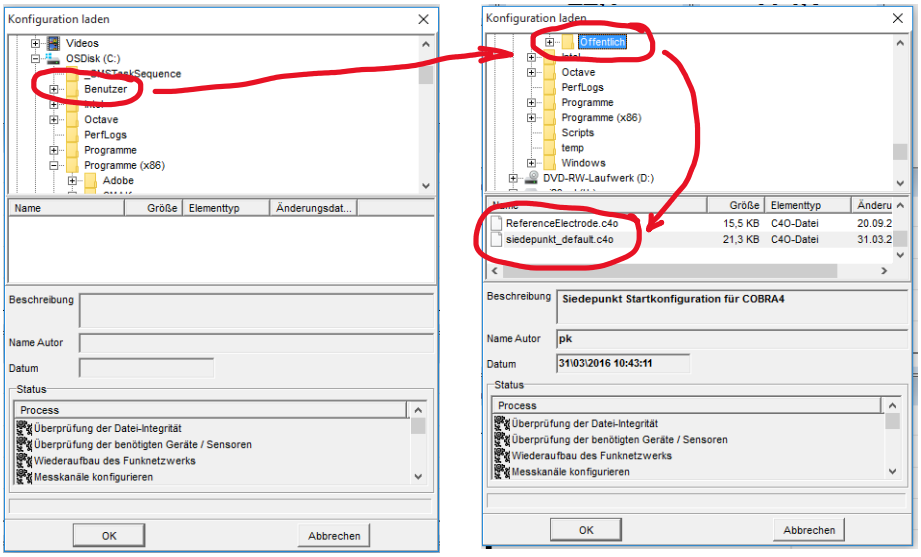

Figure 12.2: How to reach the configuration to load on the relative pop-up window.

☐ To start a measurement, click on the red button (symbol “record”) on the extreme left of the toolbar.

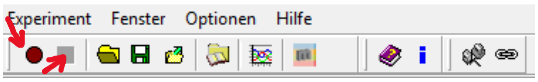

Figure 12.3: Toolbar of the software “measure”. The arrows point to the “start measurement” button (left arrow, symbol “record”) and to the “stop measurement” button (right arrow).

☐ To stop the measurement, click on the black button (symbol “stop”) on the left of the toolbar.

☐ When the measurement is stopped, a window opens automatically and asks whether the collected data should be saved or discarded. Click the first option, “Transfer all measurements to the main window of the software measure,” then click OK.

Figure 12.4: Pop-up window that opens when the measurement is stopped. Please select the first option and click OK.

☐ On the "Messung" menu of the software "measure", please select "Messwerte exportieren". In the pop-up window that appears, select the option you prefer: either exporting the collected data from the main window to your LRZ folder as a CSV file, or exporting the measurement data to the clipboard and pasting it directly into an opened Excel file.

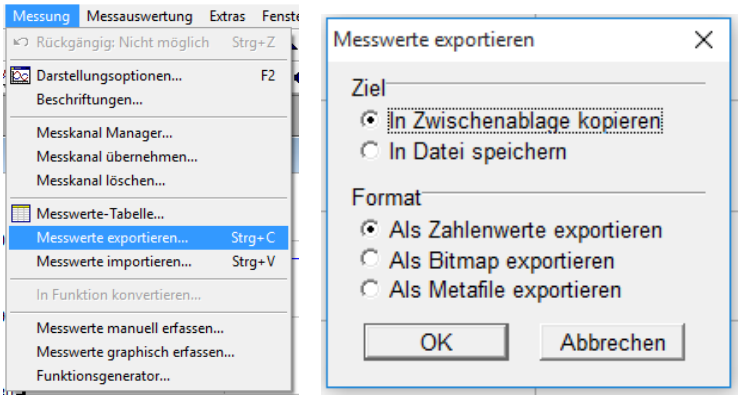

Figure 12.5: Left, dropdown menu after selecting "Messung" in the software "measure". Please click on "Messwerte exportieren". Right: in the pop-up window that opens after clicking, please select the saving option you prefer and click OK.